



Solar thermal collectors and applications

Soteris A. Kalogirou*

Department of Mechanical Engineering, Higher Technical Institute, P.O. Box 20423, Nicosia 2152, Cyprus

Received 18 June 2003; accepted 10 February 2004

Abstract

In this paper a survey of the various types of solar thermal collectors and applications is presented. Initially, an analysis of the environmental problems related to the use of conventional sources of energy is presented and the benefits offered by renewable energy systems are outlined. A historical introduction into the uses of solar energy is attempted followed by a description of the various types of collectors including flat-plate, compound parabolic, evacuated tube, parabolic trough, Fresnel lens, parabolic dish and heliostat field collectors. This is followed by an optical, thermal and thermodynamic analysis of the collectors and a description of the methods used to evaluate their performance. Typical applications of the various types of collectors are presented in order to show to the reader the extent of their applicability. These include solar water heating, which comprise thermosyphon, integrated collector storage, direct and indirect systems and air systems, space heating and cooling, which comprise, space heating and service hot water, air and water systems and heat pumps, refrigeration, industrial process heat, which comprise air and water systems and steam generation systems, desalination, thermal power systems, which comprise the parabolic trough, power tower and dish systems, solar furnaces, and chemistry applications. As can be seen solar energy systems can be used for a wide range of applications and provide significant benefits, therefore, they should be used whenever possible.

© 2004 Elsevier Ltd. All rights reserved.

Keywords: Solar collectors; Optical and thermal analysis; Water heating; Space heating; Cooling; Industrial process heat; Solar power generation; Desalination; Solar chemistry

Contents

1. Introduction	235
1.1. Energy related environmental problems.	235
1.1.1. Acid rain	236
1.1.2. Ozone layer depletion.	236
1.1.3. Global climate change	237
1.1.4. Renewable energy technologies.	237
1.2. History of solar energy.	238
2. Solar collectors.	240
2.1. Stationary collectors.	240
2.1.1. Flat-plate collectors	241
2.1.1.1. Glazing materials	242
2.1.1.2. Collector absorbing plates.	242
2.1.2. Compound parabolic collectors	244
2.1.3. Evacuated tube collectors	246
2.2. Sun tracking concentrating collectors	247
2.2.1. Parabolic trough collectors	248
2.2.2. Linear Fresnel reflector.	250
2.2.3. Parabolic dish reflector (PDR).	251
2.2.4. Heliostat field collector.	251

* Tel.: +357-2240-6466; fax: +357-2249-4953.

E-mail address: skalogir@spidernet.com.cy (S.A. Kalogirou).

3. Thermal analysis of collectors	252
3.1. Flat-plate collectors performance	253
3.2. Concentrating collectors performance	255
3.2.1. Optical analysis	256
3.2.2. Thermal analysis	257
3.3. Second law analysis	259
3.3.1. Minimum entropy generation rate	260
3.3.2. Optimum collector temperature	260
3.3.3. Non-isothermal collector	261
4. Performance of solar collectors	262
4.1. Collector thermal efficiency	262
4.2. Collector incidence angle modifier	263
4.2.1. Flat-plate collectors	263
4.2.2. Concentrating collectors	263
4.3. Concentrating collector acceptance angle	264
4.4. Collector time constant	264
4.5. Collector test results and preliminary collector selection	265
4.6. Modelling of solar systems	266
4.6.1. TRNSYS simulation program	266
4.6.2. WATSUN simulation program	267
4.6.3. Polysun simulation program	267
4.6.4. F-Chart method and program	268
4.6.5. Artificial neural networks in solar energy systems modelling and prediction	269
4.6.6. Limitations of simulations	269
4.7. Economic analysis	269
4.7.1. Time value of money	269
4.7.2. Method description	270
5. Solar collector applications	270
5.1. Solar water heating systems	270
5.1.1. Thermosyphon systems (passive)	271
5.1.2. Integrated collector storage systems (passive)	272
5.1.3. Direct circulation systems (active)	273
5.1.4. Indirect water heating systems (active)	274
5.1.5. Air systems	275
5.2. Solar space heating and cooling	275
5.2.1. Space heating and service hot water	277
5.2.2. Air systems	277
5.2.3. Water systems	277
5.2.4. Heat pump systems	278
5.3. Solar refrigeration	279
5.3.1. Adsorption units	279
5.3.2. Absorption units	279
5.4. Industrial process heat	281
5.4.1. Solar industrial air and water systems	283
5.4.2. Solar steam generation systems	283
5.5. Solar desalination systems	284
5.6. Solar thermal power systems	286
5.6.1. Parabolic trough collector systems	286
5.6.2. Power tower systems	288
5.6.3. Parabolic dish systems	289
5.7. Solar furnaces	289
5.8. Solar chemistry applications	290
6. Conclusions	290
References	290

Nomenclature	
A_a	absorber area (m^2)
A_c	total collector aperture area (m^2)
A_f	collector geometric factor
A_r	receiver area (m^2)
b	bond width (m)
b_0	incidence angle modifier constant
b_1	incidence angle modifier constant
c_p	specific heat at constant pressure (J/kg K)
c_0	intercept efficiency [= $F_R \tau \alpha$]
c_1	first-order coefficient of the collector efficiency ($W/m^2 \text{ } ^\circ C$)
c_2	second-order coefficient of the collector efficiency ($W/m^2 \text{ } ^\circ C^2$)
C	collector concentration ratio [= A_a/A_r], factor given by Eq. (26), investment cost (\$)
C_b	bond conductance ($W/m \text{ } ^\circ C$)
C_{FA}	cost rate for auxiliary energy (\$/kJ)
C_{FL}	cost rate for conventional fuel (\$/kJ)
d	market discount rate (%), interest rate (%)
d_r	displacement of receiver from focus (m)
d^*	universal non-random error parameter due to receiver mislocation and reflector profile errors ($d^* = d_r/D$)
D	riser tube outside diameter (m), monthly total heating load for space heating and hot water or demand (J)
D_i	tube inside diameter (m)
D_o	tube outside diameter (m)
$E_{x,in}$	exergy in (W)
$E_{x,out}$	exergy out (W)
f	focal distance (m), solar contribution, factor given by Eq. (25)
F'	collector efficiency factor
F	fin efficiency, cash flow
F_R	heat removal factor
F'_R	collector heat exchanger efficiency factor
G_b	beam (or direct) irradiation (W/m^2)
G_t	total (direct plus diffuse) solar energy incident on the collector aperture (W/m^2)
h	hour angle (degrees)
\bar{H}_T	monthly average daily radiation incident on the collector surface per unit area (J/m^2)
h_{fi}	heat transfer coefficient inside absorber tube ($W/m^2 \text{ } ^\circ C$)
h_w	wind heat transfer coefficient ($W/m^2 \text{ } ^\circ C$)
h_p	height of the parabola (m)
i	inflation rate (%)
I	total horizontal radiation per unit area (W/m^2)
I_{bT}	incident beam radiation per unit area (W/m^2)
I_d	horizontal diffuse radiation per unit area (W/m^2)
k	absorber thermal conductivity ($W/m \text{ } ^\circ C$)
$k_{\alpha\tau}$	incidence angle modifier
k_b	bond thermal conductivity ($W/m \text{ } ^\circ C$)
k_0	intercept efficiency [= $F_R n_o$]
k_1	first-order coefficient of the collector efficiency ($W/m^2 \text{ } ^\circ C$) [= c_1/C]
k_2	second-order coefficient of the collector efficiency ($W/m^2 \text{ } ^\circ C^2$) [= c_2/C]
L	half distance between two consecutive riser pipes [= $(W - D)/2$], collector length (m)
m	mass flow rate of fluid (kg/s), factor given in Eq. (6)
M	mass flow number
n_c	collector efficiency
n_o	collector optical efficiency
N	days in month, number of years
N_g	number of glass covers
N_s	entropy generation number
PW_N	present worth after N years
q^*	irradiation per unit of collector area (W/m^2)
q_u	rate of useful energy delivered by the collector (W)
q'_u	useful energy gain per unit length (J/m)
q'_{fin}	useful energy conducted per unit fin length (J/m)
q'_{tube}	useful energy conducted per unit tube length (J/m)
q_o^*	radiation falling on the receiver (W/m^2)
Q	rate of heat transfer output (W)
Q_{aux}	auxiliary energy (J)
Q_{load}	load or demand energy (J)
Q^*	solar radiation incident on collector (W)
Q_o	rate of heat loss to ambient (W)
R	receiver radius (m)
s	specific entropy (J/kg K)
S	absorbed solar energy (kJ/m^2)
S_{gen}	generated entropy (J/K)
t	time
T	absolute temperature (K)
T_a	ambient temperature ($^\circ C$)
T_b	local base temperature ($^\circ C$)
\bar{T}_a	monthly average ambient temperature ($^\circ C$)
T_{av}	average collector fluid temperature ($^\circ C$)
T_f	local fluid temperature ($^\circ C$)
T_{fi}	temperatures of the fluid entering the collector ($^\circ C$)
T_i	temperatures of the fluid entering the collector ($^\circ C$)
T_o	ambient temperature (K), temperature of the fluid leaving the collector ($^\circ C$)
T_{oi}	collector outlet initial water temperature ($^\circ C$)
T_{ot}	collector outlet water temperature after time t ($^\circ C$)
T_p	average temperature of the absorbing surface ($^\circ C$), stagnation temperature ($^\circ C$)
T_r	temperature of the absorber ($^\circ C$), receiver temperature (K)

T_{ref}	an empirically derived reference temperature [= 100 °C]	Φ	zenith angle (degrees)
T_s	apparent black body temperature of the sun (~ 6000 K)	Ψ	factor given in Eq. (7)
T_*	apparent sun temperature as an exergy source (~ 4500 K)	σ	Stefan–Boltzmann constant [= $5.67 \times 10^{-8} \text{ W/m}^2 \text{ K}^4$]
U_b	bottom heat loss coefficient ($\text{W/m}^2 \text{ }^\circ\text{C}$)	σ^*	universal random error parameter ($\sigma^* = \sigma C$)
U_e	edges heat loss coefficient ($\text{W/m}^2 \text{ }^\circ\text{C}$)	σ_{sun}	standard deviation of the energy distribution of the sun's rays at normal incidence
U_L	solar collector heat transfer loss coefficient ($\text{W/m}^2 \text{ }^\circ\text{C}$)	σ_{slope}	standard deviation of the distribution of local slope errors at normal incidence
U_o	heat transfer coefficient from fluid to ambient air ($\text{W/m}^2 \text{ }^\circ\text{C}$)	σ_{mirror}	standard deviation of the variation in diffusivity of the reflective material at normal incidence
U_r	receiver-ambient heat transfer coefficient based on A_r ($\text{W/m}^2 \text{ }^\circ\text{C}$)	τ_α	absorber transmittance
U_t	top heat loss coefficient ($\text{W/m}^2 \text{ }^\circ\text{C}$)	$\tau\alpha$	transmittance–absorptance product
W	distance between riser tubes (m), wind velocity (m/s)	$\overline{\tau\alpha}$	monthly average transmittance–absorptance product
W_a	collector aperture (m)	$(\tau\alpha)_b$	transmittance–absorptance product for estimating incidence angle modifier for beam radiation
x	factor used in Eq. (72) [= $(T_i - T_a)/G_i$]	$(\tau\alpha)_s$	transmittance–absorptance product for estimating incidence angle modifier for sky radiation
X	dimensionless parameter given by Eq. (83)	$(\tau\alpha)_g$	transmittance–absorptance product for estimating incidence angle modifier for ground reflected radiation
X_c	corrected value of X	φ	parabolic angle (degrees): the angle between the axis and the reflected beam at focus of the parabola
y	factor used in Eq. (74) [= $(T_i - T_a)/G_b$]	φ_r	collector rim angle (degrees)
Y	dimensionless parameter given by Eq. (84)		
<i>Greek symbols</i>			
α_α	absorber absorptance		
α	fraction of solar energy reaching surface that is absorbed, absorptivity		
β	incidence angle (degrees), collector slope (degrees), misalignment angle error (degrees)		
β^*	universal non-random error parameter due to angular errors ($\beta^* = \beta C$)		
δ	absorber (fin) thickness (m), declination angle (degrees)		
ΔT	temperature difference [= $T_i - T_a$]		
Δx	elemental fin or riser tube distance (m)		
ε_g	emissivity of glass covers		
ε_p	absorber plate emittance		
γ	collector intercept factor, average bond thickness (m)		
ρ	density (kg/m^3), mirror reflectance		
ρ_m	mirror reflectance		
$\rho_{(\theta)}$	distance, ρ , along a tangent from the receiver to the curve given by Eq. (101)		
θ	dimensionless temperature [= T/T_o], angle of incidence (degrees)		
θ_A	acceptance half angle for CPC collectors (degrees)		
θ_m	collector half acceptance angle (degrees)		
θ_{sky}	effective incidence angle for evaluating the incidence angle modifier of flat-plate collector for sky diffuse radiation		
θ_{gnd}	effective incidence angle for evaluating the incidence angle modifier of flat-plate collector for ground reflected radiation		
<i>Abbreviations</i>			
AFP	advanced flat-plate		
CLFR	compact linear Fresnel reflector		
CPC	compound parabolic collector		
CTC	cylindrical trough collector		
ED	electrodialysis		
ER	energy recovery		
E–W	east–west		
ETC	evacuated tube collector		
FPC	flat-plate collector		
HFC	heliostat field collector		
ICPC	integrated compound parabolic collector		
LCR	local concentration ratio		
LCS	life cycle savings		
LFR	linear Fresnel reflector		
MEB	multiple effect boiling		
MSF	multistage flash		
N–S	north–south		
PDR	parabolic dish reflector		
PTC	parabolic trough collector		
PWF	present worth factor		
RO	reverse osmosis		
TI	transparent insulation		
VC	vapor compression		

1. Introduction

The sun is a sphere of intensely hot gaseous matter with a diameter of 1.39×10^9 m. The solar energy strikes our planet a mere 8 min and 20 s after leaving the giant furnace, the sun which is 1.5×10^{11} m away. The sun has an effective blackbody temperature of 5762 K [1]. The temperature in the central region is much higher and it is estimated at 8×10^6 to 40×10^6 K. In effect the sun is a continuous fusion reactor in which hydrogen is turned into helium. The sun's total energy output is 3.8×10^{20} MW which is equal to 63 MW/m^2 of the sun's surface. This energy radiates outwards in all directions. Only a tiny fraction, 1.7×10^{14} kW, of the total radiation emitted is intercepted by the earth [1]. However, even with this small fraction it is estimated that 30 min of solar radiation falling on earth is equal to the world energy demand for one year.

Man realised that a good use of solar energy is in his benefit, from the prehistoric times. The Greek historian Xenophon in his 'memorabilia' records some of the teachings of the Greek Philosopher Socrates (470–399 BC) regarding the correct orientation of dwellings in order to have houses which were cool in summer and warm in winter.

Since prehistory, the sun has dried and preserved man's food. It has also evaporated sea water to yield salt. Since man began to reason, he has recognised the sun as a motive power behind every natural phenomenon. This is why many of the prehistoric tribes considered Sun as 'God'. Many scripts of ancient Egypt say that the Great Pyramid, one of the man's greatest engineering achievements, was built as a stairway to the sun [2].

Basically, all the forms of energy in the world as we know it are solar in origin. Oil, coal, natural gas and woods were originally produced by photosynthetic processes, followed by complex chemical reactions in which decaying vegetation was subjected to very high temperatures and pressures over a long period of time [1]. Even the wind and tide energy have a solar origin since they are caused by differences in temperature in various regions of the earth.

The greatest advantage of solar energy as compared with other forms of energy is that it is clean and can be supplied without any environmental pollution. Over the past century fossil fuels have provided most of our energy because these are much cheaper and more convenient than energy from alternative energy sources, and until recently environmental pollution has been of little concern.

Twelve winter days of 1973 changed the economic relation of fuel and energy when the Egyptian army stormed across the Suez Canal on October the 12th provoking an international crisis and for the first time, involved as part of Arab strategy, the threat of the 'oil weapon'. Both the price and the political weapon issues quickly came to a head when the six Gulf members of

the Organisations of Petroleum Exporting Countries (OPEC), met in Kuwait and quickly abandoned the idea of holding any more price consultations with the oil companies, announcing that they were raising the price of their crude oil by 70%.

The reason for the rapid increase in oil demand occurred mainly because increasing quantities of oil, produced at very low cost, became available during the 50s and 60s from the Middle East and North Africa. For the consuming countries imported oil was cheap compared with indigenously produced energy from solid fuels.

But the main problem is that proved reserves of oil and gas, at current rates of consumption, would be adequate to meet demand for another 40 and 60 years, respectively. The reserves for coal are in better situation as they would be adequate for at least the next 250 years.

If we try to see the implications of these limited reserves we will be faced with a situation in which the price of fuels will be accelerating as the reserves are decreased. Considering that the price of oil has become firmly established as the price leader for all fuel prices then the conclusion is that energy prices will increase over the next decades at something greater than the rate of inflation or even more. In addition to this is also the concern about the environmental pollution caused by the burning of the fossil fuels. This issue is examined in Section 1.1.

In addition to the thousands of ways in which the sun's energy has been used by both nature and man through time, to grow food or dry clothes, it has also been deliberately harnessed to perform a number of other jobs. Solar energy is used to heat and cool buildings (both active and passive), to heat water for domestic and industrial uses, to heat swimming pools, to power refrigerators, to operate engines and pumps, to desalinate water for drinking purposes, to generate electricity, for chemistry applications, and many more. The objective of this paper is to present the various types of collectors used to harness solar energy, their thermal analysis and performance, and a review of applications.

There are many alternative energy sources which can be used instead of fossil fuels. The decision as to what type of energy source should be utilised must, in each case, be made on the basis of economic, environmental and safety considerations. Because of the desirable environmental and safety aspects it is widely believed that solar energy should be utilised instead of other alternative energy forms, even when the costs involved are slightly higher.

1.1. Energy related environmental problems

Energy is considered a prime agent in the generation of wealth and a significant factor in economic development. The importance of energy in economic development is recognised universally and historical data verify that there is

a strong relationship between the availability of energy and economic activity. Although at the early 70s, after the oil crisis, the concern was on the cost of energy, during the past two decades, the risk and reality of environmental degradation have become more apparent. The growing evidence of environmental problems is due to a combination of several factors since the environmental impact of human activities has grown dramatically. This is due to the increase of the world population, energy consumption and industrial activities. Achieving solutions to environmental problems that humanity faces today requires long-term potential actions for sustainable development. In this respect, renewable energy resources appear to be one of the most efficient and effective solutions.

A few years ago, most environmental analysis and legal control instruments concentrated on conventional pollutants such as sulphur dioxide (SO_2), nitrogen oxides (NO_x), particulates, and carbon monoxide (CO). Recently however, environmental concern has extended to the control of hazardous air pollutants, which are usually toxic chemical substances which are harmful even in small doses, as well as to other globally significant pollutants such as carbon dioxide (CO_2). Additionally, developments in industrial processes and structures have led to new environmental problems. A detailed description of these gaseous and particulate pollutants and their impacts on the environment and human life is presented by Dincer [3,4].

One of the most widely accepted definitions of sustainable development is: "development that meets the needs of the present without compromising the ability of future generations to meet their own needs". There are many factors that can help to achieve sustainable development. Today, one of the main factors that must be considered is energy and one of the most important issues is the requirement for a supply of energy that is fully sustainable [5,6]. A secure supply of energy is generally agreed to be a necessary, but not a sufficient requirement for development within a society. Furthermore, for a sustainable development within a society it is required that a sustainable supply of energy and effective and efficient utilization of energy resources are secured. Such a supply in the long-term should be readily available at reasonable cost, be sustainable and be able to be utilized for all the required tasks without causing negative societal impacts. This is why there is a close connection between renewable sources of energy and sustainable development.

Pollution depends on energy consumption. Today the world daily oil consumption is 76 million barrels. Despite the well-known consequences of fossil fuel combustion on the environment, this is expected to increase to 123 million barrels per day by the year 2025 [7]. There are a large number of factors which are significant in the determination of the future level of the energy consumption and production. Such factors include population growth, economic performance, consumer tastes and technological

developments. Furthermore, governmental policies concerning energy and developments in the world energy markets will certainly play a key role in the future level and pattern of energy production and consumption [8].

Another parameter to be considered is the world population. This is expected to double by the middle of this century and as economic development will certainly continue to grow, the global demand for energy is expected to increase. Today much evidence exists, which suggests that the future of our planet and of the generations to come will be negatively impacted if humans keep degrading the environment. Currently, three environmental problems are internationally known; these are the acid precipitation, the stratospheric ozone depletion, and the global climate change. These are analysed in more detail below.

1.1.1. Acid rain

This is a form of pollution depletion in which SO_2 and NO_x produced by the combustion of fossil fuels are transported over great distances through the atmosphere and deposited via precipitation on the earth, causing damage to ecosystems that are exceedingly vulnerable to excessive acidity. Therefore, it is obvious that the solution to the issue of acid rain deposition requires an appropriate control of SO_2 and NO_x pollutants. These pollutants cause both regional and transboundary problems of acid precipitation.

Recently, attention is also given to other substances such as volatile organic compounds (VOCs), chlorides, ozone and trace metals that may participate in a complex set of chemical transformations in the atmosphere resulting in acid precipitation and the formation of other regional air pollutants. A number of evidences that show the damages of acid precipitation are reported by Dincer and Rosen [6].

It is well known that some energy-related activities are the major sources of acid precipitation. Additionally, VOCs are generated by a variety of sources and comprise a large number of diverse compounds. Obviously, the more energy we spend the more we contribute to acid precipitation; therefore, the easiest way to reduce acid precipitation is by reducing energy consumption.

1.1.2. Ozone layer depletion

The ozone present in the stratosphere, at altitudes between 12 and 25 km, plays a natural equilibrium-maintaining role for the earth, through absorption of ultraviolet (UV) radiation (240–320 nm) and absorption of infrared radiation [3]. A global environmental problem is the depletion of the stratospheric ozone layer which is caused by the emissions of CFCs, halons (chlorinated and brominated organic compounds) and NO_x . Ozone depletion can lead to increased levels of damaging UV radiation reaching the ground, causing increased rates of skin cancer and eye damage to humans and is harmful to many biological species. It should be noted that energy related activities are only partially (directly or indirectly) responsible for the emissions which lead to stratospheric ozone

depletion. The most significant role in ozone depletion have the CFCs, which are mainly used in air conditioning and refrigerating equipment as refrigerants, and NO_x emissions which are produced by the fossil fuel and biomass combustion processes, the natural denitrification and nitrogen fertilizers.

In 1998 the size of the ozone hole over Antarctica was 25 million km^2 . It was about 3 million km^2 in 1993 [7]. Researchers expect the Antarctic ozone hole to remain severe in the next 10–20 years, followed by a period of slow healing. Full recovery is predicted to occur in 2050; however, the rate of recovery is affected by the climate change [8].

1.1.3. Global climate change

The term greenhouse effect has generally been used for the role of the whole atmosphere (mainly water vapour and clouds) in keeping the surface of the earth warm. Recently however, it has been increasingly associated with the contribution of CO_2 which is estimated that contributes about 50% to the anthropogenic greenhouse effect. Additionally, several other gasses such as CH_4 , CFCs, halons, N_2O , ozone and peroxyacetylnitrate (also called greenhouse gasses) produced by the industrial and domestic activities can also contribute to this effect, resulting in a rise of the earth's temperature. Increasing atmospheric concentrations of greenhouse gasses increase the amount of heat trapped (or decrease the heat radiated from the earth's surface), thereby raising the surface temperature of the earth. According to Colombo [9] the earth's surface temperature has increased by about 0.6°C over the last century, and as a consequence the sea level is estimated to have risen by perhaps 20 cm. These changes can have a wide range of effects on human activities all over the world. The role of various greenhouse gasses is summarized in Ref. [6].

Humans contribute through many of their economic and other activities to the increase of the atmospheric concentrations of various greenhouse gasses. For example, CO_2 releases from fossil fuel combustion, methane emissions from increased human activity and CFC releases all contribute to the greenhouse effect. Predictions show that if atmospheric concentrations of greenhouse gasses, mainly due to fossil fuels combustion, continue to increase at the present rates, the earth's temperature may increase by another $2\text{--}4^\circ\text{C}$ in the next century. If this prediction is realized, the sea level could rise by between 30 and 60 cm before the end of this century [9]. The impacts of such sea level increase could easily be understood and include flooding of coastal settlements, displacement of fertile zones for agriculture toward higher latitudes, and decrease the availability of fresh water for irrigation and other essential uses. Thus, such consequences could put in danger the survival of entire populations.

1.1.4. Renewable energy technologies

Renewable energy technologies produce marketable energy by converting natural phenomena into useful forms

of energy. These technologies use the sun's energy and its direct and indirect effects on the earth (solar radiation, wind, falling water and various plants, i.e. biomass), gravitational forces (tides), and the heat of the earth's core (geothermal) as the resources from which energy is produced. These resources have massive energy potential, however, they are generally diffused and not fully accessible, most of them are intermittent, and have distinct regional variabilities. These characteristics give rise to difficult, but solvable, technical and economical challenges. Nowadays, significant progress is made by improving the collection and conversion efficiencies, lowering the initial and maintenance costs, and increasing the reliability and applicability.

A worldwide research and development in the field of renewable energy resources and systems is carried out during the last two decades. Energy conversion systems that are based on renewable energy technologies appeared to be cost effective compared to the projected high cost of oil. Furthermore, renewable energy systems can have a beneficial impact on the environmental, economic, and political issues of the world. At the end of 2001 the total installed capacity of renewable energy systems was equivalent to 9% of the total electricity generation [10]. By applying a renewable energy intensive scenario the global consumption of renewable sources by 2050 would reach 318 exajoules [11].

The benefits arising from the installation and operation of renewable energy systems can be distinguished into three categories; energy saving, generation of new working posts and the decrease of environmental pollution.

The energy saving benefit derives from the reduction in consumption of the electricity and/or diesel which are used conventionally to provide energy. This benefit can be directly translated into monetary units according to the corresponding production or avoiding capital expenditure for the purchase of imported fossil fuels.

Another factor which is of considerable importance in many countries is the ability of renewable energy technologies to generate jobs. The penetration of a new technology leads to the development of new production activities contributing to the production, market distribution and operation of the pertinent equipment. Specifically in the case of solar energy collectors job creation mainly relates to the construction and installation of the collectors. The latter is a decentralised process since it requires the installation of equipment in every building or every individual consumer.

The most important benefit of renewable energy systems is the decrease of environmental pollution. This is achieved by the reduction of air emissions due to the substitution of electricity and conventional fuels. The most important effects of air pollutants on the human and natural environment are their impact on the public health, agriculture and on ecosystems. It is relatively simple to measure the financial impact of these effects when they relate to tradable goods such as the agricultural crops;

however when it comes to non-tradable goods, like human health and ecosystems, things become more complicated. It should be noted that the level of the environmental impact and therefore the social pollution cost largely depends on the geographical location of the emission sources. Contrary to the conventional air pollutants, the social cost of CO₂ does not vary with the geographical characteristics of the source as each unit of CO₂ contributes equally to the climate change threat and the resulting cost.

In this paper emphasis is given to solar thermal systems. Solar thermal systems are non-polluting and offer significant protection of the environment. The reduction of greenhouse gas pollution is the main advantage of utilising solar energy. Therefore, solar thermal systems should be employed whenever possible in order to achieve a sustainable future.

1.2. History of solar energy

The idea of using solar energy collectors to harness the sun's power is recorded from the prehistoric times when at 212 BC the Greek scientist/physician Archimedes devised a method to burn the Roman fleet. Archimedes reputedly set the attacking Roman fleet afire by means of concave metallic mirror in the form of hundreds of polished shields; all reflecting on the same ship [2].

The Greek historian Plutarch (AD 46–120) referred to the incident saying that the Romans, seeing that indefinite mischief overwhelmed them from no visible means, began to think they were fighting with the gods. The basic question was whether or not Archimedes knew enough about the science of optics to devise a simple way to concentrate sunlight to a point where ships could be burned from a distance. Archimedes had written a book "On burning Mirrors" but no copy has survived to give evidence [12].

Eighteen hundred years after Archimedes, Athanasius Kircher (1601–1680) carried out some experiments to set fire to a woodpile at a distance in order to see whether the story of Archimedes had any scientific validity but no report of his findings survived [12].

Amazingly, the very first applications of solar energy refer to the use of concentrating collectors, which are by their nature (accurate shape construction) and the requirement to follow the sun, more 'difficult' to apply. During the 18th century, solar furnaces capable of melting iron, copper and other metals were being constructed of polished-iron, glass lenses and mirrors. The furnaces were in use throughout Europe and the Middle East. One furnace designed by the French scientist Antoine Lavoisier, attained the remarkable temperature of 1750 °C. The furnace used a 1.32 m lens plus a secondary 0.2 m lens to obtain such temperature which turned out to be the maximum achieved by man for one hundred years.

During the 19th century the attempts to convert solar energy into other forms based upon the generation of low-pressure steam to operate steam engines. August Mouchot

pioneered this field by constructing and operating several solar-powered steam engines between the years 1864 and 1878 [12]. Evaluation of one built at Tours by the French government showed that it was too expensive to be considered feasible. Another one was set up in Algeria. In 1875, Mouchot made a notable advance in solar collector design by making one in the form of a truncated cone reflector. Mouchot's collector consisted of silver-plated metal plates and had a diameter of 5.4 m and a collecting area of 18.6 m². The moving parts weighed 1400 kg.

Abel Pifre was a contemporary of Mouchot who also made solar engines [12,13]. Pifre's solar collectors were parabolic reflectors made of very small mirrors. In shape they looked rather similar to Mouchot's truncated cones.

In 1901 A.G. Eneas installed a 10 m diameter focusing collector which powered a water pumping apparatus at a California farm. The device consisted of a large umbrella-like structure open and inverted at an angle to receive the full effect of sun's rays on the 1788 mirrors which lined the inside surface. The sun's rays were concentrated at a focal point where the boiler was located. Water within the boiler was heated to produce steam which in turn powered a conventional compound engine and centrifugal pump [1,12].

In 1904 a Portuguese priest, Father Himalaya, constructed a large solar furnace. This was exhibited at the St Louis World's fair. This furnace appeared quite modern in structure, being a large, off-axis, parabolic horn collector [12].

In 1912 Shuman, in collaboration with C.V. Boys, undertook to build the world's largest pumping plant in Meadi, Egypt. The system was placed in operation in 1913 and it was using long parabolic cylinders to focus sunlight onto a long absorbing tube. Each cylinder was 62 m long, and the total area of the several banks of cylinders was 1200 m². The solar engine developed as much as 37–45 kW continuously for a 5 h period [1,12,13]. Despite the plant's success, it was completely shut down in 1915 due to the onset of World War I and cheaper fuel prices.

During the last 50 years many variations were designed and constructed using focusing collectors as a means of heating the transfer or working fluid which powered mechanical equipment. The two primary solar technologies used are the central receivers and the distributed receivers employing various point and line-focus optics to concentrate sunlight. Central receiver systems use fields of heliostats (two-axis tracking mirrors) to focus the sun's radiant energy onto a single tower-mounted receiver [14]. Distributed receiver technology includes parabolic dishes, Fresnel lenses, parabolic troughs, and special bowls. Parabolic dishes track the sun in two axes and use mirrors to focus radiant energy onto a point-focus receiver. Troughs and bowls are line-focus tracking reflectors that concentrate sunlight onto receiver tubes along their focal lines. Receiver temperatures range from 100 °C in low-temperature troughs to close 1500 °C in dish and central receiver systems [14].

More details of the basic types of collectors are given in Section 2.

Another area of interest, the hot water and house heating appeared in the mid 1930s, but gained interest in the last half of the 40s. Until then millions of houses were heated by coal burn boilers. The idea was to heat water and fed it to the radiator system that was already installed.

The manufacture of solar water heaters (SWH) began in the early 60s. The industry of SWH expanded very quickly in many countries of the world. Typical SWH in many cases are of the thermosyphon type and consist of two flat-plate solar collectors having an absorber area between 3 and 4 m², a storage tank with capacity between 150 and 180 l and a cold water storage tank, all installed on a suitable frame. An auxiliary electric immersion heater and/or a heat exchanger, for central heating assisted hot water production, are used in winter during periods of low solar insolation. Another important type of SWH is the force circulation type. In this system only the solar panels are visible on the roof, the hot water storage tank is located indoors in a plantroom and the system is completed with piping, pump and a differential thermostat. Obviously, this latter type is more appealing mainly due to architectural and aesthetic reasons, but also more expensive especially for small-size installations [15]. These together with a variety of other systems are described in Section 5.

Becquerel had discovered the photovoltaic effect in selenium in 1839. The conversion efficiency of the 'new' silicon cells developed in 1958 was 11% although the cost was prohibitively high (\$1000/W) [12]. The first practical application of solar cells was in space where cost was not a barrier and no other source of power is available. Research in the 1960s, resulted in the discovery of other photovoltaic materials such as gallium arsenide (GaAs). These could operate at higher temperatures than silicon but were much more expensive. The global installed capacity of photovoltaics at the end of 2002 was near 2 GWp [16]. Photovoltaic (PV) cells are made of various semiconductors, which are materials that are only moderately good conductors of electricity. The materials most commonly used are silicon (Si) and compounds of cadmium sulphide (CdS), cuprous sulphide (Cu₂S), and GaAs.

Amorphous silicon cells are composed of silicon atoms in a thin homogenous layer rather than a crystal structure. Amorphous silicon absorbs light more effectively than crystalline silicon, so the cells can be thinner. For this reason, amorphous silicon is also known as a 'thin film' PV technology. Amorphous silicon can be deposited on a wide range of substrates, both rigid and flexible, which makes it ideal for curved surfaces and 'fold-away' modules. Amorphous cells are, however, less efficient than crystalline based cells, with typical efficiencies of around 6%, but they are easier and therefore cheaper to produce. Their low cost makes them ideally suited for many applications where high efficiency is not required and low cost is important.

Amorphous silicon (a-Si) is a glassy alloy of silicon and hydrogen (about 10%). Several properties make it an attractive material for thin-film solar cells:

1. Silicon is abundant and environmentally safe.
2. Amorphous silicon absorbs sunlight extremely well, so that only a very thin active solar cell layer is required (about 1 μm as compared to 100 μm or so for crystalline solar cells), thus greatly reducing solar-cell material requirements.
3. Thin films of a-Si can be deposited directly on inexpensive support materials such as glass, sheet steel, or plastic foil.

A number of other promising materials such as cadmium telluride and copper indium diselenide are now being used for PV modules. The attraction of these technologies is that they can be manufactured by relatively inexpensive industrial processes, in comparison to crystalline silicon technologies, yet they typically offer higher module efficiencies than amorphous silicon.

The PV cells are packed into modules which produce a specific voltage and current when illuminated. PV modules can be connected in series or in parallel to produce larger voltages or currents. Photovoltaic systems can be used independently or in conjunction with other electrical power sources. Applications powered by PV systems include communications (both on earth and in space), remote power, remote monitoring, lighting, water pumping and battery charging.

The two basic types of PV applications are the stand alone and the grid connected. Stand-alone PV systems are used in areas that are not easily accessible or have no access to mains electricity. A stand-alone system is independent of the electricity grid, with the energy produced normally being stored in batteries. A typical stand-alone system would consist of PV module or modules, batteries and charge controller. An inverter may also be included in the system to convert the direct current generated by the PV modules to the alternating current form (AC) required by normal appliances.

In the grid connected applications the PV system is connect to the local electricity network. This means that during the day, the electricity generated by the PV system can either be used immediately (which is normal for systems installed in offices and other commercial buildings), or can be sold to one of the electricity supply companies (which is more common for domestic systems where the occupier may be out during the day). In the evening, when the solar system is unable to provide the electricity required, power can be bought back from the network. In effect, the grid is acting as an energy storage system, which means the PV system does not need to include battery storage.

When PVs started to be used for large-scale commercial applications, about 20 years ago, their efficiency was well below 10%. Nowadays, their efficiency increased to about 15%. Laboratory or experimental units can give efficiencies

of more than 30%, but these have not been commercialized yet. Although 20 years ago PVs were considered as a very expensive solar system the present cost is around 5000\$ per kW_e and there are good prospects for further reduction in the coming years. More details on photovoltaics are beyond the scope of this paper.

The lack of water was always a problem to humanity. Therefore among the first attempts to harness solar energy were the development of equipment suitable for the desalination of sea-water. Solar distillation has been in practice for a long time. According to Malik et al. [17], the earliest documented work is that of an Arab alchemist in the 15th century reported by Mouchot in 1869. Mouchot reported that the Arab alchemist had used polished Damascus mirrors for solar distillation.

The great French chemist Lavoisier (1862) used large glass lenses, mounted on elaborate supporting structures, to concentrate solar energy on the contents of distillation flasks [17]. The use of silver or aluminium coated glass reflectors to concentrate solar energy for distillation has also been described by Mouchot.

The use of solar concentrators in solar distillation has been reported by Pasteur (1928) [17] who used a concentrator to focus solar rays onto a copper boiler containing water. The steam generated from the boiler was piped to a conventional water cooled condenser in which distilled water was accumulated.

Solar stills are one of the simplest type of desalination equipment which uses the greenhouse effect to evaporate salty water. Solar stills were the first to be used on large-scale distilled water production. The first water distillation plant constructed was a system built at Las Salinas, Chile, in 1874 [12,17]. The still covered 4700 m² and produced up to 23 000 l of fresh water per day (4.9 l/m²), in clear sun. The still was operated for 40 years and was abandoned only after a fresh-water pipe was installed supplying water to the area from the mountains.

The renewal of interest on solar distillation occurred after the First World War at which time several new devices had been developed such as: roof type, tilted wick, inclined tray and inflated stills. Some more details on solar stills are given in Section 5.5. In this section it is also indicated how solar collectors can be used to power conventional desalination equipment. More information on solar desalination is given in Ref. [18].

Another application of solar energy is solar drying. Solar dryers have been used primarily by the agricultural industry. The objective in drying an agricultural product is to reduce its moisture contents to that level which prevents deterioration within a period of time regarded as the safe storage period. Drying is a dual process of heat transfer to the product from the heating source, and mass transfer of moisture from the interior of the product to its surface and from the surface to the surrounding air.

The objective of a dryer is to supply the product with more heat than is available under ambient conditions,

increasing sufficiently the vapour pressure of the moisture held within the crop, thus enhancing moisture migration from within the crop and decreasing significantly the relative humidity of the drying air, thus increasing its moisture carrying capability and ensuring a sufficiently low equilibrium moisture content.

In solar drying, solar energy is used as either the sole source of the required heat or as a supplemental source, and the air flow can be generated by either forced or natural convection. The heating procedure could involve the passage of the pre-heated air through the product, by directly exposing the product to solar radiation or a combination of both. The major requirement is the transfer of heat to the moist product by convection and conduction from surrounding air mass at temperatures above that of the product, or by radiation mainly from the sun and to a little extent from surrounding hot surfaces, or conduction from heated surfaces in contact with the product. Details of solar dryers are beyond the scope of this paper. More information on solar dryers can be found in Ref. [19].

Section 2 gives a brief description of several of the most common collectors available in the market.

2. Solar collectors

Solar energy collectors are special kind of heat exchangers that transform solar radiation energy to internal energy of the transport medium. The major component of any solar system is the solar collector. This is a device which absorbs the incoming solar radiation, converts it into heat, and transfers this heat to a fluid (usually air, water, or oil) flowing through the collector. The solar energy thus collected is carried from the circulating fluid either directly to the hot water or space conditioning equipment, or to a thermal energy storage tank from which can be drawn for use at night and/or cloudy days.

There are basically two types of solar collectors: non-concentrating or stationary and concentrating. A non-concentrating collector has the same area for intercepting and for absorbing solar radiation, whereas a sun-tracking concentrating solar collector usually has concave reflecting surfaces to intercept and focus the sun's beam radiation to a smaller receiving area, thereby increasing the radiation flux. A large number of solar collectors are available in the market. A comprehensive list is shown in Table 1 [20].

In this section a review of the various types of collectors currently available will be presented. This includes FPC, ETC, and concentrating collectors.

2.1. Stationary collectors

Solar energy collectors are basically distinguished by their motion, i.e. stationary, single axis tracking and two-axes tracking, and the operating temperature. Initially,

Table 1
Solar energy collectors

Motion	Collector type	Absorber type	Concentration ratio	Indicative temperature range (°C)
Stationary	Flat plate collector (FPC)	Flat	1	30–80
	Evacuated tube collector (ETC)	Flat	1	50–200
	Compound parabolic collector (CPC)	Tubular	1–5	60–240
Single-axis tracking			5–15	60–300
	Linear Fresnel reflector (LFR)	Tubular	10–40	60–250
	Parabolic trough collector (PTC)	Tubular	15–45	60–300
	Cylindrical trough collector (CTC)	Tubular	10–50	60–300
Two-axes tracking	Parabolic dish reflector (PDR)	Point	100–1000	100–500
	Heliostat field collector (HFC)	Point	100–1500	150–2000

Note: Concentration ratio is defined as the aperture area divided by the receiver/absorber area of the collector.

the stationary solar collectors are examined. These collectors are permanently fixed in position and do not track the sun. Three types of collectors fall in this category:

1. Flat plate collectors (FPC);
2. Stationary compound parabolic collectors (CPC);
3. Evacuated tube collectors (ETC).

2.1.1. Flat-plate collectors

A typical flat-plate solar collector is shown in Fig. 1. When solar radiation passes through a transparent cover and impinges on the blackened absorber surface of high absorptivity, a large portion of this energy is absorbed by the plate and then transferred to the transport medium in the fluid tubes to be carried away for storage or use. The underside of the absorber plate and the side of casing are well insulated to reduce conduction losses. The liquid tubes can be welded to the absorbing plate, or they can be an

integral part of the plate. The liquid tubes are connected at both ends by large diameter header tubes.

The transparent cover is used to reduce convection losses from the absorber plate through the restraint of the stagnant air layer between the absorber plate and the glass. It also reduces radiation losses from the collector as the glass is transparent to the short wave radiation received by the sun but it is nearly opaque to long-wave thermal radiation emitted by the absorber plate (greenhouse effect).

FPC are usually permanently fixed in position and require no tracking of the sun. The collectors should be oriented directly towards the equator, facing south in the northern hemisphere and north in the southern. The optimum tilt angle of the collector is equal to the latitude of the location with angle variations of 10–15° more or less depending on the application [20].

A FPC generally consists of the following components as shown in Fig. 2:

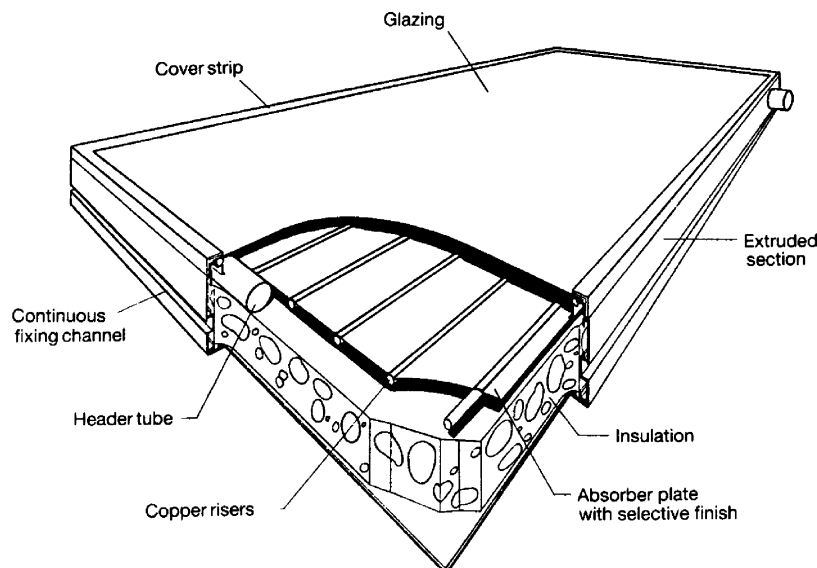


Fig. 1. Pictorial view of a flat-plate collector.

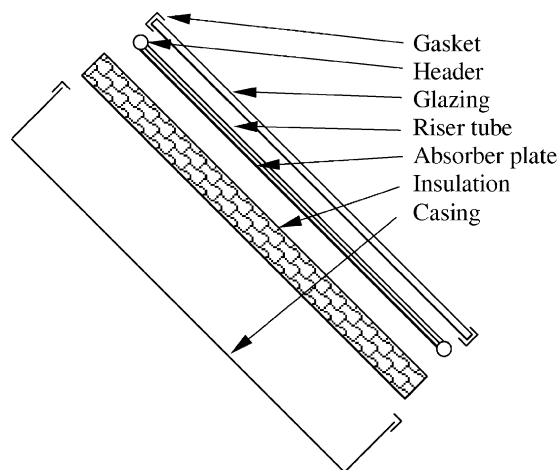


Fig. 2. Exploded view of a flat-plate collector.

Glazing. One or more sheets of glass or other diathermanous (radiation-transmitting) material.

Tubes, fins, or passages. To conduct or direct the heat transfer fluid from the inlet to the outlet.

Absorber plates. Flat, corrugated, or grooved plates, to which the tubes, fins, or passages are attached. The plate may be integral with the tubes.

Headers or manifolds. To admit and discharge the fluid.

Insulation. To minimise the heat loss from the back and sides of the collector.

Container or casing. To surround the aforementioned components and keep them free from dust, moisture, etc.

FPC have been built in a wide variety of designs and from many different materials. They have been used to heat fluids such as water, water plus antifreeze additive, or air. Their major purpose is to collect as much solar energy as possible at the lower possible total cost. The collector should also have a long effective life, despite the adverse effects of the sun's ultraviolet radiation, corrosion and clogging because of acidity, alkalinity or hardness of the heat transfer fluid, freezing of water, or deposition of dust or moisture on the glazing, and breakage of the glazing because of thermal expansion, hail, vandalism or other causes. These causes can be minimised by the use of tempered glass.

More details are given about the glazing and absorber plate materials in Sections 2.1.1.1 and 2.1.1.2, respectively. Most of these details apply also to other types of collectors.

2.1.1.1. Glazing materials. Glass has been widely used to glaze solar collectors because it can transmit as much as 90% of the incoming shortwave solar irradiation while transmitting virtually none of the longwave radiation emitted outward by the absorber plate. Glass with low iron content has a relatively high transmittance for solar radiation (approximately 0.85–0.90 at normal incidence), but its transmittance is essentially zero for the longwave

thermal radiation (5.0–50 μm) emitted by sun-heated surfaces.

Plastic films and sheets also possess high shortwave transmittance, but because most usable varieties also have transmission bands in the middle of the thermal radiation spectrum, they may have longwave transmittances as high as 0.40. Plastics are also generally limited in the temperatures they can sustain without deteriorating or undergoing dimensional changes. Only a few types of plastics can withstand the sun's ultraviolet radiation for long periods. However, they are not broken by hail or stones, and, in the form of thin films, they are completely flexible and have low mass.

The commercially available grades of window and green-house glass have normal incidence transmittances of about 0.87 and 0.85, respectively. For direct radiation, the transmittance varies considerably with the angle of incidence [21].

Antireflective coatings and surface texture can also improve transmission significantly. The effect of dirt and dust on collector glazing may be quite small, and the cleansing effect of an occasional rainfall is usually adequate to maintain the transmittance within 2–4% of its maximum value.

The glazing should admit as much solar irradiation as possible and reduce the upward loss of heat as much as possible. Although glass is virtually opaque to the longwave radiation emitted by collector plates, absorption of that radiation causes an increase in the glass temperature and a loss of heat to the surrounding atmosphere by radiation and convection. These are analysed in more details in Section 3.

Various prototypes of transparently insulated FPC and CPC have been built and tested in the last decade [22,23]. Low cost and high temperature resistant transparent insulating (TI) materials have been developed so that the commercialisation of these collectors becomes feasible. A prototype FPC covered by TI was developed by Benz et al. [24]. It was experimentally proved that the efficiency of the collector was comparable with that of ETC. However, no commercial collectors of this type are available in the market.

2.1.1.2. Collector absorbing plates. The collector plate absorbs as much of the irradiation as possible through the glazing, while losing as little heat as possible upward to the atmosphere and downward through the back of the casing. The collector plates transfer the retained heat to the transport fluid. The absorptance of the collector surface for shortwave solar radiation depends on the nature and colour of the coating and on the incident angle. Usually black colour is used, however various colour coatings have been proposed in Refs. [25–27] mainly for aesthetic reasons.

By suitable electrolytic or chemical treatments, surfaces can be produced with high values of solar radiation absorptance (α) and low values of longwave emittance (ϵ).

Essentially, typical selective surfaces consist of a thin upper layer, which is highly absorbent to shortwave solar radiation but relatively transparent to longwave thermal radiation, deposited on a surface that has a high reflectance and a low emittance for longwave radiation. Selective surfaces are particularly important when the collector surface temperature is much higher than the ambient air temperature. Lately, a low-cost mechanically manufactured selective solar absorber surface method has been proposed [28].

An energy efficient solar collector should absorb incident solar radiation, convert it to thermal energy and deliver the thermal energy to a heat transfer medium with minimum losses at each step. It is possible to use several different design principles and physical mechanisms in order to create a selective solar absorbing surface. Solar absorbers are based on two layers with different optical properties, which are referred as tandem absorbers. A semiconducting or dielectric coating with high solar absorbance and high infrared transmittance on top of a non-selective highly reflecting material such as metal constitutes one type of tandem absorber. Another alternative is to coat a non-selective highly absorbing material with a heat mirror having a high solar transmittance and high infrared reflectance [29].

Today, commercial solar absorbers are made by electroplating, anodization, evaporation, sputtering and by applying solar selective paints. Much of the progress during recent years has been based on the implementation of vacuum techniques for the production of fin type absorbers used in low temperature applications. The chemical and electrochemical processes used for their commercialization were readily taken over from the metal finishing industry. The requirements of solar absorbers used in high temperature applications, however, namely extremely low thermal emittance and high temperature stability, were difficult to fulfil with conventional wet processes. Therefore, large-scale sputter deposition was developed in the late 70s. The vacuum techniques are nowadays mature, characterized by low cost and have the advantage of being less environmentally polluting than the wet processes.

For fluid-heating collectors, passages must be integral with or firmly bonded to the absorber plate. A major problem is obtaining a good thermal bond between tubes and absorber plates without incurring excessive costs for labour or materials. Material most frequently used for collector plates are copper, aluminium, and stainless steel. UV-resistant plastic extrusions are used for low temperature applications. If the entire collector area is in contact with the heat transfer fluid, the thermal conductance of the material is not important.

Fig. 3 shows a number of absorber plate designs for solar water and air heaters that have been used with varying degrees of success [30]. Fig. 3A shows a bonded sheet design, in which the fluid passages are integral with the plate to ensure good thermal conduct between the metal

and the fluid. Fig. 3B and C shows fluid heaters with tubes soldered, brazed, or otherwise fastened to upper or lower surfaces of sheets or strips of copper. Copper tubes are used most often because of their superior resistance to corrosion.

Thermal cement, clips, clamps, or twisted wires have been tried in the search for low-cost bonding methods. Fig. 3D shows the use of extruded rectangular tubing to obtain a larger heat transfer area between tube and plate. Mechanical pressure, thermal cement, or brazing may be used to make the assembly. Soft solder must be avoided because of the high plate temperature encountered at stagnation conditions.

Air or other gases can be heated with FPC, particularly if some type of extended surface (Fig. 3E) is used to counteract the low heat transfer coefficients between metal and air [30]. Metal or fabric matrices (Fig. 3F) [13,30], or thin corrugated metal sheets (Fig. 3G) may be used, with selective surfaces applied to the latter when a high level of performance is required. The principal requirement is a large contact area between the absorbing surface and the air. Various applications of solar air collectors are reported in Refs. [31–37]. A design procedure for solar air heating systems is presented in Ref. [38] whereas the optimisation of the flow passage geometry is presented in Ref. [39].

Reduction of heat loss from the absorber can be accomplished either by a selective surface to reduce radiative heat transfer or by suppressing convection. Francia [40] showed that a honeycomb made of transparent material, placed in the airspace between the glazing and the absorber, was beneficial.

Another category of collectors which is not shown in Fig. 3 is the uncovered or unglazed solar collector [41]. These are usually low-cost units which can offer cost-effective solar thermal energy in applications such as water preheating for domestic or industrial use, heating of swimming pools [42,43], space heating and air heating for industrial or agricultural applications.

FPC are by far the most used type of collector. FPC are usually employed for low temperature applications up to 100 °C, although some new types of collectors employing vacuum insulation and/or TI can achieve slightly higher values [24]. Due to the introduction of highly selective coatings actual standard FPC can reach stagnation temperatures of more than 200 °C. With these collectors good efficiencies can be obtained up to temperatures of about 100 °C.

The characteristics of a typical water FPC are shown in Table 2.

Lately some modern manufacturing techniques have been introduced by the industry like the use of ultrasonic welding machines, which improve both the speed and the quality of welds. This is used for the welding of fins on risers in order to improve heat conduction. The greatest advantage of this method is that the welding is performed at room temperature therefore deformation of the welded parts is avoided. These collectors with selective coating are called

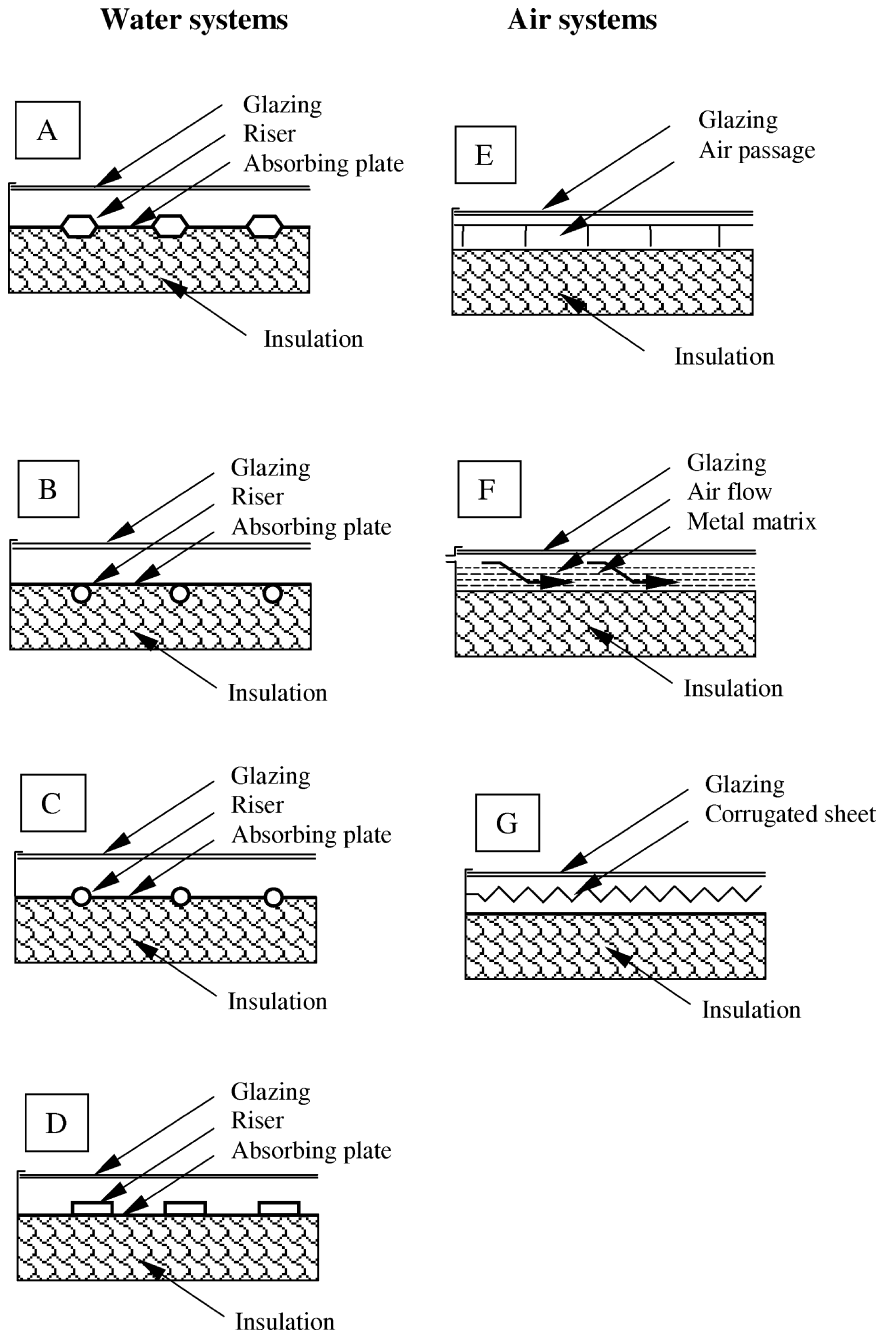


Fig. 3. Various types of flat-plate solar collectors.

advance FPC and the characteristics of a typical type are also shown in Table 2.

2.1.2. Compound parabolic collectors

CPC are non-imaging concentrators. These have the capability of reflecting to the absorber all of the incident radiation within wide limits. Their potential as collectors of solar energy was pointed out by Winston [44]. The necessity

of moving the concentrator to accommodate the changing solar orientation can be reduced by using a trough with two sections of a parabola facing each other, as shown in Fig. 4.

Compound parabolic concentrators can accept incoming radiation over a relatively wide range of angles. By using multiple internal reflections, any radiation that is entering the aperture, within the collector acceptance angle, finds its way to the absorber surface located at the bottom of

Table 2
Characteristics of a typical water FPC system

Parameter	Simple flat plate collector	Advanced flat plate collector
Fixing of risers on the absorber plate	Embedded	Ultrasonically welded
Absorber coating	Black mat paint	Chromium selective coating
Glazing	Low-iron glass	Low-iron glass
Efficiency mode	$nv_s(T_i - T_a)/G$	$nv_s(T_i - T_a)/G$
G_{test} -flow rate per unit area at test conditions (kg/s m ²)	0.015	0.015
c_0 -intercept efficiency	0.79	0.80
c_1 -negative of the first-order coefficient of the efficiency (W/m ² °C)	6.67	4.78
b_0 -incidence angle modifier constant	0.1	0.1
Collector slope angle	Latitude + 5 to 10°	Latitude + 5 to 10°

the collector. The absorber can take a variety of configurations. It can be cylindrical as shown in Fig. 4 or flat. In the CPC shown in Fig. 4 the lower portion of the reflector (AB and AC) is circular, while the upper portions (BD and CE) are parabolic. As the upper part of a CPC contribute little to the radiation reaching the absorber, they are usually truncated thus forming a shorter version of the CPC, which is also cheaper. CPCs are usually covered with glass to avoid dust and other materials from entering the collector and thus reducing the reflectivity of its walls.

These collectors are more useful as linear or trough-type concentrators. The acceptance angle is defined as the angle through which a source of light can be moved and still converge at the absorber. The orientation of a CPC collector is related to its acceptance angle (θ_c , in Fig. 4). Also depending on the collector acceptance angle, the collector can be stationary or tracking. A CPC concentrator can be orientated with its long axis along either the north–south or the east–west direction and its aperture is tilted directly towards the equator at an angle equal to the local latitude. When orientated along the north–south direction the collector must track the sun by turning its axis so as to face the sun continuously. As the acceptance angle of the concentrator along its long axis is wide, seasonal tilt adjustment is not necessary. It can also be stationary but radiation will only be received the hours when the sun is within the collector acceptance angle. When the concentrator is orientated with its long axis along the east–west direction, with a little seasonal adjustment in tilt angle the collector is able to catch the sun's rays effectively through its wide acceptance angle along its long axis. The minimum acceptance angle in this case should be equal to the maximum incidence angle projected in a north–south vertical plane during the times when output is needed from the collector. For stationary CPC collectors mounted in this mode the minimum acceptance angle is equal to 47°. This angle covers the declination of the sun from summer to winter solstices ($2 \times 23.5^\circ$). In practice bigger angles are used to enable the collector to collect diffuse radiation at the expense of a lower concentration ratio. Smaller (less than 3) concentration ratio CPCs are of greatest practical interest.

These according to Pereira [45] are able to accept a large proportion of diffuse radiation incident on their apertures and concentrate it without the need of tracking the sun.

A method to estimate the optical and thermal properties of CPCs is presented in Ref. [46]. In particular, a simple analytic technique was developed for the calculation of the average number of reflections for radiation passing through a CPC, which is useful for computing optical losses. Many numerical examples are presented which are helpful in designing a CPC.

Two basic types of CPC collectors have been designed; the symmetric and the asymmetric. These usually employ two main types of absorbers; fin type with pipe and tubular absorbers [47–50].

Practical design considerations such as the choice of the receiver type, the optimum method for introducing a gap between receiver and reflector to minimise optical and thermal losses and the effect of a glass envelope around the receiver are given in Ref. [51]. Other practical design considerations for CPCs with multichannel and bifacial absorbers are given in Refs. [52] and [53], respectively, whereas design considerations and performance evaluation of cost-effective asymmetric CPCs are given in Ref. [54].

The characteristics of a typical CPC are shown in Table 3.

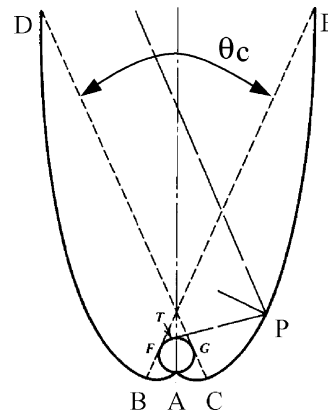


Fig. 4. Schematic diagram of a compound parabolic collector.

Table 3
Characteristics of a typical CPC system

Parameter	Value
F' : collector fin efficiency factor	0.9
U_L : overall loss coefficient of collector per unit aperture area ($W/m^2 \text{ } ^\circ C$)	1.5
ρ_R : reflectivity of walls of CPC	0.85
θ_c : half-acceptance angle of CPC (degrees)	45
Ratio of truncated to full height of CPC	0.67
Axis orientation	Receiver axis is horizontal and in a plane with a slope of 35° (transverse)
a: absorbtance of absorber plate	0.95
N_G : number of cover plates	1
η_R : index of refraction of cover material	1.526
K_L : product of extinction coefficient and the thickness of each cover plate	0.0375
Collector slope angle	(local latitude)

2.1.3. Evacuated tube collectors

Conventional simple flat-plate solar collectors were developed for use in sunny and warm climates. Their benefits however are greatly reduced when conditions become unfavourable during cold, cloudy and windy days. Furthermore, weathering influences such as condensation and moisture will cause early deterioration of internal materials resulting in reduced performance and system failure. Evacuated heat pipe solar collectors (tubes) operate differently than the other collectors available on the market. These solar collectors consist of a heat pipe inside a vacuum-sealed tube, as shown in Fig. 5.

ETC have demonstrated that the combination of a selective surface and an effective convection suppressor can result in good performance at high temperatures [21]. The vacuum envelope reduces convection and conduction losses, so the collectors can operate at higher temperatures than FPC. Like FPC, they collect both direct and diffuse radiation. However, their efficiency is higher at low incidence angles. This effect tends to give ETC an advantage over FPC in day-long performance.

ETC use liquid–vapour phase change materials to transfer heat at high efficiency. These collectors feature a heat pipe (a highly efficient thermal conductor) placed inside a vacuum-sealed tube. The pipe, which is a sealed copper pipe, is then attached to a black copper fin that fills the tube (absorber plate). Protruding from the top of each tube is a metal tip attached to the sealed pipe (condenser). The heat pipe contains a small amount of fluid

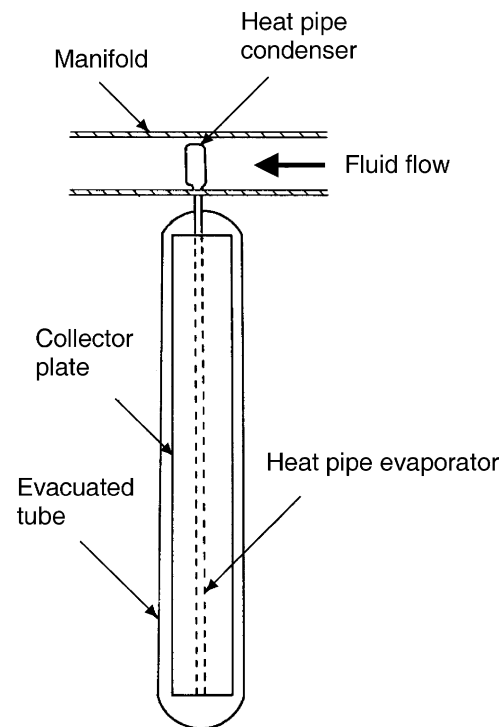


Fig. 5. Schematic diagram of an evacuated tube collector.

(e.g. methanol) that undergoes an evaporating–condensing cycle. In this cycle, solar heat evaporates the liquid, and the vapour travels to the heat sink region where it condenses and releases its latent heat. The condensed fluid return back to the solar collector and the process is repeated. When these tubes are mounted, the metal tips up, into a heat exchanger (manifold) as shown in Fig. 5. Water, or glycol, flows through the manifold and picks up the heat from the tubes. The heated liquid circulates through another heat exchanger and gives off its heat to a process or to water that is stored in a solar storage tank.

Because no evaporation or condensation above the phase-change temperature is possible, the heat pipe offers inherent protection from freezing and overheating. This self-limiting temperature control is a unique feature of the evacuated heat pipe collector.

ETC basically consist of a heat pipe inside a vacuum-sealed tube. A large number of variations of the absorber shape of ETC are on the market [55]. Evacuated tubes with CPC-reflectors are also commercialised by several manufacturers. One manufacturer recently presented an all-glass ETC, which may be an important step to cost reduction and increase of lifetime. Another variation of this type of collector is what is called Dewar tubes. In this two concentric glass tubes are used and the space in between the tubes is evacuated (vacuum jacket). The advantage of this design is that it is made entirely of glass and it is not necessary to penetrate the glass envelope in order to extract

Table 4
Characteristics of a typical ETC system

Parameter	Value
Glass tube diameter	65 mm
Glass thickness	1.6 mm
Collector length	1965 mm
Absorber plate	Copper
Coating	Selective
Absorber area for each collector	0.1 m ²
Efficiency mode	$\eta_{vs}(T_i - T_a)/G$
G_{test} : flow rate per unit area at test conditions (kg/s m ²)	0.014
c_0 : intercept efficiency	0.82
c_1 : negative of the first-order coefficient of the efficiency (W/m ² °C)	2.19
b_0 : incidence angle modifier constant	0.2
Collector slope angle	Latitude +5 to 10°

heat from the tube thus leakage losses are not present and it is also less expensive than the single envelope system [56]. The characteristics of a typical ETC are shown in Table 4.

Another type of collector developed recently is the integrated compound parabolic collector (ICPC). This is an ETC in which at the bottom part of the glass tube a reflective material is fixed [57]. The collector combines the vacuum insulation and non-imaging stationary concentration into a single unit. In another design a tracking ICPC is developed which is suitable for high temperature applications [58].

2.2. Sun tracking concentrating collectors

Energy delivery temperatures can be increased by decreasing the area from which the heat losses occur. Temperatures far above those attainable by FPC can be reached if a large amount of solar radiation is concentrated on a relatively small collection area. This is done by interposing an optical device between the source of radiation and the energy absorbing surface. Concentrating collectors exhibit certain advantages as compared with the conventional flat-plate type [59]. The main ones are:

1. The working fluid can achieve higher temperatures in a concentrator system when compared to a flat-plate system of the same solar energy collecting surface. This means that a higher thermodynamic efficiency can be achieved.
2. It is possible with a concentrator system, to achieve a thermodynamic match between temperature level and task. The task may be to operate thermionic, thermodynamic, or other higher temperature devices.
3. The thermal efficiency is greater because of the small heat loss area relative to the receiver area.
4. Reflecting surfaces require less material and are structurally simpler than FPC. For a concentrating

collector the cost per unit area of the solar collecting surface is therefore less than that of a FPC.

5. Owing to the relatively small area of receiver per unit of collected solar energy, selective surface treatment and vacuum insulation to reduce heat losses and improve the collector efficiency are economically viable.

Their disadvantages are:

1. Concentrator systems collect little diffuse radiation depending on the concentration ratio.
2. Some form of tracking system is required so as to enable the collector to follow the sun.
3. Solar reflecting surfaces may lose their reflectance with time and may require periodic cleaning and refurbishing.

Many designs have been considered for concentrating collectors. Concentrators can be reflectors or refractors, can be cylindrical or parabolic and can be continuous or segmented. Receivers can be convex, flat, cylindrical or concave and can be covered with glazing or uncovered. Concentration ratios, i.e. the ratio of aperture to absorber areas, can vary over several orders of magnitude, from as low as unity to high values of the order of 10 000. Increased ratios mean increased temperatures at which energy can be delivered but consequently these collectors have increased requirements for precision in optical quality and positioning of the optical system.

Because of the apparent movement of the sun across the sky, conventional concentrating collectors must follow the sun's daily motion. There are two methods by which the sun's motion can be readily tracked. The first is the altazimuth method which requires the tracking device to turn in both altitude and azimuth, i.e. when performed properly, this method enables the concentrator to follow the sun exactly. Paraboloidal solar collectors generally use this system. The second one is the one-axis tracking in which the collector tracks the sun in only one direction either from east to west or from north to south. Parabolic trough collectors (PTC) generally use this system. These systems require continuous and accurate adjustment to compensate for the changes in the sun's orientation. Relations on how to estimate the angle of incidence of solar radiation for these tracking modes are given in Section 3.2.

The first type of a solar concentrator, shown in Fig. 6, is effectively a FPC fitted with simple flat reflectors which can markedly increase the amount of direct radiation reaching the collector. This is a concentrator because the aperture is bigger than the absorber but the system is stationary. A comprehensive analysis of such a system is presented in Ref. [60]. The model facilitates the prediction of the total energy absorbed by the collector at any hour of the day for any latitude for random tilt angles and azimuth angles of the collector and reflectors. This simple enhancement of FPC was initially suggested by Tabor in 1966 [61].

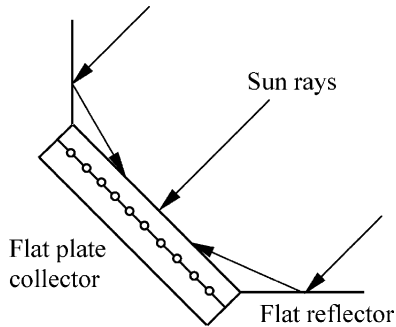


Fig. 6. Flat plate collector with flat reflectors.

Other important studies on this area were presented by Seitel [62] and Perers et al. [63].

Another type of collector, already covered under the stationary collectors, the CPC is also classified as concentrator. This, depending on the acceptance angle, can be stationary or tracking. When tracking is used this is very rough or intermitted as concentration ratio is usually small and radiation can be collected and concentrated by one or more reflections on the parabolic surfaces.

As was seen above one disadvantage of concentrating collectors is that, except at low concentration ratios, they can use only the direct component of solar radiation, because the diffuse component cannot be concentrated by most types. However, an additional advantage of concentrating collectors is that, in summer, when the sun rises well to the north of the east–west line, the sun-follower, with its axis oriented north–south, can begin to accept radiation directly from the sun long before a fixed, south-facing flat-plate can receive anything other than diffuse radiation from the portion of the sky that it faces. Thus, in relatively cloudless areas, the concentrating collector may capture more radiation per unit of aperture area than a FPC.

In concentrating collectors solar energy is optically concentrated before being transferred into heat. Concentration can be obtained by reflection or refraction of solar radiation by the use of mirrors or lens. The reflected or refracted light is concentrated in a focal zone, thus increasing the energy flux in the receiving target. Concentrating collectors can also be classified into non-imaging

and imaging depending on whether the image of the sun is focused at the receiver or not. The concentrator belonging in the first category is the CPC whereas all the other types of concentrators belong to the imaging type.

The collectors falling in this category are:

1. Parabolic trough collector;
2. Linear Fresnel reflector (LFR);
3. Parabolic dish;
4. Central receiver.

2.2.1. Parabolic trough collectors

In order to deliver high temperatures with good efficiency a high performance solar collector is required. Systems with light structures and low cost technology for process heat applications up to 400 °C could be obtained with parabolic through collectors (PTCs). PTCs can effectively produce heat at temperatures between 50 and 400 °C.

PTCs are made by bending a sheet of reflective material into a parabolic shape. A metal black tube, covered with a glass tube to reduce heat losses, is placed along the focal line of the receiver (Fig. 7). When the parabola is pointed towards the sun, parallel rays incident on the reflector are reflected onto the receiver tube. It is sufficient to use a single axis tracking of the sun and thus long collector modules are produced. The collector can be orientated in an east–west direction, tracking the sun from north to south, or orientated in a north–south direction and tracking the sun from east to west. The advantages of the former tracking mode is that very little collector adjustment is required during the day and the full aperture always faces the sun at noon time but the collector performance during the early and late hours of the day is greatly reduced due to large incidence angles (cosine loss). North–south orientated troughs have their highest cosine loss at noon and the lowest in the mornings and evenings when the sun is due east or due west.

Over the period of one year, a horizontal north–south trough field usually collects slightly more energy than a horizontal east–west one. However, the north–south field collects a lot of energy in summer and much less in winter. The east–west field collects more energy in the winter than a north–south field and less in summer, providing a more

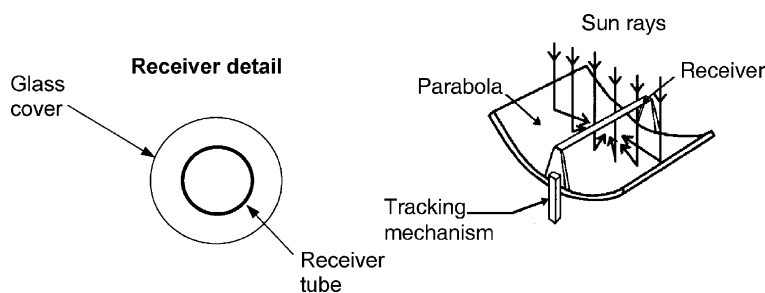


Fig. 7. Schematic of a parabolic trough collector.

constant annual output. Therefore, the choice of orientation usually depends on the application and whether more energy is needed during summer or during winter [64].

Parabolic trough technology is the most advanced of the solar thermal technologies because of considerable experience with the systems and the development of a small commercial industry to produce and market these systems. PTCs are built in modules that are supported from the ground by simple pedestals at either end.

PTCs are the most mature solar technology to generate heat at temperatures up to 400 °C for solar thermal electricity generation or process heat applications. The biggest application of this type of system is the Southern California power plants, known as solar electric generating systems (SEGS), which have a total installed capacity of 354 MW_e [65]. More details on this system are given in Section 5.6.1. Another important application of this type of collector is installed at Plataforma Solar de Almeria (PSA) in Southern Spain mainly for experimental purposes. The total installed capacity of the PTCs is equal to 1.2 MW [66].

The receiver of a parabolic trough is linear. Usually, a tube is placed along the focal line to form an external surface receiver (Fig. 7). The size of the tube, and therefore the concentration ratio, is determined by the size of the reflected sun image and the manufacturing tolerances of the trough. The surface of the receiver is typically plated with selective coating that has a high absorptance for solar radiation, but a low emittance for thermal radiation loss.

A glass cover tube is usually placed around the receiver tube to reduce the convective heat loss from the receiver, thereby further reducing the heat loss coefficient. A disadvantage of the glass cover tube is that the reflected light from the concentrator must pass through the glass to reach the absorber, adding a transmittance loss of about 0.9, when the glass is clean. The glass envelope usually has an antireflective coating to improve transmissivity. One way to further reduce convective heat loss from the receiver tube and thereby increase the performance of the collector, particularly for high temperature applications, is to evacuate the space between the glass cover tube and the receiver.

In order to achieve cost effectiveness in mass production, not only the collector structure must feature a high stiffness to weight ratio so as to keep the material content to a minimum, but also the collector structure must be amenable to low-labour manufacturing processes. A number of structural concepts have been proposed such as steel framework structures with central torque tubes or double V-trusses, or fibreglass [67]. A recent development in this type of collectors is the design and manufacture of EuroTrough, a new PTC, in which an advance lightweight structure is used to achieve cost efficient solar power generation [68,69]. Based on environmental test data to date, mirrored glass appears to be the preferred mirror material although self-adhesive reflective materials with 5–7 years life exists in the market.

The design of this type of collector is given in a number of publications. The optimization of the collector aperture

and rim angle is given in Ref. [59]. Design of other aspects of the collector is given in Refs. [70,71].

A tracking mechanism must be reliable and able to follow the sun with a certain degree of accuracy, return the collector to its original position at the end of the day or during the night, and also track during periods of intermittent cloud cover. Additionally, tracking mechanisms are used for the protection of collectors, i.e. they turn the collector out of focus to protect it from the hazardous environmental and working conditions, like wind gust, overheating and failure of the thermal fluid flow mechanism. The required accuracy of the tracking mechanism depends on the collector acceptance angle. This is described in detail in Section 4.3.

Various forms of tracking mechanisms, varying from complex to very simple, have been proposed. They can be divided into two broad categories, namely mechanical [72–74] and electrical/electronic systems. The electronic systems generally exhibit improved reliability and tracking accuracy. These can be further subdivided into the following:

1. Mechanisms employing motors controlled electronically through sensors, which detect the magnitude of the solar illumination [75–77].
2. Mechanisms using computer controlled motors with feedback control provided from sensors measuring the solar flux on the receiver [78–80].

A tracking mechanism developed by the author uses three light dependent resistors which detect the focus, sun/cloud, and day or night conditions and give instruction to a DC motor through a control system to focus the collector, to follow approximately the sun path when cloudy conditions exist and return the collector to the east during night. More details are given in Ref. [81].

New developments in the field of PTC aim at cost reduction and improvements of the technology. In one system the collector can be washed automatically thus reducing drastically the maintenance cost.

After a period of research and commercial development of the PTC in the 80s a number of companies entered into the field producing this type of collectors, for the temperature range between 50 and 300 °C, all of them with one-axis tracking. One such example is the solar collector produced by the Industrial Solar Technology (IST) Corporation. IST erected several process heat installations in the United States with up to 2700 m² of collector aperture area [82].

The IST parabolic trough has thoroughly been tested and evaluated by Sandia [83] and the German Aerospace Centre (DLR) [82] for efficiency and durability. Improvements of the optical performance, which recently have been discussed [84], would lead to a better incident angle modifier and a higher optical efficiency.

The characteristics of the IST collector system are shown in Table 5.

Table 5
Characteristics of the IST PTC system

Parameter	Value/type
Collector rim angle	70°
Reflective surface	Silvered acrylic
Receiver material	Steel
Collector aperture	2.3 m
Receiver surface treatment	Highly selective blackened nickel
Absorptance	0.97
Emittance (80 °C)	0.18
Glass envelope transmittance	0.96
Absorber outside diameter	50.8 mm
G_{test} : flow rate per unit area at test conditions (kg/s m ²)	0.015
k_0 : intercept efficiency	0.762
k_1 : negative of the first-order coefficient of the efficiency (W/m ² °C)	0.2125
k_2 : negative of the second-order coefficient of the efficiency (W/m ² °C ²)	0.001672
b_0 : incidence angle modifier constant	0.958
b_1 : incidence angle modifier constant	-0.298
Tracking mechanism accuracy	0.05°
Collector orientation	Axis in N–S direction
Mode of tracking	E–W horizontal

2.2.2. Linear Fresnel reflector

LFR technology relies on an array of linear mirror strips which concentrate light on to a fixed receiver mounted on a linear tower. The LFR field can be imagined as a broken-up parabolic trough reflector (Fig. 8), but unlike parabolic troughs, it does not have to be of parabolic shape, large absorbers can be constructed and the absorber does not have to move. A representation of an element of an LFR collector field is shown in Fig. 9. The greatest advantage of this type of system is that it uses flat or elastically curved reflectors which are cheaper compared to parabolic glass reflectors. Additionally, these are mounted close to the ground, thus minimizing structural requirements.

The first to apply this principle was the great solar pioneer Giorgio Francia [85] who developed both linear

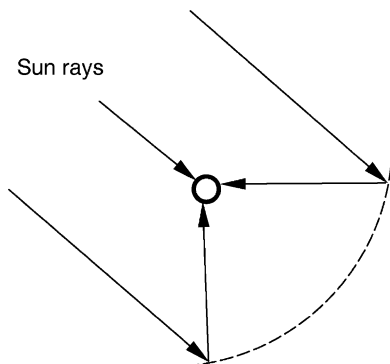


Fig. 8. Fresnel type parabolic trough collector.

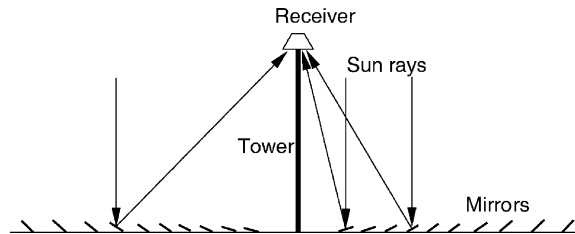


Fig. 9. Schematic diagram of a downward facing receiver illuminated from an LFR field.

and two-axis tracking Fresnel reflector systems at Genoa, Italy in the 60s. These systems showed that elevated temperatures could be reached using such systems but he moved on to two-axis tracking, possibly because advanced selective coatings and secondary optics were not available [86]. Two of the early published works on this area are given in Refs. [87,88], whereas some later papers are given in Refs. [89,90].

In 1979, the FMC Corporation produced a detailed project design study for 10 and 100 MW_e LFR power plants for the Department of Energy (DOE) of the US. The larger plant would have used a 1.68 km linear cavity absorber mounted on 61 m towers. The project however was never put into practice as it ran out of DOE funding [86].

A latter effort to produce a tracking LFR was made by the Israeli Paz company in the early 90s by Feuermann and Gordon [91]. This used an efficient secondary CPC-like optics and an evacuated tube absorber.

One difficulty with the LFR technology is that avoidance of shading and blocking between adjacent reflectors leads to increased spacing between reflectors. Blocking can be reduced by increasing the height of the absorber towers, but this increases cost. Compact linear Fresnel reflector (CLFR) technology has been recently developed at Sydney University in Australia. This is in effect a second type of solution for the Fresnel reflector field problem which has been overlooked until recently. In this design adjacent linear elements can be interleaved to avoid shading. The classical LFR system has only one receiver, and there is no choice about the direction and orientation of a given reflector. However, if it is assumed that the size of the field will be large, as it must be in technology supplying electricity in the MW class, it is reasonable to assume that there will be many towers in the system. If they are close enough then individual reflectors have the option of directing reflected solar radiation to at least two towers. This additional variable in the reflector orientation provides the means for much more densely packed arrays, because patterns of alternating reflector orientation can be such that closely packed reflectors can be positioned without shading and blocking [86]. The interleaving of mirrors between two receiving towers is shown in Fig. 10. The arrangement minimizes beam blocking by adjacent reflectors and allows high reflector densities and low tower heights to be used. Close spacing of reflectors reduces land usage but this is in many cases not a serious issue

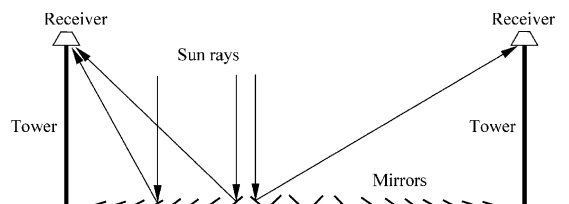


Fig. 10. Schematic diagram showing interleaving of mirrors in a CLFR with reduced shading between mirrors.

as in deserts. The avoidance of large reflector spacing and tower heights is an important cost issue when the cost of ground preparation, array substructure cost, tower structure cost, steam line thermal losses and steam line cost are considered. If the technology is to be located in an area with limited land availability such as in urban areas or next to existing power plants, high array ground coverage can lead to maximum system output for a given ground area [86].

2.2.3. Parabolic dish reflector (PDR)

A parabolic dish reflector, shown schematically in Fig. 11, is a point-focus collector that tracks the sun in two axes, concentrating solar energy onto a receiver located at the focal point of the dish. The dish structure must track fully the sun to reflect the beam into the thermal receiver. For this purpose tracking mechanisms similar to the ones described in previous section are employed in double so as the collector is tracked in two axes.

The receiver absorbs the radiant solar energy, converting it into thermal energy in a circulating fluid. The thermal energy can then either be converted into electricity using an engine-generator coupled directly to the receiver, or it can be transported through pipes to a central power-conversion system. Parabolic-dish systems can achieve temperatures in excess of 1500 °C. Because the receivers are distributed throughout a collector field, like parabolic troughs, parabolic dishes are often called distributed-receiver systems.

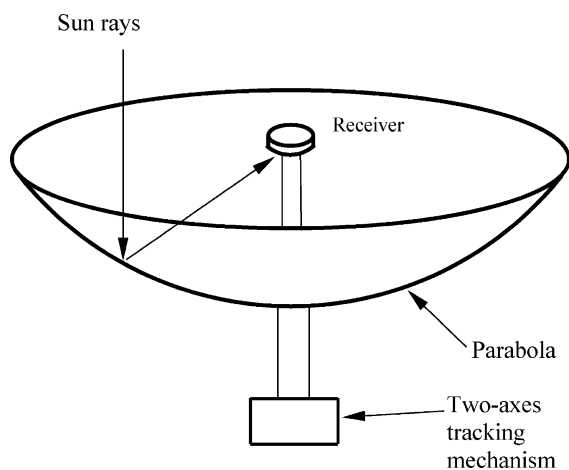


Fig. 11. Schematic of a parabolic dish collector.

Parabolic dishes have several important advantages:

1. Because they are always pointing the sun, they are the most efficient of all collector systems;
2. They typically have concentration ratio in the range of 600–2000, and thus are highly efficient at thermal-energy absorption and power conversion systems;
3. They have modular collector and receiver units that can either function independently or as part of a larger system of dishes.

The main use of this type of concentrator is for parabolic dish engines. A parabolic dish-engine system is an electric generator that uses sunlight instead of crude oil or coal to produce electricity. The major parts of a system are the solar dish concentrator and the power conversion unit. More details on this system are given in Section 5.6.3.

Parabolic-dish systems that generate electricity from a central power converter collect the absorbed sunlight from individual receivers and deliver it via a heat-transfer fluid to the power-conversion systems. The need to circulate heat-transfer fluid throughout the collector field raises design issues such as piping layout, pumping requirements, and thermal losses.

Systems that employ small generators at the focal point of each dish provide energy in the form of electricity rather than as heated fluid. The power conversion unit includes the thermal receiver and the heat engine. The thermal receiver absorbs the concentrated beam of solar energy, converts it to heat, and transfers the heat to the heat engine. A thermal receiver can be a bank of tubes with a cooling fluid circulating through it. The heat transfer medium usually employed as the working fluid for an engine is hydrogen or helium. Alternate thermal receivers are heat pipes wherein the boiling and condensing of an intermediate fluid is used to transfer the heat to the engine. The heat engine system takes the heat from the thermal receiver and uses it to produce electricity. The engine-generators have several components; a receiver to absorb the concentrated sunlight to heat the working fluid of the engine, which then converts the thermal energy into mechanical work; an alternator attached to the engine to convert the work into electricity, a waste-heat exhaust system to vent excess heat to the atmosphere, and a control system to match the engine's operation to the available solar energy. This distributed parabolic dish system lacks thermal storage capabilities, but can be hybridised to run on fossil fuel during periods without sunshine. The Stirling engine is the most common type of heat engine used in dish-engine systems. Other possible power conversion unit technologies that are evaluated for future applications are microturbines and concentrating photovoltaics [92].

2.2.4. Heliostat field collector

For extremely high inputs of radiant energy, a multiplicity of flat mirrors, or heliostats, using altazimuth mounts,

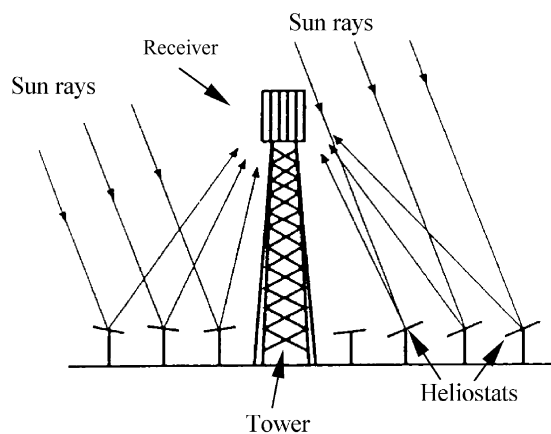


Fig. 12. Schematic of central receiver system.

can be used to reflect their incident direct solar radiation onto a common target as shown in Fig. 12. This is called the heliostat field or central receiver collector. By using slightly concave mirror segments on the heliostats, large amounts of thermal energy can be directed into the cavity of a steam generator to produce steam at high temperature and pressure.

The concentrated heat energy absorbed by the receiver is transferred to a circulating fluid that can be stored and later used to produce power. Central receivers have several advantages:

1. They collect solar energy optically and transfer it to a single receiver, thus minimizing thermal-energy transport requirements;
2. They typically achieve concentration ratios of 300–1500 and so are highly efficient both in collecting energy and in converting it to electricity;
3. They can conveniently store thermal energy;
4. They are quite large (generally more than 10 MW) and thus benefit from economies of scale.

Each heliostat at a central-receiver facility has from 50 to 150 m² of reflective surface. The heliostats collect and concentrate sunlight onto the receiver, which absorbs the concentrated sunlight, transferring its energy to a heat-transfer fluid. The heat-transport system, which consists primarily of pipes, pumps, and valves, directs the transfer fluid in a closed loop between the receiver, storage, and power-conversion systems. A thermal-storage system typically stores the collected energy as sensible heat for later delivery to the power-conversion system. The storage system also decouples the collection of solar energy from its conversion to electricity. The power-conversion system consists of a steam generator, turbine generator, and support equipment, which convert the thermal energy into electricity and supply it to the utility grid.

In this case incident sunrays are reflected by large tracking mirrored collectors, which concentrate the energy flux towards radiative/convective heat exchangers, where energy is transferred to a working thermal fluid. After

energy collection by the solar system, the conversion of thermal energy to electricity has many similarities with the conventional fossil-fuelled thermal power plants [93].

The average solar flux impinging on the receiver has values between 200 and 1000 kW/m². This high flux allows working at relatively high temperatures of more than 1500 °C and to integrate thermal energy in more efficient cycles. Central receiver systems can easily integrate in fossil-fuelled plants for hybrid operation in a wide variety of options and have the potential to operate more than half the hours of each year at nominal power using thermal energy storage.

Central receiver systems are considered to have a large potential for mid-term cost reduction of electricity compared to parabolic trough technology since they allow many intermediate steps between the integration in a conventional Rankine cycle up to the higher energy cycles using gas turbines at temperatures above 1000 °C, and this subsequently leads to higher efficiencies and larger throughputs [94,95]. Another alternative is to use Brayton cycle turbines, which require higher temperature than the ones employed in Rankine cycle.

There are three general configurations for the collector and receiver systems. In the first, heliostats completely surround the receiver tower, and the receiver, which is cylindrical, has an exterior heat-transfer surface. In the second, the heliostats are located north of the receiver tower (in the northern hemisphere), and the receiver has an enclosed heat-transfer surface. In the third, the heliostats are located north of the receiver tower, and the receiver, which is a vertical plane, has a north-facing heat-transfer surface.

In the final analysis, however, it is the selection of the heat-transfer fluid, thermal-storage medium, and power-conversion cycle that defines a central-receiver plant. The heat-transfer fluid may either be water/steam, liquid sodium, or molten nitrate salt (sodium nitrate/potassium nitrate), whereas the thermal-storage medium may be oil mixed with crushed rock, molten nitrate salt, or liquid sodium. All rely on steam-Rankine power-conversion systems, although a more advanced system has been proposed that would use air as the heat-transfer fluid, ceramic bricks for thermal storage, and either a steam-Rankine or open-cycle Brayton power-conversion system.

3. Thermal analysis of collectors

In this section the thermal analysis of the collectors is presented. The two major types of collectors, i.e. flat-plate and concentrating are examined separately. The basic parameter to consider is the collector thermal efficiency. This is defined as the ratio of the useful energy delivered to the energy incident on the collector aperture. The incident solar flux consists of direct and diffuse radiation. While FPC can collect both, concentrating collectors can only

utilise direct radiation if the concentration ratio is greater than 10 [96].

3.1. Flat-plate collectors performance

In this section various relations that are required in order to determine the useful energy collected and the interaction of the various constructional parameters on the performance of a collector are presented.

Under steady-state conditions, the useful heat delivered by a solar collector is equal to the energy absorbed by the heat transfer fluid minus the direct or indirect heat losses from the surface to the surroundings. The useful energy collected from a collector can be obtained from the following formula:

$$q_u = A_c[G_t\tau\alpha - U_L(T_p - T_a)] = mc_p[T_o - T_i] \quad (1)$$

Eq. (1) can be modified by substituting inlet fluid temperature (T_i) for the average plate temperature (T_p), if a suitable correction factor is included. The resulting equation is

$$q_u = A_c F_R [G_t(\tau\alpha) - U_L(T_i - T_a)] \quad (2)$$

where F_R is the correction factor, or collector heat removal factor.

Heat removal factor can be considered as the ratio of the heat actually delivered to that delivered if the collector plate were at uniform temperature equal to that of the entering fluid. In Eq. (2) the temperature T_i of the inlet fluid depends on the characteristics of the complete solar heating system and the hot water demand or heat demand of the building. However, F_R is affected only by the solar collector characteristics, the fluid type, and the fluid flow rate through the collector. F_R may be obtained from Ref. [97]

$$F_R = \frac{mc_p}{A_c U_L} \left(1 - \exp \left[\frac{U_L F' A_c}{mc_p} \right] \right) \quad (3)$$

where F' is the collector efficiency factor. It represents the ratio of the actual useful energy gain that would result if the collector-absorbing surface had been at the local fluid temperature.

The collector efficiency factor can be calculated by considering the temperature distribution between two pipes of the collector absorber and by assuming that the temperature gradient in the flow direction is negligible [97]. This analysis can be performed by considering the sheet tube configuration shown in Fig. 13, where the distance between the tubes is W , the tube diameter is D , and the sheet thickness is δ . As the sheet metal is usually made from copper or aluminum which are good conductors of heat, the temperature gradient through the sheet is negligible, therefore the region between the centerline separating the tubes and the tube base can be considered as a classical fin problem.

The fin, shown in Fig. 13(a) is of length $L = (W - D)/2$. An elemental region of width Δx and unit length in the flow direction is shown in Fig. 13(b). An energy balance on this element gives

$$S \Delta x - U_L \Delta x (T - T_a) + \left(-k\delta \frac{dT}{dx} \right) \Big|_x - \left(-k\delta \frac{dT}{dx} \right) \Big|_{x+\Delta x} = 0 \quad (4)$$

where S is the absorbed solar energy. By dividing through with Δx and finding the limit as Δx approaches zero, gives:

$$\frac{d^2 T}{dx^2} = \frac{U_L}{k\delta} \left(T - T_a - \frac{S}{U_L} \right) \quad (5)$$

The two boundary conditions necessary to solve this second-order differential equation are:

$$\frac{dT}{dx} \Big|_{x=0} = 0, \quad \text{and} \quad T \Big|_{x=L} = T_b$$

For convenience the following two variables are defined:

$$m = \sqrt{\frac{U_L}{k\delta}} \quad (6)$$

$$\Psi = T - T_a - \frac{S}{U_L} \quad (7)$$

Therefore, Eq. (5) becomes

$$\frac{d^2 \Psi}{dx^2} - m^2 \Psi = 0 \quad (8)$$

which has the boundary conditions:

$$\frac{d\Psi}{dx} \Big|_{x=0} = 0 \quad \text{and} \quad \Psi \Big|_{x=L} = T_b - T_a - \frac{S}{U_L}$$

Eq. (8) is a second-order homogeneous linear differential equation whose general solution is:

$$\Psi = C_1 e^{mx} + C_2 e^{-mx} = C_1 \sinh(mx) + C_2 \cosh(mx) \quad (9)$$

The first boundary yields $C_1 = 0$, and the second boundary condition yields:

$$\Psi = T_b - T_a - \frac{S}{U_L} = C_2 \cosh(mL) \quad \text{or}$$

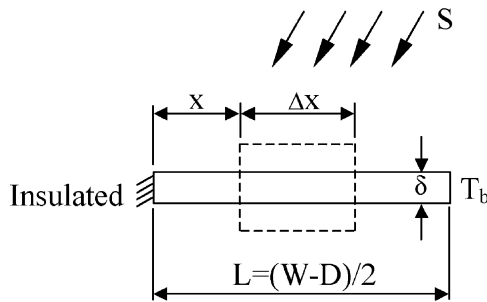
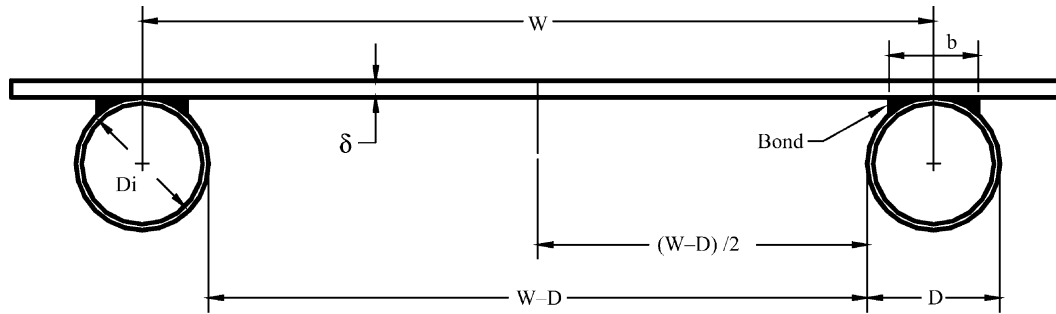
$$C_2 = \frac{T_b - T_a - S/U_L}{\cosh(mL)}$$

With C_1 and C_2 known, Eq. (9) becomes:

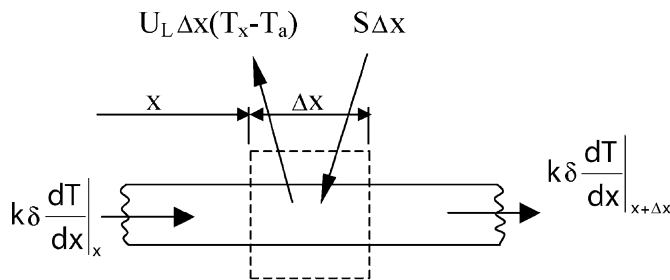
$$\frac{T - T_a - S/U_L}{T_b - T_a - S/U_L} = \frac{\cosh(mx)}{\cosh(mL)} \quad (10)$$

This equation gives the temperature distribution in the x -direction at any given y .

The energy conducted to the region of the tube per unit length in the flow direction can be found by evaluating



(a) Energy balance for the fin element



(b) Energy balance for the tube element

Fig. 13. Flat-plate sheet and tube configuration.

the Fourier's law at the fin base:

$$q'_{fin} = -k\delta \frac{dT}{dx} \Big|_{x=L} = \frac{k\delta m}{U_L} [S - U_L(T_b - T_a)] \tanh(mL) \quad (11)$$

but $k\delta m/U_L$ is just $1/m$. Eq. (11) accounts for the energy collected on only one side of the tube; for both sides, the energy collection is

$$q'_{fin} = (W - D)[S - U_L(T_b - T_a)] \frac{\tanh[m(W - D)/2]}{m(W - D)/2} \quad (12)$$

or with the help of fin efficiency

$$q'_{fin} = (W - D)F[S - U_L(T_b - T_a)] \quad (13)$$

where factor F in Eq. (13) is the standard fin efficiency for straight fins with rectangular profile, obtained from:

$$F = \frac{\tanh[m(W - D)/2]}{m(W - D)/2} \quad (14)$$

The useful gain of the collector also includes the energy collected above the tube region. This is given by:

$$q'_{tube} = D[S - U_L(T_b - T_a)] \quad (15)$$

Accordingly, the useful energy gain per unit length in the direction of the fluid flow is:

$$q'_u = q'_{fin} + q'_{tube} = [(W - D)F + D][S - U_L(T_b - T_a)] \quad (16)$$

This energy must be ultimately transferred to the fluid, which can be expressed in terms of two resistances as:

$$q'_u = \frac{T_b - T_f}{\frac{1}{h_{fi}\pi D_i} + \frac{1}{C_b}} \quad (17)$$

In Eq. (17), C_b is the bond conductance which can be estimated from knowledge of the bond thermal conductivity k_b , the average bond thickness γ , and the bond width b . The bond conductance on a per unit length basis is given by:

$$C_b = \frac{k_b b}{\gamma} \quad (18)$$

The bond conductance can be very important in accurately describing the collector performance and generally it is necessary to have good metal-to-metal contact so that the bond conductance is greater than 30 W/m K and preferably the tube should be welded to the fin.

Solving Eq. (17) for T_b , substituting it into Eq. (16) and solving the result for the useful gain, we get

$$q'_u = WF'[S - U_L(T_f - T_a)] \quad (19)$$

where the collector efficiency factor F' is given by:

$$F' = \frac{\frac{1}{U_L}}{W \left[\frac{1}{U_L[D + (W - D)F]} + \frac{1}{C_b} + \frac{1}{\pi D_i h_{fi}} \right]} \quad (20)$$

A physical interpretation of F' is that it represents the ratio of the actual useful energy gain to the useful energy gain that would result if the collector absorbing surface had been at the local fluid temperature. It should be noted that the denominator of Eq. (20) is the heat transfer resistance from the fluid to the ambient air. This resistance can be represented as $1/U_o$. Therefore, another interpretation of F' is:

$$F' = \frac{U_o}{U_L} \quad (21)$$

The collector efficiency factor is essentially a constant factor for any collector design and fluid flow rate. The ratio of U_L to C_b , the ratio of U_L to h_{fi} , and the fin efficiency F are the only variables appearing in Eq. (20) that may be functions of temperature. For most collector designs F is the most important of these variables in determining F' . The factor F' is a function of U_L and h_{fi} , each of which has some temperature dependence, but it is not a strong function of temperature. Additionally, the collector efficiency factor decreases with increased tube center-to-center distances and increases with increases in both material thicknesses and thermal conductivity. Increasing the overall loss coefficient decreases F' while increasing the fluid-tube heat transfer coefficient increases F' .

The overall heat loss coefficient is a complicated function of the collector construction and its operating conditions and it is given by the following expression

$$U_L = U_t + U_b + U_c \quad (22)$$

i.e. it is the heat transfer resistance from the absorber plate to the ambient air.

In addition to serving as a heat trap by admitting shortwave solar radiation and retaining longwave thermal radiation, the glazing also reduces heat loss by convection. The insulating effect of the glazing is enhanced by the use of several sheets of glass, or glass plus plastic. The top loss coefficient in Eq. (22) is given by [98]:

$$U_t = \frac{1}{\frac{N_g}{\frac{C}{T_p} \left[\frac{T_{av} - T_a}{N_g + f} \right]^{0.33} + \frac{1}{h_w}} + \frac{\sigma(T_{av}^2 + T_a^2)(T_{av} + T_a)}{\frac{1}{\epsilon_p + 0.05N_g(1 - \epsilon_p)} + \frac{2N_g + f - 1}{\epsilon_g} - N_g} \quad (23)$$

where

$$h_w = 5.7 + 3.8W \quad (24)$$

$$f = (1 - 0.04h_w + 0.0005h_w^2)(1 + 0.091N_g) \quad (25)$$

$$C = 365.9(1 - 0.00883\beta + 0.0001298\beta^2) \quad (26)$$

and T_p is the collector stagnation temperature, i.e. the temperature of the absorbing plate when the flow rate is equal to zero, and is obtained from:

$$T_p = \frac{G_t(\tau\alpha)}{U_L} + T_a \quad (27)$$

As usually good insulation is used in the collector construction, the loss coefficient for the bottom and edges of the collector, U_b and U_c , in Eq. (22) is constant, and its estimation is straightforward. The heat loss from the back of the plate rarely exceeds 10% of the upward loss.

The overall transmittance-absorptance product ($\tau\alpha$) is determined as:

$$(\tau\alpha) = \frac{I_{bT}(\tau\alpha)_b + I_d \left(\frac{1 + \cos \beta}{2} \right) (\tau\alpha)_s + \rho I \left(\frac{1 - \cos \beta}{2} \right) (\tau\alpha)_g}{I} \quad (28)$$

Finally, the collector efficiency can be obtained by dividing q_u by $(G_t A_c)$. Therefore,

$$n = F_R \left[\tau\alpha - \frac{U_L(T_i - T_a)}{G_t} \right] \quad (29)$$

For incident angles below about 35°, the product τ times α is essentially constant and Eqs. (2) and (29) are linear with respect to the parameter $(T_i - T_a)/G_t$, as long as U_L remains constant.

3.2. Concentrating collectors performance

For concentrating collector both optical and thermal analyses are required.

3.2.1. Optical analysis

The concentration ratio (C) is defined as the ratio of the aperture area to the receiver/absorber area, i.e.

$$C = \frac{A_a}{A_r} \quad (30)$$

For FPC with no reflectors, $C = 1$. For concentrators C is always greater than 1. For a single axis tracking collector the maximum possible concentration is given by [1,97]:

$$C_{\max} = \frac{1}{\sin(\theta_m)} \quad (31)$$

and for two-axes tracking collector [1,97]

$$C_{\max} = \frac{1}{\sin^2(\theta_m)} \quad (32)$$

where θ_m is the half acceptance angle. The half acceptance angle denotes coverage of one-half of the angular zone within which radiation is accepted by the concentrator's receiver. Radiation is accepted over an angle of $2\theta_m$ because radiation incident within this angle reaches the receiver after passing through the aperture. This angle describes the angular field within which radiation can be collected by the receiver without having to track the concentrator.

Eqs. (31) and (32) define the upper limit of concentration that may be obtained for a given collector viewing angle. For a stationary CPC the angle θ_m depends on the motion of the sun in the sky. For example, for a CPC having its axis in a N–S direction and tilted from the horizontal such that the plane of the sun's motion is normal to the aperture, the acceptance angle is related to the range of hours over which sunshine collection is required, e.g. for 6 h of useful sunshine collection $2\theta_m = 90^\circ$ (sun travels $15^\circ/\text{h}$). In this case $C_{\max} = 1/\sin(45^\circ) = 1.41$.

For a tracking collector θ_m is limited by the size of the sun's disk, small scale errors and irregularities of the reflector surface and tracking errors. For a perfect collector and tracking system C_{\max} depends only on the sun's disk which has a width of 0.53° ($32'$) [97]. Therefore,

$$\text{For single axis tracking: } C_{\max} = 1/\sin(16') = 216$$

$$\text{For full tracking: } C_{\max} = 1/\sin^2(16') = 46\,747$$

It can, therefore, be concluded that the concentration ratio for moving collectors is much higher. However, high accuracy of the tracking mechanism and careful construction of the collector is required with increased concentration ratio as θ_m is very small. In practice, due to various errors, much lower values than the above maximum ones are employed.

Another factor that needs to be determined is the incidence angle for the various modes of tracking. This can be about a single axis or about two axes. In the case of single axis mode the motion can be in various ways, i.e. east–west, north–south or parallel to the earth's axis.

The mode of tracking affects the amount of incident radiation falling on the collector surface in proportion to

Table 6

Comparison of energy absorbed for various modes of tracking

Tracking mode	Solar energy (kW h/m ²)			Percent to full tracking		
	E	SS	WS	E	SS	WS
Full tracking	8.43	10.60	5.70	100.0	100.0	100.0
E–W polar	8.43	9.73	5.23	100.0	91.7	91.7
N–S horizontal	6.22	7.85	4.91	73.8	74.0	86.2
E–W horizontal	7.51	10.36	4.47	89.1	97.7	60.9

Note: E: equinoxes, SS: summer solstice, WS: winter solstice.

the cosine of the incidence angle. The amount of energy falling on a surface of 1 m^2 for four modes of tracking for the summer and winter solstices and the equinoxes is shown in Table 6 [64]. The amount of energy shown in Table 6 is obtained by applying a radiation model [12]. This is affected by the incidence angle which is different for each mode.

The performance of the various modes of tracking can be compared to the full tracking mode, which collects the maximum amount of solar radiation, shown as 100% in Table 6. Relations for the estimation of the angle of incidence for the various modes of tracking are given in Table 7.

The optical efficiency is defined as the ratio of the energy absorbed by the receiver to the energy incident on the collector's aperture. The optical efficiency depends on the optical properties of the materials involved, the geometry of the collector, and the various imperfections arising from the construction of the collector. In equation form [99]:

$$n_o = \rho\tau\alpha\gamma[(1 - A_f \tan(\theta))\cos(\theta)] \quad (33)$$

The geometry of the collector dictates the geometric factor A_f , which is a measure of the effective reduction of the aperture area due to abnormal incidence effects. For a PTC, its value can be obtained by the following relation [100]:

$$A_f = \frac{2}{3} W_a h_p + f W_a \left[1 + \frac{W_a^2}{48f^2} \right] \quad (34)$$

The most complex parameter involved in determining the optical efficiency of a PTC is the intercept factor. This is defined as the ratio of the energy intercepted by the receiver to the energy reflected by the focusing device, i.e. parabola [99]. Its value depends on the size of the receiver, the surface angle errors of the parabolic mirror, and solar beam spread.

The errors associated with the parabolic surface are of two types, random and non-random [101]. Random errors are defined as those errors which are truly random in nature and, therefore, can be represented by normal probability distributions. Random errors are identified as apparent changes in the sun's width, scattering effects caused by random slope errors (i.e. distortion of the parabola due to wind loading) and scattering effects associated with the reflective surface. Non-random errors arise in

Table 7
Relations for the estimation of the angle of incidence (θ) for the various modes of tracking

Mode of tracking	Incidence angle	Remarks
Full tracking	$\cos(\theta) = 1$	This depends on the accuracy of the tracking mechanism.
Collector axis in N–S axis polar E–W tracking	$\cos(\theta) = \cos(\delta)$	This mode collects the maximum possible sunshine For this mode the sun is normal to the collector at equinoxes ($\delta = 0^\circ$) and the cosine effect is maximum at the solstices. When more than one collector is used, front collectors cast shadows on adjacent ones
Collector axis in N–S axis horizontal E–W tracking	$\cos(\theta) = \sqrt{\sin^2(\alpha) + \cos^2(\delta)\sin^2(h)}$ or $\cos(\theta) = \cos(\Phi)\cos(h) + \cos(\delta)\sin^2(h)$	The greatest advantage of this arrangement is that very small shadowing effects are encountered when more than one collector is used. These are present in the first and last hours of the day
Collector axis in E–W axis horizontal N–S tracking	$\cos(\theta) = \sqrt{1 - \cos^2(\delta)\sin^2(h)}$ or $\cos(\theta) = \sqrt{\sin^2(\delta) + \cos^2(\delta)\cos^2(h)}$	The shadowing effects of this arrangement are minimal. The principal shadowing is caused when the collector is tipped to a maximum degree south ($\delta = 23.5^\circ$) at winter solstice. In this case the sun casts a shadow toward the collector at the north

Notes: δ : declination angle, h : hour angle, Φ : zenith angle. Relations to determine these angles can be found in many solar energy books [1,97].

manufacture/assembly and/or in the operation of the collector. These can be identified as reflector profile imperfections, misalignment errors and receiver location errors. Random errors are modeled statistically, by determining the standard deviation of the total reflected energy distribution, at normal incidence [102] and are given by:

$$\sigma = \sqrt{\sigma_{\text{sun}}^2 + 4\sigma_{\text{slope}}^2 + \sigma_{\text{mirror}}^2} \quad (35)$$

Non-random errors are determined from a knowledge of the misalignment angle error β (i.e. the angle between the reflected ray from the centre of sun and the normal to the reflector’s aperture plane) and the displacement of the receiver from the focus of the parabola (d_r). As reflector profile errors and receiver mislocation along the Y axis essentially have the same effect a single parameter is used to account for both. According to Guven and Bannerot [102] random and non-random errors can be combined with the collector geometric parameters, concentration ratio (C) and receiver diameter (D) to yield error parameters universal to all collector geometries. These are called ‘universal error parameters’ and an asterisk is used to distinguish them from the already defined parameters. Using the universal error parameters the formulation of the intercept factor γ is possible [101]:

$$\gamma = \frac{1 - \cos \phi_r}{2 \sin \phi_r} \times \int_0^{\phi_r} \text{Erf} \left(\frac{\sin \phi_r (1 + \cos \phi) (1 - 2d^* \sin \phi) - \pi \beta^* (1 + \cos \phi_r)}{\sqrt{2\pi\sigma^* (1 + \cos \phi_r)}} \right) - \text{Erf} \left(- \frac{\sin \phi_r (1 + \cos \phi) (1 + 2d^* \sin \phi) + \pi \beta^* (1 + \cos \phi_r)}{\sqrt{2\pi\sigma^* (1 + \cos \phi_r)}} \right) \times \frac{d\phi}{(1 + \cos \phi)} \quad (36)$$

where

- d^* universal non-random error parameter due to receiver mislocation and reflector profile errors ($d^* = d_r/D$)
- β^* universal non-random error parameter due to angular errors ($\beta^* = \beta C$)
- σ^* universal random error parameter ($\sigma^* = \sigma C$)
- C collector concentration ratio [= A_a/A_r]
- D riser tube outside diameter (m)
- d_r displacement of receiver from focus (m)
- β misalignment angle error (degrees)

Another parameter that needs to be determined is the radiation concentration distribution on the receiver of the collector, called local concentration ratio (LCR). For the PTC this distribution is as shown in Fig. 14. The shape of the curves depends on the same type or errors mentioned above and on the angle of incidence. Analysis of these effects is presented in Ref. [103] and may not be repeated here. It should be noted that the distribution for half the receiver is shown in Fig. 14. Another more representative way to show this distribution for the whole receiver is shown in Fig. 15. As can be seen from these figures, the top part of the receiver receives essentially only direct sunshine from the sun and the maximum concentration, about 36 suns, occurs at zero incidence angle and at an angle β , shown in Fig. 14, of 120° .

3.2.2. Thermal analysis

The generalised thermal analysis of a concentrating solar collector is similar to that of a FPC. It is necessary to derive appropriate expressions for the collector efficiency factor F' , the loss coefficient U_L and the collector heat removal factor F_R . For the loss coefficient standard heat transfer relations for glazed tubes can be used.

The instantaneous efficiency of a concentrating collector may be calculated from an energy balance of its receiver.

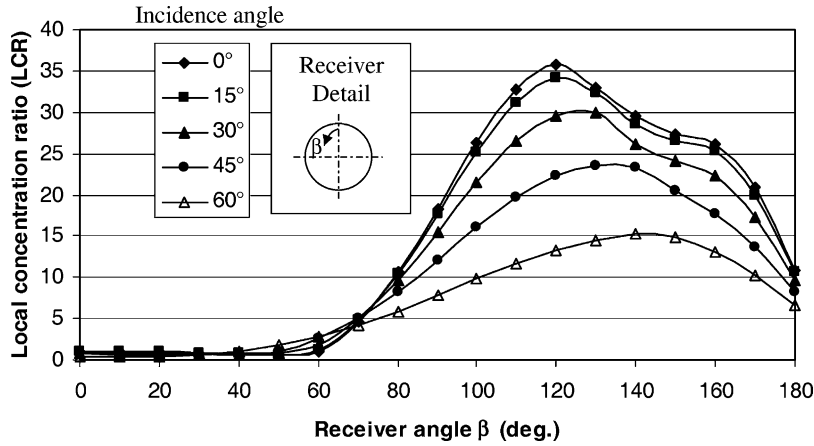


Fig. 14. Local concentration ratio on the receiver of a parabolic trough collector.

Eq. (1) also may be adapted for use with concentrating collectors. Therefore, the useful energy delivered from a concentrator is:

$$q_u = G_b n_o A_a - A_r U_L (T_r - T_a) \tag{37}$$

The useful energy gain per unit of collector length can be expressed in terms of the local receiver temperature T_r as:

$$q'_u = \frac{q_u}{L} = \frac{A_a n_o G_b}{L} - \frac{A_r U_L}{L} (T_r - T_a) \tag{38}$$

In terms of the energy transfer to the fluid at local fluid temperature T_f :

$$q'_u = \frac{\left(\frac{A_r}{L}\right)(T_r - T_f)}{\frac{D_o}{h_{fi} D_i} + \left(\frac{D_o}{2k} \ln \frac{D_o}{D_i}\right)} \tag{39}$$

If T_r is eliminated from Eqs. (38) and (39) we have:

$$q'_u = F' \frac{A_a}{L} \left[n_o G_b - \frac{U_L}{C} (T_f - T_a) \right] \tag{40}$$

where F' is the collector efficiency factor given by:

$$F' = \frac{1/U_L}{\frac{1}{U_L} + \frac{D_o}{h_{fi} D_i} + \left(\frac{D_o}{2k} + \ln \frac{D_o}{D_i}\right)} \tag{41}$$

Similarly as for the FPC the heat removal factor can be used and Eq. (37) can be written as:

$$q_u = F_R [G_b n_o A_a - A_r U_L (T_i - T_a)] \tag{42}$$

And the collector efficiency can be obtained by dividing q_u by $(G_b A_a)$. Therefore,

$$n = F_R \left[n_o - U_L \left(\frac{T_i - T_a}{G_b C} \right) \right] \tag{43}$$

where C is the concentration ratio [$C = A_a/A_r$]. For the F_R a relation similar to Eq. (3) is used by replacing A_c to A_r .

Another analysis usually performed for PTCs is by applying a piecewise two-dimensional model of the receiver by considering the circumferential variation of solar flux shown in Figs. 14 and 15. Such an analysis can be performed by dividing the receiver into longitudinal and isothermal nodal sections as shown in Fig. 16 and applying the principle

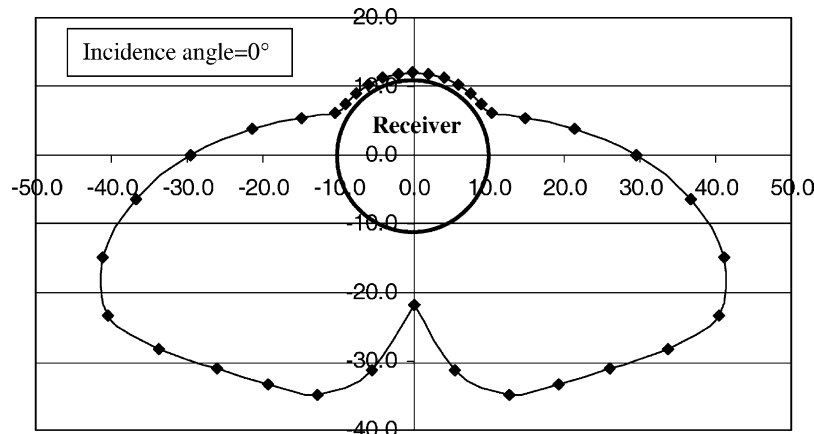


Fig. 15. More representative view of LCR for a collector with receiver diameter of 22 mm and rim angle of 90°.

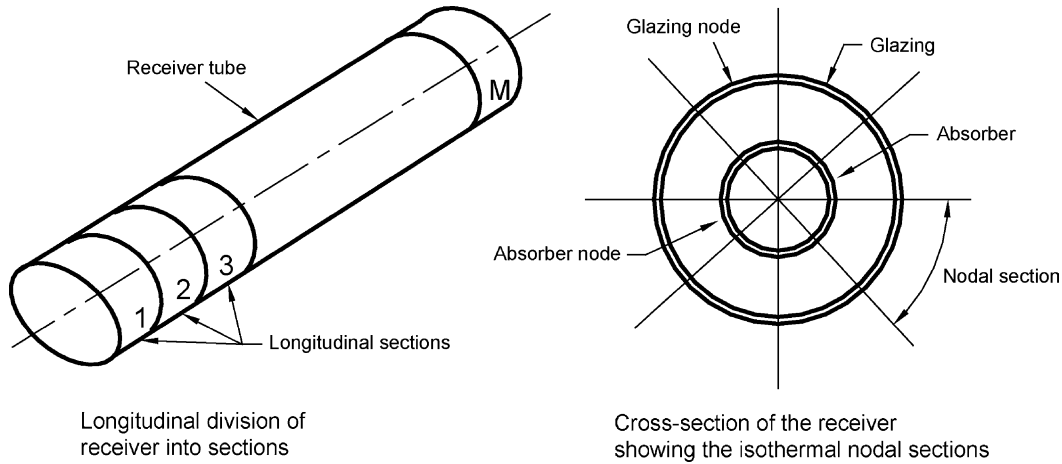


Fig. 16. Piecewise two-dimensional model of the receiver assembly.

of energy balance to the glazing and receiver nodes [104]. This analysis can give the temperature distribution along the circumference and length of the receiver, thus any points of high temperature, which might reach a temperature above the degradation temperature of the receiver selective coating, can be determined.

3.3. Second law analysis

The analysis presented here is based on Bejan’s work [105,106]. The analysis however is adapted to imaging collectors because entropy generation minimisation is more important to high temperature systems. Consider that the collector has an aperture area (or total heliostat area) A_a and receives solar radiation at the rate Q^* from the sun as shown in Fig. 17. The net solar heat transfer Q^* is proportional to the collector area A_a and the proportionality factor q^* (W/m^2) which varies with geographical position on the earth, the orientation of the collector, meteorological conditions and the time of day. In the present analysis q^* is assumed to be constant and the system is in steady state, i.e.

$$Q^* = q^* A_a \tag{44}$$

For concentrating systems q^* is the solar energy falling on the reflector. In order to obtain the energy falling on the collector receiver the tracking mechanism accuracy, the optical errors of the mirror including its reflectance and the optical properties of the receiver glazing must be considered.

Therefore, the radiation falling on the receiver q_o^* is a function of the optical efficiency, which accounts for all the above errors. For the concentrating collectors, Eq. (33) can be used. The radiation falling on the receiver is:

$$q_o^* = n_o q^* = \frac{n_o Q^*}{A_a} \tag{45}$$

The incident solar radiation is partly delivered to a power cycle (or user) as heat transfer Q at the receiver temperature

T_r . The remaining fraction Q_o represents the collector–ambient heat loss:

$$Q_o = Q^* - Q \tag{46}$$

For imaging concentrating collectors Q_o is proportional to the receiver–ambient temperature difference and to the receiver area as:

$$Q_o = U_r A_r (T_r - T_o) \tag{47}$$

where U_r is the overall heat transfer coefficient based on A_r . It should be noted that U_r is a characteristic constant of the collector.

Combining Eqs. (46) and (47) it is apparent that the maximum receiver temperature occurs when $Q = 0$, i.e. when the entire solar heat transfer Q^* is lost to the ambient. The maximum collector temperature is given in dimensionless form by:

$$\theta_{max} = \frac{T_{r,max}}{T_o} = 1 + \frac{Q^*}{U_r A_r T_o} \tag{48}$$

Combining Eqs. (45) and (48):

$$\theta_{max} = 1 + \frac{q_o^* A_a}{n_o U_r A_r T_o} \tag{49}$$

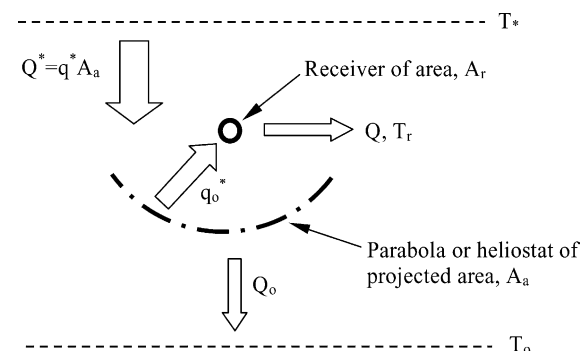


Fig. 17. Imaging concentrating collector model.

Considering that $C = A_a/A_r$, then:

$$\theta_{\max} = 1 + \frac{q_0^* C}{n_o U_r T_o} \quad (50)$$

As can be seen from Eq. (50), θ_{\max} is proportional to C , i.e. the higher the concentration ratio of the collector the higher is θ_{\max} and $T_{r,\max}$. The term $T_{r,\max}$ in Eq. (48) is also known as the stagnation temperature of the collector, i.e. the temperature that can be obtained at no flow condition. In dimensionless form the collector temperature $\theta = T_r/T_o$ will vary between 1 and θ_{\max} , depending on the heat delivery rate Q . The stagnation temperature θ_{\max} is the parameter that describes the performance of the collector with regard to collector–ambient heat loss as there is no flow through the collector and all the energy collected is used to raise the temperature of the working fluid to stagnation temperature which is fixed at a value corresponding to the energy collected equal to energy loss to ambient. Thus the collector efficiency is given by:

$$\eta_c = \frac{Q}{Q^*} = 1 - \frac{\theta - 1}{\theta_{\max} - 1} \quad (51)$$

Therefore, η_c is a linear function of collector temperature. At stagnation point the heat transfer Q carries zero exergy or zero potential for producing useful work.

3.3.1. Minimum entropy generation rate

The minimization of the entropy generation rate is the same as the maximization of the power output. The process of solar energy collection is accompanied by the generation of entropy upstream of the collector, downstream of the collector and inside the collector as shown in Fig. 18.

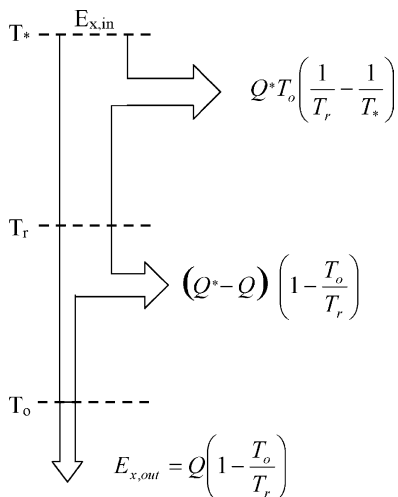


Fig. 18. Exergy flow diagram.

The exergy inflow coming from the solar radiation falling on the collector surface is:

$$E_{x,in} = Q^* \left(1 - \frac{T_o}{T_*} \right) \quad (52)$$

where T_* is the apparent sun temperature as an exergy source. In this analysis the value suggested by Petela [107] is adopted, i.e. T_* is approximately equal to $3/4 T_s$, where T_s is the apparent black body temperature of the sun, which is about 6000 K. Therefore, T_* considered here is 4500 K. It should be noted that in this analysis T_* is also considered constant and as its value is much greater than T_o , $E_{x,in}$ is very near Q^* . The output exergy from the collector is given by:

$$E_{x,out} = Q \left(1 - \frac{T_o}{T_r} \right) \quad (53)$$

whereas the difference between the $E_{x,in} - E_{x,out}$ represents the destroyed exergy. From Fig. 18, the entropy generation rate can be written as:

$$S_{gen} = \frac{Q_o}{T_o} + \frac{Q}{T_r} - \frac{Q^*}{T_*} \quad (54)$$

This equation can be written with the help of Eq. (46) as:

$$S_{gen} = \frac{1}{T_o} \left[Q^* \left(1 - \frac{T_o}{T_*} \right) - Q \left(1 - \frac{T_o}{T_r} \right) \right] \quad (55)$$

By using Eqs. (52) and (53), Eq. (55) can be written as:

$$S_{gen} = \frac{1}{T_o} (E_{x,in} - E_{x,out}) \quad (56)$$

or

$$E_{x,out} = E_{x,in} - T_o S_{gen} \quad (57)$$

Therefore, if we consider $E_{x,in}$ constant, the maximisation of the exergy output ($E_{x,out}$) is the same as the minimisation of the total entropy generation S_{gen} .

3.3.2. Optimum collector temperature

By substituting Eqs (46) and (47) into Eq. (55) the rate of entropy generation can be written as:

$$S_{gen} = \frac{U_r A_r (T_r - T_o)}{T_o} - \frac{Q^*}{T_*} + \frac{Q^* - U_r A_r (T_r - T_o)}{T_r} \quad (58)$$

By applying Eq. (50) in Eq. (58) and by performing various manipulations:

$$\frac{S_{gen}}{U_r A_r} = \theta - 2 - \frac{q_0^* C}{n_o U_r T_*} + \frac{\theta_{\max}}{\theta} \quad (59)$$

The dimensionless term $S_{gen}/U_r A_r$ accounts for the fact that the entropy generation rate scales with the finite size of the system which is described by $A_r = A_a/C$.

By differentiating Eq. (59) with respect to θ and setting to zero the optimum collector temperature (θ_{opt}) for

Table 8
Optimum collector temperatures for various types of concentrating collectors

Collector type	Concentration ratio	Stagnation temperature (°C)	Optimal temperature (°C)
Parabolic trough	50	565	227
Parabolic dish	500	1285	408
Central receiver	1500	1750	503

Notes: Ambient temperature considered = 25 °C.

minimum entropy generation is obtained:

$$\theta_{opt} = \sqrt{\theta_{max}} = \left(1 + \frac{q_o^* C}{n_o U_r T_o}\right)^{1/2} \quad (60)$$

By substituting θ_{max} by $T_{r,max}/T_o$ and θ_{opt} by $T_{r,opt}/T_o$, Eq. (60) can be written as:

$$T_{r,opt} = \sqrt{T_{r,max} T_o} \quad (61)$$

This equation states that the optimal collector temperature is the geometric average of the maximum collector (stagnation) temperature and the ambient temperature. Typical stagnation temperatures and the resulting optimum operating temperatures for various types of concentrating collectors are shown in Table 8. The stagnation temperatures shown in Table 8 are estimated by considering mainly the collector radiation losses.

As can be seen from the data presented in Table 8 for high performance collectors, like the central receiver, it is better to operate the system at high flow rates in order to lower the temperature around the value shown instead of operating at very high temperature, in order to obtain higher thermodynamic efficiency from the collector system.

By applying Eq. (60) to Eq. (59), the corresponding minimum entropy generation rate is:

$$\frac{S_{gen,min}}{U_r A_r} = 2(\sqrt{\theta_{max}} - 1) - \frac{\theta_{max} - 1}{\theta_*} \quad (62)$$

where $\theta_* = T_*/T_o$. It should be noted that for flat-plate and low concentration ratio collectors, the last term of Eq. (62) is negligible as θ_* is much bigger than $\theta_{max} - 1$, but it is not for higher concentration collectors, like the central receiver and the parabolic dish ones, which have stagnation temperatures of several thousands of degrees.

By applying the stagnation temperatures shown in Table 8 to Eq. (62), the dimensionless entropy generated against the collector concentration ratios considered here as shown in Fig. 19 is obtained.

3.3.3. Non-isothermal collector

So far the analysis was carried out by considering an isothermal collector. For a non-isothermal one, which is a more realistic model particularly for the long PTC, and by applying the principle of energy conservation:

$$q^* = U_r(T - T_o) + mc_p \frac{dT}{dx} \quad (63)$$

where x is from 0 to L (the collector length). The generated entropy can be obtained from:

$$S_{gen} = mc_p \ln \frac{T_{out}}{T_{in}} - \frac{Q^*}{T_*} + \frac{Q_o}{T_o} \quad (64)$$

From an overall energy balance, the total heat loss is:

$$Q_o = Q^* - mc_p(T_{out} - T_{in}) \quad (65)$$

Substituting Eq. (65) into Eq. (64) and performing the necessary manipulations the following relation is obtained:

$$N_s = M \left(\ln \frac{\theta_{out}}{\theta_{in}} - \theta_{out} + \theta_{in} \right) - \frac{1}{\theta_*} + 1 \quad (66)$$

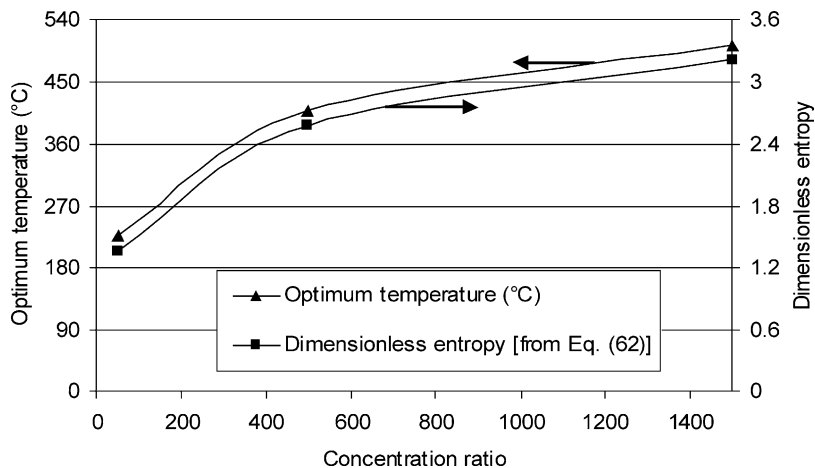


Fig. 19. Entropy generated and optimum temperatures against collector concentration ratio.

where $\theta_{\text{out}} = T_{\text{out}}/T_o$, $\theta_{\text{in}} = T_{\text{in}}/T_o$, N_s is the entropy generation number and M is the mass flow number given by:

$$N_s = \frac{S_{\text{gen}} T_o}{Q^*}, \quad \text{and} \quad M = \frac{m c_p T_o}{Q^*} \quad (67)$$

If the inlet temperature is fixed $\theta_{\text{in}} = 1$, then the entropy generation rate is a function of only M and θ_{out} . These parameters are interdependent because the collector outlet temperature depends on the mass flow rate.

4. Performance of solar collectors

ASHRAE Standard 93:1986 [108] for testing the thermal performance of collectors is undoubtedly the one most often used to evaluate the performance of flat-plate and concentrating solar collectors. The thermal performance of the solar collector is determined partly by obtaining values of instantaneous efficiency for different combinations of incident radiation, ambient temperature, and inlet fluid temperature. This requires experimental measurement of the rate of incident solar radiation falling onto the solar collector as well as the rate of energy addition to the transfer fluid as it passes through the collector, all under steady state or quasi-steady-state conditions. In addition, tests must be performed to determine the transient thermal response characteristics of the collector. The variation of steady-state thermal efficiency with incident angles between the direct beam and the normal to collector aperture area at various sun and collector positions is also required [108].

ASHRAE Standard 93:1986 [108] gives information on testing solar energy collectors using single-phase fluids and no significant internal storage. The data can be used to predict performance in any location and under any weather conditions where load, weather, and insolation are known.

4.1. Collector thermal efficiency

In reality the heat loss coefficient U_L in Eqs (2) and (42) is not constant but is a function of collector inlet and ambient temperatures. Therefore:

$$F_R U_L = c_1 + c_2(T_i - T_a) \quad (68)$$

Applying Eq. (68) in Eqs. (2) and (42) we have:
For FPC:

$$q_u = A_a F_R [\tau \alpha G_t - c_1(T_i - T_a) - c_2(T_i - T_a)^2] \quad (69)$$

and for concentrating collectors:

$$q_u = F_R [G_b n_o A_a - A_r c_1(T_i - T_a) - A_r c_2(T_i - T_a)^2] \quad (70)$$

Therefore for FPC, the efficiency can be written as:

$$n = F_R \tau \alpha - c_1 \frac{(T_i - T_a)}{G_t} - c_2 \frac{(T_i - T_a)^2}{G_t} \quad (71)$$

and if we denote $c_0 = F_R \tau \alpha$ and $x = (T_i - T_a)/G_t$ then:

$$n = c_0 - c_1 x - c_2 G_t x^2 \quad (72)$$

And for concentrating collectors the efficiency can be written as:

$$n = F_R n_o - \frac{c_1(T_i - T_a)}{C G_b} - \frac{c_2(T_i - T_a)^2}{C G_b} \quad (73)$$

and if we denote $k_0 = F_R n_o$, $k_1 = c_1/C$, $k_2 = c_2/C$ and $y = (T_i - T_a)/G_b$: then:

$$n = k_0 - k_1 y - k_2 G_b y^2 \quad (74)$$

Usually, the second-order terms are neglected in which case $c_2 = 0$ and $k_2 = 0$ (or third-term in above equations is neglected). Therefore, Eqs. (71) and (73) plot as a straight line on a graph of efficiency versus the heat loss parameter $(T_i - T_a)/G_t$ for the case of FPCs and $(T_i - T_a)/G_b$ for the case of concentrating collectors. The intercept (intersection of the line with the vertical efficiency axis) equals to $F_R \tau \alpha$ for the FPCs and $F_R n_o$ for the concentrating ones. The slope of the line, i.e. the efficiency difference divided by the corresponding horizontal scale difference, equals to $-F_R U_L$ and $-F_R U_L/C$, respectively. If experimental data on collector heat delivery at various temperatures and solar conditions are plotted, with efficiency as the vertical axis and $\Delta T/G$ (G_t or G_b is used according to the type of collector) as the horizontal axis, the best straight line through the data points correlates collector performance with solar and temperature conditions. The intersection of the line with the vertical axis is where the temperature of the fluid entering the collector equals the ambient temperature, and collector efficiency is at its maximum. At the intersection of the line with the horizontal axis, collector efficiency is zero. This condition corresponds to such a low radiation level, or to such a high temperature of the fluid into the collector, that heat losses equal solar absorption, and the collector delivers no useful heat. This condition, normally called stagnation, usually occurs when no fluid flows in the collector.

A comparison of the efficiency of various collectors at irradiation levels of 500 and 1000 W/m² is shown in Fig. 20. Five representative collector types are considered:

- Flat-plate collector.
- Advanced flat-plate collector (AFP). In this collector the risers are ultrasonically welded to the absorbing plate, which is also electroplated with chromium selective coating.
- Stationary CPC orientated with its long axis in the east–west direction.
- Evacuated tube collector.
- Parabolic trough collector with E–W tracking.

As seen in Fig. 20 the higher the irradiation level the better the efficiency and the higher performance collectors like the CPC, ETC and PTC retain high efficiency even at

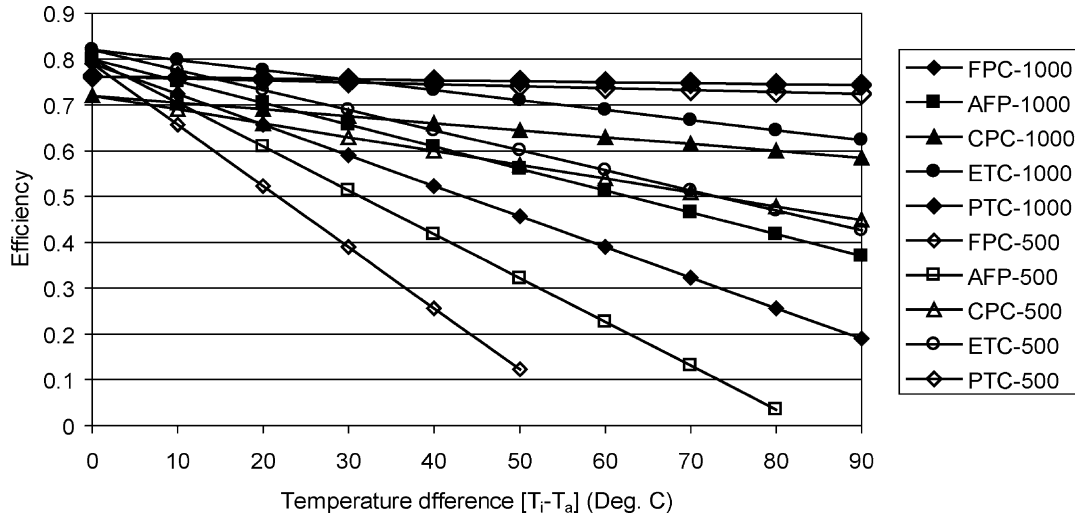


Fig. 20. Comparison of the efficiency of various collectors at two irradiation levels, 500 and 1000 W/m².

higher collector inlet temperatures. It should be noted that the radiation levels examined are considered as global radiation for all collector types except the PTC for which the same radiation values are used but considered as beam radiation.

As it can be seen from Fig. 20 the advantage of concentrating collectors is that the heat losses are inversely proportional to the concentration ratio C . This leads to the small slope of the collector performance curve. Thus the efficiency of concentrating collectors remains high at high inlet-water temperatures.

The difference in performance can also be seen from the performance equations. For example, the performance of a good FPC is given by

$$n = 0.792 - 6.65 \left(\frac{\Delta T}{G_t} \right) - 0.06 \left(\frac{\Delta T^2}{G_t} \right) \quad (75)$$

whereas the performance equation of the IST collector (obtained by the Sandia tests [83]) as given by the manufacturer is:

$$n = 0.762 - 0.2125 \left(\frac{\Delta T}{G_b} \right) - 0.001672 \left(\frac{\Delta T^2}{G_b} \right) \quad (76)$$

Eqs. (71)–(74) include all important design and operational factors affecting steady-state performance except collector flow rate and solar incidence angle. Flow rate inherently affects performance through the average absorber temperature. If the heat removal rate is reduced, the average absorber temperature increases, and more heat is lost. If the flow is increased, collector absorber temperature and heat loss decreases. The effect of solar incidence angle is accounted by the incidence angle modifier.

4.2. Collector incidence angle modifier

4.2.1. Flat-plate collectors

The above performance equations (69) and (71) assume that the sun is perpendicular to the plane of the collector, which rarely occurs. For the glass cover plates of a FPC, specular reflection of radiation occurs thereby reducing the $(\tau\alpha)$ product. The incident angle modifier $k_{\alpha\tau}$, defined as the ratio of $\tau\alpha$ at some incident angle θ to $\tau\alpha$ at normal radiation $(\tau\alpha)_n$, is described by the following expression:

$$k_{\alpha\tau} = 1 - b_0 \left(\frac{1}{\cos(\theta)} - 1 \right) - b_1 \left(\frac{1}{\cos(\theta)} - 1 \right)^2 \quad (77)$$

For single glass cover, a single-order equation can be used with $b_0 = -0.1$ and $b_1 = 0$.

With the incidence angle modifier, the collector efficiency equation (71) can be modified as:

$$n = F_R (\tau\alpha)_n k_{\alpha\tau} - c_1 \frac{(T_i - T_a)}{G_t} - c_2 \frac{(T_i - T_a)^2}{G_t} \quad (78)$$

4.2.2. Concentrating collectors

Similarly, for concentrating collectors the performance equations (70) and (73) described previously are reasonably well defined as long as the direct beam of solar irradiation is normal to the collector aperture. However, for off-normal incidence angles, the optical efficiency term (n_o) is often difficult to be described analytically because it depends on the actual concentrator geometry, concentrator optics, receiver geometry and receiver optics which may differ significantly. As the incident angle of the beam radiation increases these terms become more complex. Fortunately, the combined effect of these three parameters at different incident angles can be accounted for with

the incident angle modifier. This is simply a correlation factor to be applied to the efficiency curve and is only a function of the incident angle between the direct solar beam and the outward drawn normal to the aperture plane of the collector. It describes how the optical efficiency of the collector changes as the incident angle changes. With the incident angle modifier Eq. (73) becomes:

$$n = F_R K_{\alpha\tau} n_o - \frac{c_1(T_i - T_a)}{CG_b} - \frac{c_2(T_i - T_a)^2}{CG_b} \quad (79)$$

If the inlet fluid temperature is maintained equal to ambient temperature, the incident angle modifier can be determined from:

$$K_{\alpha\tau} = \frac{n(T_{fi} = T_a)}{F_R [n_o]_n} \quad (80)$$

where $n(T_{fi} = T_a)$ is the measured efficiency at the desired incident angle and for an inlet fluid temperature equal to the ambient temperature. The denominator in Eq. (80) is the test intercept taken from the collector efficiency test with Eq. (73) with $[n_o]_n$ being the normal optical efficiency, i.e. at normal angle of incidence.

As an example the results obtained from such a test (Fig. 21) are denoted by the small squares. By using a curve fitting method (second-order polynomial fit), the curve that best fits the points can be obtained [59]:

$$K_{\alpha\tau} = 1 - 0.00384(\theta) - 0.000143(\theta)^2 \quad (81)$$

For the IST collector, the incidence angle modifier $k_{\alpha\tau}$ of the collector, given by the manufacturer is:

$$k_{\alpha\tau} = \cos(\theta) + 0.0003178(\theta) - 0.00003985(\theta)^2 \quad (82)$$

4.3. Concentrating collector acceptance angle

Another test required for the concentrating collectors is the determination of the collector acceptance angle, which characterises the effect of errors in the tracking mechanism angular orientation.

This can be found with the tracking mechanism disengaged and measuring the efficiency at various out of focus angles as the sun is travelling over the collector plane. An example is shown in Fig. 22 where the angle of incidence measured from the normal to the tracking axis (i.e. out of focus angle) is plotted against the efficiency factor, i.e. the ratio of the maximum efficiency at normal incidence to the efficiency at a particular out of focus angle.

A definition of the collector acceptance angle is the range of incidence angles (as measured from the normal to the tracking axis) in which the efficiency factor varies by no more than 2% from the value of normal incidence [108]. Therefore from Fig. 22, the collector half-acceptance angle, θ_m , is 0.5°. This angle determines the maximum error of the tracking mechanism.

4.4. Collector time constant

A last aspect of collector testing is the determination of the heat capacity of a collector in terms of a time constant. It is also necessary to determine the time response of the solar collector in order to be able to evaluate the transient behaviour of the collector, and to select the correct time intervals for the quasi-steady state or steady-state efficiency tests. Whenever transient conditions exist, Eqs. (69)–(74) do not govern the thermal performance of the collector since

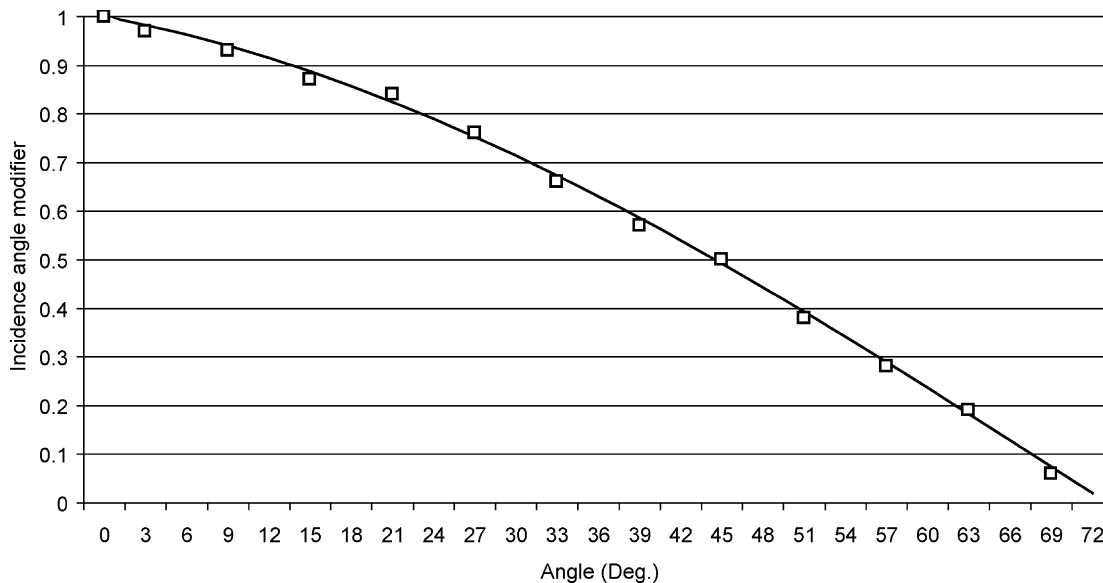


Fig. 21. Parabolic trough collector incidence angle modifier test results.

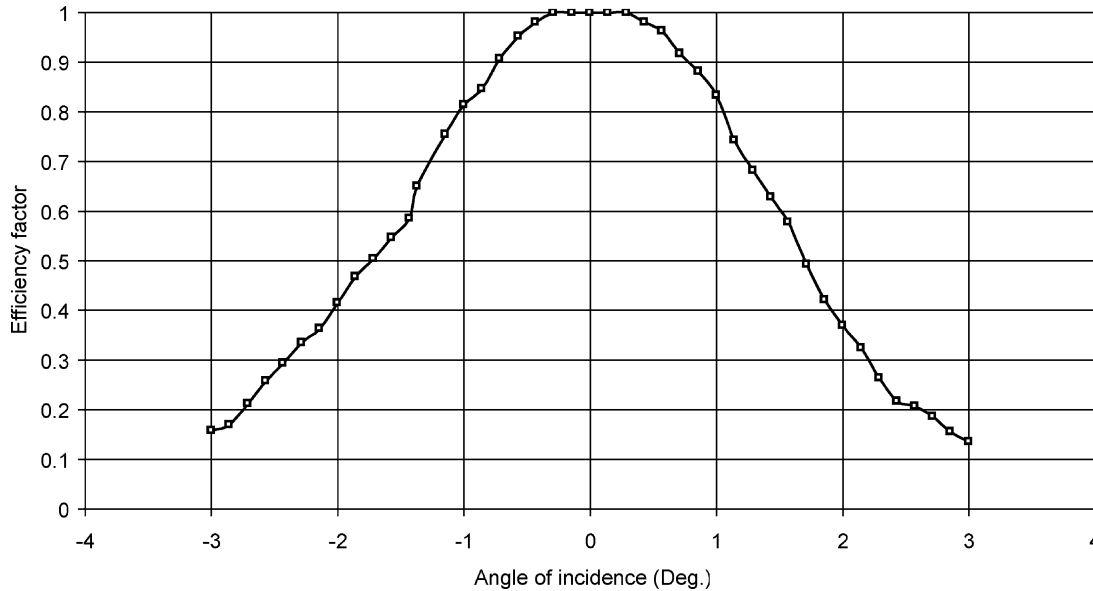


Fig. 22. Parabolic trough collector acceptance angle test results.

part of the absorbed solar energy is used for heating up the collector and its components.

The time constant of a collector is the time required for the fluid leaving the collector to reach 63% of its ultimate steady value after a step change in incident radiation. The collector time constant is a measure of the time required for the following relationship to apply [108]:

$$\frac{T_{ot} - T_i}{T_{oi} - T_i} = \frac{1}{e} = 0.368 \quad (83)$$

where T_{ot} is the collector outlet water temperature after time t (°C); T_{oi} is the collector outlet initial water temperature (°C); T_i is the collector inlet water temperature (°C).

The procedure for performing this test is to operate the collector with the fluid inlet temperature maintained at the ambient temperature. The incident solar energy is then abruptly reduced to zero by either shielding a FPC, or defocusing a concentrating one. The temperatures of the transfer fluid are continuously monitored as a function of time until Eq. (83) is satisfied. Results of tests carried out on a PTC constructed by the author are given in Ref. [71].

4.5. Collector test results and preliminary collector selection

Collector testing is required in order to evaluate the performance of solar collectors and compare different collectors to select the most appropriate one for a specific application. As can be seen from Sections 4.1–4.4 the tests show how a collector absorbs solar energy, how it loses heat, the effects of angle of incidence of solar radiation and the significant heat capacity effects which are determined from the collector time constant.

Finally tests are performed on the solar collectors in order to determine their quality. In particular the ability of a collector to resist extreme operating conditions are examined as specified in International Standard ISO 9806-2 (1995) [109]. The tests are required to be applied in the sequence specified in Table 9 so that possible degradation in one test will be exposed in a later test.

Final selection of a collector should be made only after energy analyses of the complete system, including realistic weather conditions and loads, have been conducted for one year. Also, a preliminary screening of collectors with various performance parameters should be conducted in order to identify those that best match the load. The best way to accomplish this is to identify the expected range of the parameter $\Delta T/G$ for the load and climate on a plot of efficiency n as a function of the heat loss parameter, as indicated in Fig. 23.

Table 9
Sequence of quality tests for solar collectors [109]

Sequence	Test
1	Internal pressure
2	High temperature resistance
3	Exposure
4	External thermal shock
5	Internal thermal shock
6	Rain penetration
7	Freeze resistance
8	Internal pressure (re-test)
9	Thermal performance
10	Impact resistance
11	Final inspection

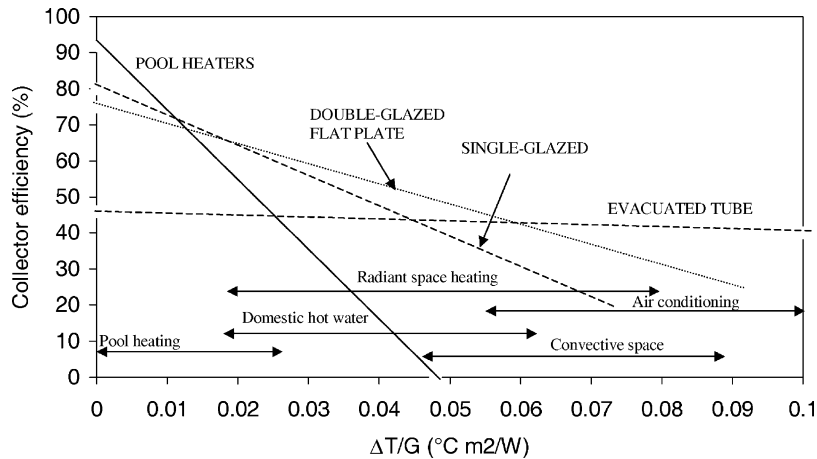


Fig. 23. Collector efficiencies of various liquid collectors.

Collector efficiency curves may be used for preliminary collector selection. However, efficiency curves illustrate only the instantaneous performance of a collector. They do not include incidence angle effects, which vary throughout the year, heat exchanger effects, probabilities of occurrence of T_1, T_a , solar irradiation, system heat loss, or control strategies. Final selection requires determining the long-term energy output of a collector as well as performance cost-effectiveness studies. Estimating the annual performance of a particular collector and system requires the aid of appropriate analysis tools such as *F*-Chart, Watsun, or TRNSYS. These are analysed briefly in Section 4.6.

4.6. Modelling of solar systems

The proper sizing of the components of a solar system is a complex problem which includes both predictable (collector and other components performance characteristics) and unpredictable (weather data) components. In this section an overview of the simulation techniques and programs suitable for solar heating and cooling systems is presented.

Computer modelling of thermal systems presents many advantages the most important of which are the following [110]:

1. Eliminate the expense of building prototypes.
2. Complex systems are organised in an understandable format.
3. Provide thorough understanding of system operation and component interactions.
4. It is possible to optimise the system components.
5. Estimate the amount of energy delivery from the system.
6. Provide temperature variations of the system.
7. Estimate the design variable changes on system performance by using the same weather conditions.

The initial step in modelling a system is the derivation of a structure to be used to represent the system. It will become

apparent that there is no unique way of representing a given system. Since the way the system is represented often strongly suggests specific modelling approaches, the possibility of using alternative system structures should be left open while the modelling approach selection is being made. The structure that represents the system should not be confused with the real system. The structure will always be an imperfect copy of reality. However, the act of developing a system structure and the structure itself will foster an understanding of the real system. In developing a structure to represent a system, system boundaries consistent with the problem being analysed are first established. This is accomplished by specifying what items, processes, and effects are internal to the system and what items, processes, and effects are external.

Simplified analysis methods have advantages of computational speed, low cost, rapid turnaround, which is especially important during iterative design phases, and easy of use by persons with little technical experience. Disadvantages include limited flexibility for design optimisation, lack of control over assumptions, and a limited selection of systems that can be analysed. Thus, if the system application, configuration, or load characteristics under consideration are significantly non-standard, a detailed computer simulation may be required to achieve accurate results. The following sections describe briefly four software programs TRNSYS, WATSUN, Polysun and *F*-Chart as well as artificial neural networks applied in solar energy systems modelling and prediction.

4.6.1. TRNSYS simulation program

TRNSYS is an acronym for a 'transient simulation' which is a quasi-steady simulation model. This program [111] was developed by the University of Wisconsin by the members of the Solar Energy Laboratory. The program consists of many subroutines that model subsystem components. The mathematical models for the subsystem components are given in terms of their ordinary differential

or algebraic equations. With a program such as TRNSYS which has the capability of interconnecting system components in any desired manner, solving differential equations and facilitating information output, the entire problem of system simulation reduces to a problem of identifying all the components that comprise the particular system and formulating a general mathematical description of each.

Once all the components of the system have been identified and a mathematical description of each component is available, it is necessary to construct an information flow diagram for the system. The purpose of the information flow diagram is to facilitate identification of the components and the flow of information between them. Each component is represented as a box, which requires a number of constant PARAMETERS and time dependent INPUTS and produces time dependent OUTPUTS. An information flow diagram shows the manner in which all system components are interconnected. A given OUTPUT may be used as an INPUT to any number of other components. From the flow diagram a deck file has to be constructed containing information on all the components of the system, weather data file, and the output format.

Subsystem components in the TRNSYS include solar collectors, differential controllers, pumps, auxiliary heaters, heating and cooling loads, thermostats, pebble-bed storage, relief valves, hot water cylinders, heat pumps and many more. There are also subroutines for processing radiation data, performing integrations, and handling input and output. Time steps down to 1/1000 h (3.6 s) can be used for reading weather data which makes the program very flexible with respect to using measured data in simulations. Simulation time steps at a fraction of an hour is also possible.

Model validation studies have been conducted in order to determine the degree to which the TRNSYS program serves as a valid simulation program for a physical system. It has been shown by analysing the results of these validation studies that the TRNSYS program provides results with a mean error between the simulation results and the measured results on actual operating systems under 10% [112]. The use of TRNSYS for the modelling of a thermosyphon SWH was also validated by the author and found to be accurate within 4.7% [110]. TRNSYS is not a user-friendly program, although some graphical interfacing has been developed recently, like IISiBat, but is the most versatile with respect to the detail that systems are modelled.

More details about TRNSYS program can be found in the program manual [111] and in Ref. [113]. There are numerous applications of the program in literature. Some typical examples are for the modelling of a thermosyphon system [110], modelling and performance evaluation of solar domestic hot water systems [114], investigation of the effect of load profile [115], modelling of industrial process heat applications [20,116,117] and modelling and simulation of a lithium bromide absorption system [118].

4.6.2. WATSUN simulation program

WATSUN simulates active solar systems and is developed by the Watsun Simulation Laboratory of the University of Waterloo in Canada [119]. It is a ready-made program that the user can learn and operate easily. It combines collection, storage, and load information provided by the user with hourly weather data for a specific location, and calculates the system state every hour. For convenience, a monthly summary is also provided. Both hourly and monthly reports include data about incident solar radiation, energy collected, load and auxiliary energy. WATSUN provides information necessary for long-term performance calculations. Also included with WATSUN is an economic analysis option, that can be used to assess the costs and profits generated by the use of the solar energy systems.

WATSUN uses weather data consisting of hourly values for global radiation on a horizontal surface, dry bulb temperature, wind speed and relative humidity. For those locations where hourly data is not available, synthetic hourly data can be generated using WATGEN synthetic weather generator, which needs only monthly average values as input.

The WATSUN simulation interacts with the outside world through a series of files. A file is a collection of information, labelled and placed in a specific location. Files are used by the program to input and output information. There is one input file defined by the user, called the simulation data file. The simulation program then produces three output files, a listing file, an hourly data file, and a monthly data file.

The system is an assembly of collection devices, storage devices, and load devices that the user wants to assess. The system is defined in the simulation data file. The file is made up of data blocks that contain groups of related parameters.

The simulation data file controls the simulation. The parameters in this file specify the simulation period, weather data and output options. There are many systems that can be modelled, including domestic hot water, pool systems, and industrial process heating systems. Different data must be entered for each type of system.

The simulation data file also contains information about the physical characteristics of the collector device, the storage device(s), the heat exchangers, and the load. When the simulation data file has been fully delineated, the simulation requires one more file, the weather file, before it can run.

4.6.3. Polysun simulation program

Polysun program provides dynamical annual simulations of solar thermal systems and helps to optimise them [120]. It operates with dynamic time steps from 1 s to 1 h, thus simulation can be more stable and exact. The program is user friendly and the graphic–user interface permits a comfortable and clear input of all system parameters. All aspects of the simulation are based on physical models that work without empirical correlation terms. In addition

the program performs economic viability analysis and ecological balance, which includes emissions from the eight most significant greenhouse gases, thus the emissions of systems working only with conventional fuel and systems employing solar energy can be compared. Program Polysun was validated by Gantner [121] and was found to be accurate to within 5–10%.

4.6.4. *F-Chart method and program*

The method was developed by Beckman et al. [122]. The method provides a means for estimating the fraction of a total heating and cooling that will be supplied by solar energy for a given solar heating system. The primary design variable is the collector area whereas secondary variables are collector type, storage capacity, fluid flow rates, and load and collector heat exchanger sizes. The method is a correlation of the results of many hundreds of thermal performance simulations of solar heating systems performed with TRNSYS. The conditions of simulations were varied over appropriate ranges of parameters of practical system designs. The resulting correlations give f , the fraction of the monthly load supplied by solar energy as a function of two dimensionless parameters. One is related to the ratio of collector losses to heating loads, and the other is related to the ratio of absorbed solar radiation to heating loads. The f -charts have been developed for three standard system configurations, liquid and air systems for space (and hot water) heating and systems for service hot water only. Detailed simulations of these systems have been used to develop correlations between dimensionless variables and f , the monthly fraction of loads carried by solar energy. The two dimensionless groups are:

$$X = \frac{A_c F'_R U_L (T_{\text{ref}} - \bar{T}_a) \Delta t}{D} \quad (84)$$

$$Y = \frac{A_c F'_R (\bar{\tau}\alpha) \bar{H}_T N}{D} \quad (85)$$

For the purpose of calculating the values of the dimensionless parameters X and Y , Eqs. (84) and (85) are usually rearranged to read:

$$X = F_R U_L \frac{F'_R}{F_R} (T_{\text{ref}} - \bar{T}_a) \Delta t \frac{A_c}{D} \quad (86)$$

$$Y = F_R (\tau\alpha)_n \frac{F'_R}{F_R} \left[\frac{(\bar{\tau}\alpha)}{(\tau\alpha)_n} \right] \bar{H}_T N \frac{A_c}{D} \quad (87)$$

The reason for the rearrangement is that the factors $F_R U_L$ and $F_R (\tau\alpha)_n$ are readily available from standard collector tests (Section 4.1). The dimensionless parameters X and Y have some physical significance. The parameter X represents the ratio of the reference collector total energy loss to total heating load or demand (D) during the period Δt , whereas the parameter Y represents the ratio of the total absorbed solar energy to the total heating load or demand (D) during the same period.

The method can be used to simulate standard water and air systems configurations. The fraction f of the monthly total load supplied by the solar space system and air or water heating system is given as a function of the two parameters, X and Y , which can be obtained from charts [122] or from the following equations:

For air heating systems:

$$f = 1.040Y - 0.065X - 0.159Y^2 + 0.00187X^2 - 0.0095Y^3 \quad (88)$$

For liquid-based systems:

$$f = 1.029Y - 0.065X - 0.245Y^2 + 0.0018X^2 + 0.0215Y^3 \quad (89)$$

The F -Chart was developed for a storage capacity of 0.25 m³ of pebbles per square metre of collector area for air systems and 75 l of stored water per square meter of collector area for water systems. Other storage capacities can be used by modifying X by a storage size correction factor X_c/X as given by Duffie and Beckman [97].

For air heating systems for $0.50 \leq (\text{actual/standard storage capacity}) \leq 4.0$:

$$X_c/X = (\text{Actual/Standard storage capacity})^{-0.30} \quad (90)$$

For liquid-based systems for $0.50 \leq (\text{actual/standard storage capacity}) \leq 4.0$:

$$X_c/X = (\text{Actual/Standard storage capacity})^{-0.25} \quad (91)$$

Also air heating systems must be corrected for the flow rate. The standard collector flow rate is 10 l/s of air per square meter of collector area. The performance of systems having other collector flow rates can be estimated by using appropriate values of F_R and Y and then modifying the value of X by a collector air flow rate correction factor X_c/X to account for the degree of stratification in the pebble bed.

For $0.50 \leq (\text{actual/standard air flow rate}) \leq 2.0$:

$$X_c/X = (\text{Actual/Standard air flow rate})^{0.28} \quad (92)$$

Although the F -Chart method is simple in concept, the required calculations are tedious, particularly the manipulation of radiation data. The use of computers greatly reduces the effort required. Program F -Chart [123] was developed by the originators of TRNSYS is very easy to use and gives predictions very quickly. The model is accurate only for solar heating systems of a type comparable to that which was assumed in the development of the F -Chart. However, the model does not provide the flexibility of detail simulations and performance investigations as TRNSYS does.

F -Chart method was used by Datta et al. [124] for the optimisation of the collector inclination angle. It was also used by the author for a feasibility study on the use of PTC for hot water production [125].

4.6.5. Artificial neural networks in solar energy systems modelling and prediction

Artificial neural networks mimic somewhat the learning process of a human brain. They are widely accepted as a technology offering an alternative way to tackle complex and ill specified problems. They can learn from examples, are fault tolerant in the sense that they are able to handle noisy and incomplete data, are able to deal with non-linear problems, and once trained can perform prediction and generalisation at high speed. They have been used in diverse applications in control, robotics, pattern recognition, forecasting, medicine, power systems, manufacturing, optimisation, signal processing, and social/psychological sciences. They are particularly useful in system modelling such as in implementing complex mappings and system identification. Artificial neural networks have been used by the author in the field of solar energy, for modelling the heat-up response of a solar steam generating plant, for the estimation of a PTC intercept factor, for the estimation of a PTC local concentration ratios and for the design of a solar steam generation system. A review of these models together with other applications in the field of renewable energy is given in Ref. [126]. In all those models a multiple hidden layer architecture has been used. Errors reported are well within acceptable limits, which clearly suggest that artificial neural networks can be used for modelling and prediction in other fields of solar energy production and use. What is required is to have a set of data (preferably experimental) representing the past history of a system so as a suitable neural network can be trained to learn the dependence of expected output on the input parameters.

4.6.6. Limitations of simulations

Simulations are powerful tools for process design offering a number of advantages as outlined in the previous sections. However, there are limits to their use. For example, it is easy to make mistakes, such as, assume erroneous constants and neglect factors, which may be important. Like other engineering calculations, a high level of skill and scientific judgement is required in order to produce correct and useful results.

It is possible to model a system to a high degree of accuracy in order to extract the required information. In practice, however, it may be difficult to represent in detail some of the phenomena occurring in real systems. Additionally, physical world problems such as, leaks, plugged or restricted pipes, scale on heat exchangers, failure of controllers, poor installation of collectors and other equipment, poor insulation, etc. cannot be easily modelled or accounted for. Simulation programs are dealing only with thermal processes but mechanical and other considerations can also affect the thermal performance of solar systems.

There is no substitute to carefully executed experiments. A combination of simulation and physical experiments can lead to better systems and better understanding of how processes work. These can reveal whether or not theory is

adequate and where difficulties are present in the design and/or operation of the systems. As a conclusion, simulations are powerful tools for the modelling, design, prediction of performance and research and development. They must, however, be used with care and skill.

No study of solar systems is complete unless an economic analysis is carried out. For this purpose a life cycle analysis is usually performed as explained briefly in the following section.

4.7. Economic analysis

The economic analysis of solar energy systems is carried out in order to determine the least cost of meeting the energy needs, considering both solar and non-solar alternatives. The method employed for the economic analysis is called the life savings analysis. This method takes into account the time value of money and allows detailed consideration of the complete range of costs. Solar processes are generally characterised by high initial cost and low operating costs. Thus, the basic economic problem is of comparing an initial known investment with estimated future operating costs.

Life cycle cost (LCC) is the sum of all the costs associated with an energy delivery system over its lifetime in today's money, and takes into account the time value of money. The life cycle savings (LCS), for a solar plus auxiliary system, is defined as the difference between the LCC of a conventional fuel-only system and the LCC of the solar plus auxiliary system. This is equivalent to the total present worth (PW) of the gains from the solar system compared to the fuel-only system.

All software programs described in previous section have routines for the economic analysis of the modelled systems. The economic analysis of solar systems can also be performed with a spreadsheet program. Spreadsheet programs are especially suitable for economic analyses as their general format is a table with cells which can contain values or formulae and they incorporate many built-in functions. The economic analysis is carried out for every year for which various economic parameters are calculated in different columns. A detailed description of the method of economic analysis of solar systems using spreadsheets is given in Ref. [127].

4.7.1. Time value of money

It must be noted that a sum of money at hand today worth less than the same sum in the future, because the money at hand can be invested at some compounding interest to generate a bigger sum in the future. Therefore, a sum of money or cash flow in the future must be discounted and worth less at present-day value. A cash flow F occurring N years from now can be reduced to its present value P by:

$$P = \frac{F}{(1 + d)^N} \quad (93)$$

where d is the market discount rate (%).

Similarly, the amount of money needed to purchase an item is increasing because the value of money is decreasing. With an annual inflation rate i , a purchase cost C at the end of year N will become a future cost F according to:

$$F = C(1 + i)^{N-1} \quad (94)$$

4.7.2. Method description

In general, the PW (or discounted cost) of an investment or cost C at the end of year N , at a discount rate of d and interest rate of i is obtained by combining Eqs. (93) and (94) as:

$$PW_N = \frac{C(1 + i)^{N-1}}{(1 + d)^N} \quad (95)$$

Eq. (95) can easily be incorporated into a spreadsheet with the parameters d and i entered into separate cells and referencing them in the formulae as absolute cells. In this way a change in either d or i will cause automatic recalculation of the spreadsheet.

The fuel savings are obtained by subtracting the annual cost of the conventional fuel used for the auxiliary energy from the fuel needs of a fuel only system. The integrated cost of the auxiliary energy use for the first year, i.e. solar back up, is given by the formula:

$$C_{\text{aux}} = \int_0^t C_{\text{FA}} Q_{\text{aux}} dt \quad (96)$$

The integrated cost of the total load for the first year, i.e. cost of conventional fuel without solar, is:

$$C_{\text{load}} = \int_0^t C_{\text{FL}} Q_{\text{load}} dt \quad (97)$$

where C_{FA} and C_{FL} are the cost rates for auxiliary energy and conventional fuel, respectively.

Such analysis is performed annually and the following are evaluated:

- Fuel savings;
- Extra mortgage payment;
- Extra maintenance cost;
- Extra parasitic cost;
- Extra tax savings;
- Solar savings.

In some countries some other costs may be present, i.e. extra property tax to cover the new system. In this case these costs should be considered as well. The word 'extra' appearing in some of the above items assumes that the associated cost is also present for a fuel-only system and therefore only the extra part of the cost incurred by the installation of the solar system should be included. The inflation, over the period of economic analysis, of the fuel savings is estimated by using Eq. (94) with i equal to the fuel inflation rate. The parasitic cost is the energy required to power auxiliary items like

the pump, fan and controllers. This cost is also increased at an inflation rate over the period of economic analysis by using Eq. (94) with i equal to the annual increase of electricity price.

The mortgage payment is the annual value of money required to cover the funds borrowed at the beginning to install the system. This includes interest and principal payment. The estimation of the annual mortgage payment can be found by dividing the amount borrowed by the present worth factor (PWF). The PWF is estimated by using the inflation rate equal to zero (equal payments) and with the market discount rate equal to the mortgage interest rate. The PWF can be obtained from tables or calculated by the following equation [97]:

$$PWF = \frac{1}{d} \left[1 - \left(\frac{1}{1 + d} \right)^N \right] \quad (98)$$

where d is the interest rate, and N is the number of years (equal instalments).

Solar savings for each year are the sums of the items as:

$$\begin{aligned} \text{Solar savings} = & \text{Extra mortgage payment} \\ & + \text{Extra maintenance cost} \\ & + \text{Extra parasitic cost} + \text{Fuel savings} \\ & + \text{Extra tax savings} \end{aligned} \quad (99)$$

Actually, the savings are positive and the costs are negative. Finally, the PW of each year's solar savings is determined by using Eq. (95). The results are estimated for each year. These annual values are then added up to obtain the LCS according to the equation:

$$PW_{\text{LCS}} = \sum_{N=1}^N \frac{\text{Solar savings}}{(1 + d)^N} \quad (100)$$

5. Solar collector applications

Solar collectors have been used in a variety of applications. These are described in this section. In Table 10 the most important technologies in use are listed together with the type of collector that can be used in each case.

5.1. Solar water heating systems

The main part of a SWH is the solar collector array that absorbs solar radiation and converts it into heat. This heat is then absorbed by a heat transfer fluid (water, non-freezing liquid, or air) that passes through the collector. This heat can then be stored or used directly. Portions of the solar energy system are exposed to the weather conditions, so they must be protected from freezing and from overheating caused by high insolation levels during periods of low energy demand.

In solar water heating systems, potable water can either be heated directly in the collector (direct systems) or

Table 10
Solar energy applications and type of collectors used

Application	System	Collector
<i>Solar water heating</i>		
Thermosyphon systems	Passive	FPC
Integrated collector storage	Passive	CPC
Direct circulation	Active	FPC, CPC ETC
Indirect water heating systems	Active	FPC, CPC ETC
Air systems	Active	FPC
<i>Space heating and cooling</i>		
Space heating and service hot water	Active	FPC, CPC ETC
Air systems	Active	FPC
Water systems	Active	FPC, CPC ETC
Heat pump systems	Active	FPC, CPC ETC
Absorption systems	Active	FPC, CPC ETC
Adsorption (desiccant) cooling	Active	FPC, CPC ETC
Mechanical systems	Active	PDR
<i>Solar refrigeration</i>		
Adsorption units	Active	FPC, CPC ETC
Absorption units	Active	FPC, CPC ETC
<i>Industrial process heat</i>		
Industrial air and water systems	Active	FPC, CPC ETC
Steam generation systems	Active	PTC, LFR
<i>Solar desalination</i>		
Solar stills	Passive	–
Multistage flash (MSF)	Active	FPC, CPC ETC
Multiple effect boiling (MEB)	Active	FPC, CPC ETC
Vapour compression (VC)	Active	FPC, CPC ETC
<i>Solar thermal power systems</i>		
Parabolic trough collector systems	Active	PTC
Parabolic tower systems	Active	HFC
Parabolic dish systems	Active	PDR
Solar furnaces	Active	HFC, PDR
Solar chemistry systems	Active	CPC, PTC, LFR

indirectly by a heat transfer fluid that is heated in the collector, passes through a heat exchanger to transfer its heat to the domestic or service water (indirect systems). The heat transfer fluid is transported either naturally (passive systems) or by forced circulation (active systems). Natural circulation occurs by natural convection (thermosyphoning), whereas for the forced circulation systems pumps or fans are used. Except for thermosyphon and integrated collector storage (ICS) systems, which need no control, solar domestic and service hot water systems are controlled using differential thermostats.

Five types of solar energy systems can be used to heat domestic and service hot water: thermosyphon, ICS, direct circulation, indirect, and air. The first two are called passive systems as no pump is employed, whereas the others are called active systems because a pump or fan is employed in order to circulate the fluid. For freeze protection, recirculation and drain-down are used for direct solar water heating systems and drain-back is used for indirect water heating systems.

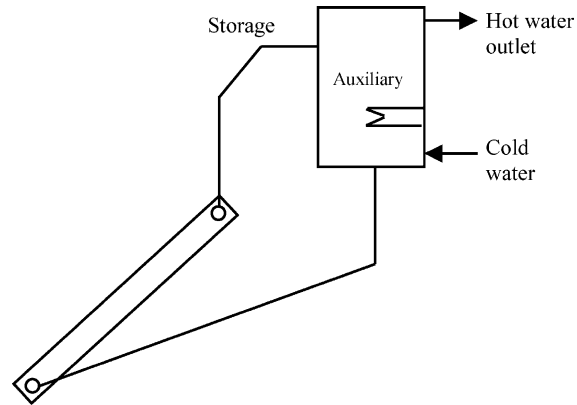


Fig. 24. Schematic diagram of a thermosyphon solar water heater.

All these systems offer significant economic benefits with payback times, depending on the type of fuel they replace, between 4 years (electricity) and 7 years (diesel oil). Of course, these payback times depend on the economic indices, like the inflation rates and fuel price applied in a country. A wide range of collectors have been used for solar water heating systems. A review of the systems manufactured in the last 20 years is given in Ref. [128].

5.1.1. Thermosyphon systems (passive)

Thermosyphon systems, shown schematically in Fig. 24, heat potable water or heat transfer fluid and use natural convection to transport it from the collector to storage. The water in the collector expands becoming less dense as the sun heats it and rises through the collector into the top of the storage tank. There it is replaced by the cooler water that has sunk to the bottom of the tank, from which it flows down the collector. The circulation continuous as long as there is sunshine. Since the driving force is only a small density difference larger than normal pipe sizes must be used to minimise pipe friction. Connecting lines must be well insulated to prevent heat losses and sloped to prevent formation of air pockets which would stop circulation. At night, or whenever the collector is cooler than the water in the tank the direction of the thermosyphon flow will reverse, thus cooling the stored water. One way to prevent this is to place the top of the collector well below (about 30 cm) the bottom of the storage tank.

The main disadvantage of thermosyphon systems is the fact that they are comparatively tall units, which makes them not very attractive aesthetically. Usually, a cold water storage tank is installed on top of the solar collector, supplying both the hot water cylinder and the cold water needs of the house, thus making the collector unit taller and even less attractive. Additionally, extremely hard or acidic water can cause scale deposits that clog or corrode the absorber fluid passages. For direct systems, pressure-reducing valves are required when the city water is used

directly (no cold water storage tank) and pressure is greater than the working pressure of the collectors.

There have been extensive analyses of the performance of thermosyphon SWH, both experimentally and analytically by numerous researchers. Some of the most important are shown here.

Gupta and Garg [129] developed one of the first models for thermal performance of a natural circulation SWH with no load. They represented solar radiation and ambient temperature by Fourier series, and were able to predict a day's performance in a manner that agreed substantially with experiments.

Ong performed two studies [130,131] to evaluate the thermal performance of a SWH. He instrumented a relatively small system with five thermocouples on the bottom surface of the water tubes and six thermocouples on the bottom surface of the collector plate. A total of six thermocouples were inserted into the storage tank and a dye tracer mass flow meter was employed. Ong's studies appear to be the first detailed ones on a thermosyphonic system.

Kudish et al. [132] in their study measured the thermosyphon flow rate directly by adapting a simple and well-known laboratory technique, a constant level device, to a solar collector in the thermosyphon mode. The thermosyphon flow data gathered were utilised to construct a standard efficiency test curve, thus showing that this technique can be applied for testing collectors in the thermosyphon mode. Also, they determined the instantaneous collector efficiency as a function of time of day.

Morrison and Braun [133] have studied system modelling and operation characteristics of thermosyphon SWH with vertical or horizontal storage tank. They found that the system performance is maximised when the daily collector volume flow is approximately equal to the daily load flow, and the system with horizontal tank did not perform as well as a vertical one.

Hobson and Norton [134] in their study developed a characteristic curve for an individual directly heated thermosyphon solar energy water heater obtained from data of a 30 days tests. Using such a curve, the calculated annual solar fraction agreed well with the corresponding value computed from the numerical simulation. Furthermore, the analysis was extended, and they produced a simple but relatively accurate design method for direct thermosyphon solar energy water heaters.

Shariah and Shalabi [135] have studied optimisation of design parameters for a thermosyphon SWH for two regions in Jordan represented by two cities, namely Amman and Aqaba through the use of TRNSYS simulation program. Their results indicate that the solar fraction of the system can be improved by 10–25% when each studied parameter is chosen properly. It was also found that the solar fraction of a system installed in Aqaba (hot climate) is less sensitive to some parameters than the solar fraction of a similar system installed in Amman (mild climate).

5.1.2. Integrated collector storage systems (passive)

ICS systems use hot water storage as part of the collector, i.e. the surface of the storage tank is used also as an absorber. As in all other systems, to improve stratification, the hot water is drawn from the top of the tank and cold make-up water enters to the bottom of the tank on the opposite side.

The main disadvantage of the ICS systems is the high thermal losses from the storage tank to the surroundings since most of the surface area of the storage tank cannot be thermally insulated as it is intentionally exposed for the absorption of solar radiation. In particular, the thermal losses are greatest during the night and overcast days with low ambient temperature. Due to these losses the water temperature drops substantially during the night especially during the winter. Various techniques have been used to avoid this from happening. Tripanagnostopoulos et al. [136] presented a number of experimental units in which the reduction of thermal losses was achieved by considering single and double cylindrical horizontal tanks properly placed in truncated symmetric and asymmetric CPC reflector troughs.

Details of an ICS unit developed by the author are presented here [137]. The system employs a non-imaging CPC cusp type collector. A fully developed cusp concentrator for a cylindrical receiver is shown in Fig. 25. The particular curve illustrated has an acceptance half-angle, θ_A , of 60° , or a full acceptance angle, $2\theta_A$, of 120° . Each side of the cusp has two mathematically distinct segments smoothly joined at a point P related to θ_A . The first segment, from the bottom of the receiver to point P , is the involute of the receiver's circular cross-section. The second segment is from point P to the top of the curve, where the curve becomes parallel to the y -axis [138].

With reference to Fig. 26, for a cylindrical receiver the radius R and acceptance half-angle, θ_A , the distance, ρ , along a tangent from the receiver to the curve, is related to the angle θ , between the radius to the bottom of the receiver and the radius to the point of tangency, T , by the following

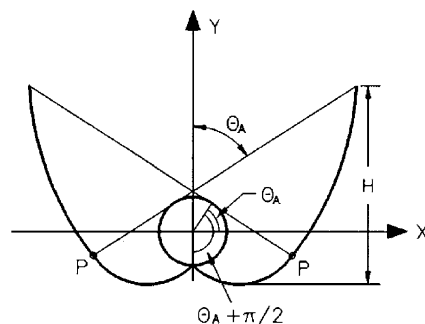


Fig. 25. Fully developed cusp.

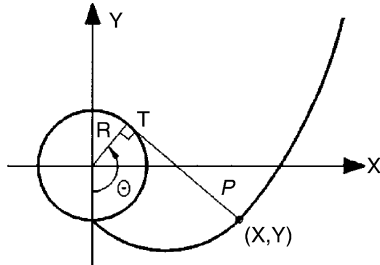


Fig. 26. Mirror co-ordinates for ideal non-imaging cusp concentrator.

expressions for the two sections of the curve [138]:

$$\rho(\theta) = R\theta, |\theta| \leq \theta_A + \pi/2 \tag{101}$$

(the involute part of the curve)

$$\rho(\theta) = R \left\{ \frac{\{\theta + \theta_A + \pi/2 - \cos(\theta - \theta_A)\}}{1 + \sin(\theta - \theta_A)} \right\}$$

$$\theta_A + \pi/2 \leq \theta \leq 3\pi/2 - \theta_A$$

The two expressions for $\rho(\theta)$ are equivalent for the point P in Fig. 25, where $\theta = \theta_A + \pi/2$. The curve is generated by incrementing θ in radians, calculating ρ , and then calculating the co-ordinates, X and Y , by:

$$X = R \sin \theta - \rho \cos \theta, \quad Y = -R \cos \theta - \rho \sin \theta \tag{102}$$

Fig. 25 shows a full untruncated curve which is the mathematical solution for a reflector shape with the maximum possible concentration ratio. The reflector shape shown in Fig. 25 is not the most practical design for a cost-effective concentrator, because reflective material is not effectively used in the upper portion of the concentrator. As in the case of the CPC, a theoretical cusp curve should be truncated to a lower height and slightly smaller concentration ratio. Graphically, this is done by drawing a horizontal line across the cusp at a selected height and discarding the part of the curve above the line. Mathematically, the curve is defined to a maximum angle θ value less than $3\pi/2 - \theta_A$. The shape of the curve below the cut-off line is not changed by truncation, so the acceptance angle used for the construction of the curve (using Eq. (101)) of a truncated cusp is equal to the acceptance angle of the fully developed cusp from which it was truncated.

A large acceptance angle of 75° is used in this design so as the collector would be able to collect as much diffuse radiation as possible [137]. The fully developed cusp together with the truncated one is shown in Fig. 27. The receiver radius considered in the construction of the cusp is 0.24 m. The actual cylinder is 0.20 m. This is done in order to create a gap at the underside of the receiver and the edge of the cusp in order to minimise the optical and conduction losses. The final design is shown in Fig. 28. The collector aperture is 1.77 m^2 , which in combination with the absorber diameter used, gives a concentration ratio of 1.47 [137].

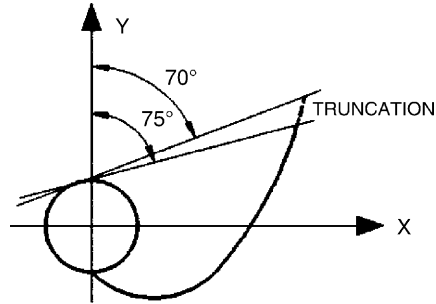


Fig. 27. Truncation of non-imaging concentrator.

It should be noted that, as shown in Fig. 28, the system is inclined at the local latitude in order to work effectively.

5.1.3. Direct circulation systems (active)

In direct circulation systems, shown schematically in Fig. 29, a pump is used to circulate potable water from storage to the collectors when there is enough available solar energy to increase its temperature and then return the heated water to the storage tank until it is needed. As a pump circulates the water, the collectors can be mounted either above or below the storage tank. The optimum flow rate for such units is about 0.015 l/m^2 of collector area. Direct circulation systems can be used in areas where freezing is not frequent. For extreme weather conditions, freeze protection is usually provided by recirculating warm water from the storage tank. Direct circulation systems often use a single storage tank equipped with an auxiliary water heater, but two-tank storage systems can also be used.

Direct circulation systems can be used with water supplied from a cold water storage tank or connected directly to city water mains. Pressure-reducing valves and pressure relief valves are required however when the city water pressure is greater than the working pressure of the collectors. Direct water heating systems should not be used in areas where the water is extremely hard or acidic because scale deposits may clog or corrode the collectors.

A variation of the direct circulation system is the drain-down systems shown in Fig. 30. In this case also potable water is pumped from storage to the collector array where it is heated. When a freezing condition or a power failure occurs, the system drains automatically by isolating

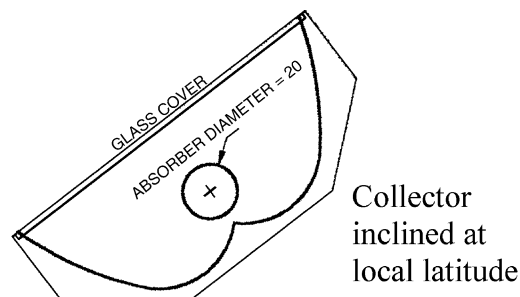


Fig. 28. The final collector.

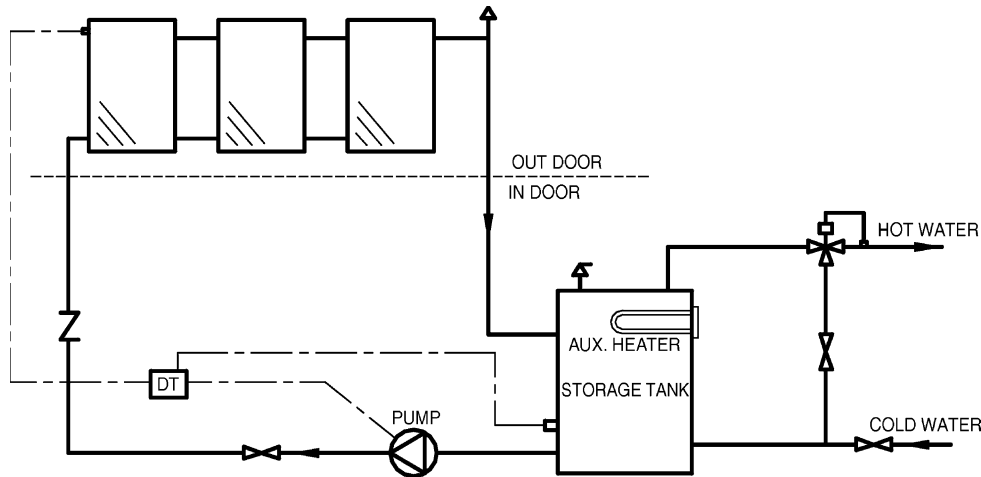


Fig. 29. Direct circulation system.

the collector array and exterior piping from the make-up water supply and draining it using the two normally open (NO) valves, shown in Fig. 30. It should be noted that the solar collectors and associated piping must be carefully sloped to drain the collector's exterior piping when circulation stops. The same comments about pressure and scale deposits apply here as for the direct circulation systems.

5.1.4. Indirect water heating systems (active)

Indirect water heating systems, shown schematically in Fig. 31, circulate a heat transfer fluid through the closed collector loop to a heat exchanger, where its heat is transferred to the potable water. The most commonly used heat transfer fluids are water/ethylene glycol solutions, although other heat transfer fluids such as silicone oils and refrigerants can also be used. When fluids that are non-potable or toxic are used double-wall heat exchangers

should be employed. The heat exchanger can be located inside the storage tank, around the storage tank (tank mantle) or can be external. It should be noted that the collector loop is closed and therefore an expansion tank and a pressure relief valve are required. Additional over-temperature protection may be needed to prevent the collector heat transfer fluid from decomposing or becoming corrosive.

A variation of indirect water heating systems is the drain-back system. Drain-back systems are generally indirect water heating systems that circulate water through the closed collector loop to a heat exchanger, where its heat is transferred to the potable water. Circulation continues as long as usable energy is available. When the circulation pump stops the collector fluid drains by gravity to a drain-back tank. If the system is pressurised the tank serves also as an expansion tank when the system is operating and in this case it must be protected with a temperature and pressure

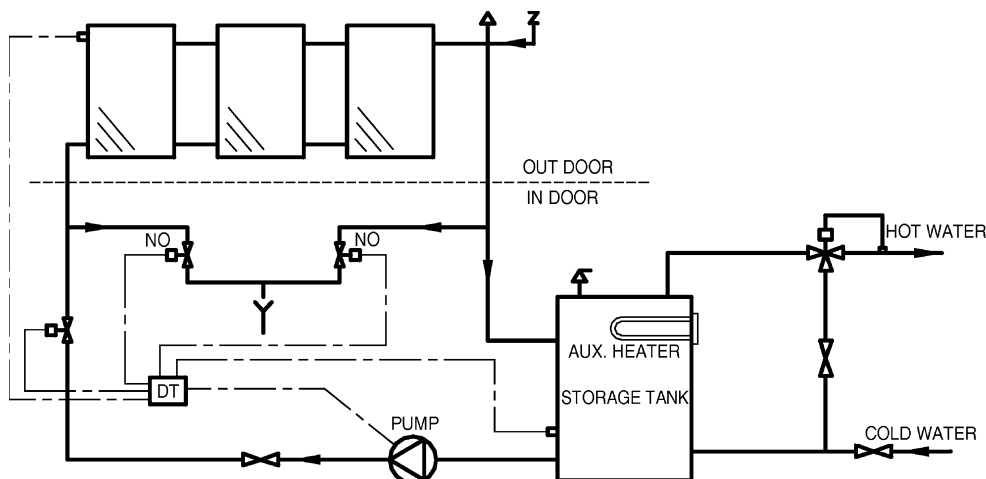


Fig. 30. Drain-down system.

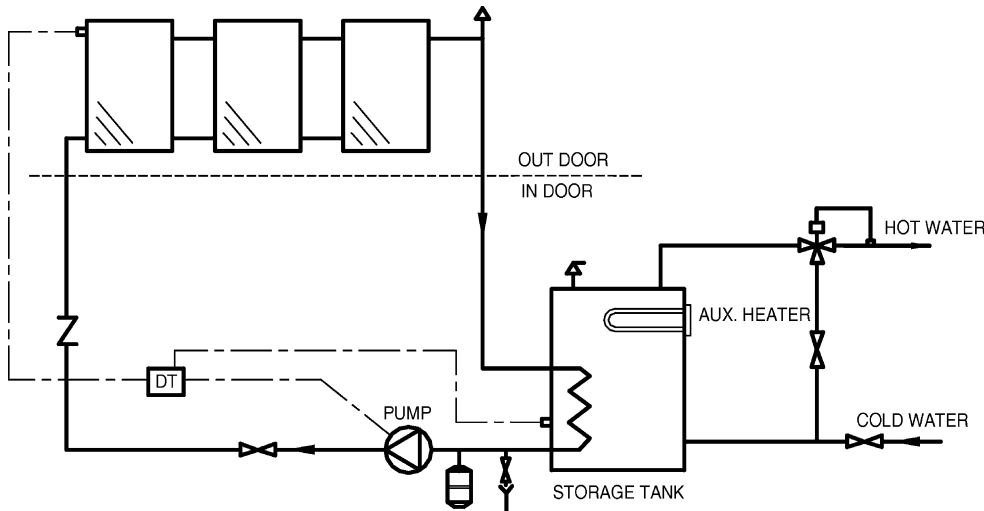


Fig. 31. Indirect water heating system.

relief valves. In the case of an unpressurised system (Fig. 32), the tank is open and vented to the atmosphere.

As the collector loop is isolated from the potable water, no valves are needed to actuate draining, and scaling is not a problem, however, the collector array and exterior piping must be adequately sloped to drain completely.

5.1.5. Air systems

Air systems are indirect water heating systems that circulate air via ductwork through the collectors to an air-to-liquid heat exchanger. In the heat exchanger, heat is transferred to the potable water, which is also circulated through the heat exchanger and returned to the storage tank. Fig. 33 shows a double storage tank system. This type of system is used most often, because air systems are generally

used for preheating domestic hot water and thus auxiliary is used only in one tank as shown.

The main advantage of the system is that air does not need to be protected from freezing or boiling, is non-corrosive, and is free. The disadvantages are that air handling equipment (ducts and fans) need more space than piping and pumps, air leaks are difficult to detect, and parasitic power consumption is generally higher than that of liquid systems.

5.2. Solar space heating and cooling

The components and subsystems discussed in Section 5.1 may be combined to create a wide variety of building solar heating and cooling systems. There are again two principal categories of such systems, passive and active.

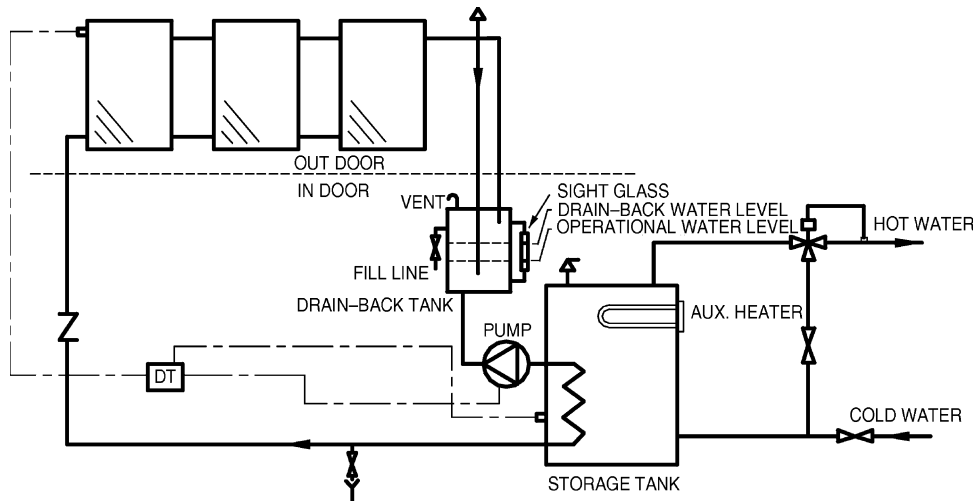


Fig. 32. Drain-back system.

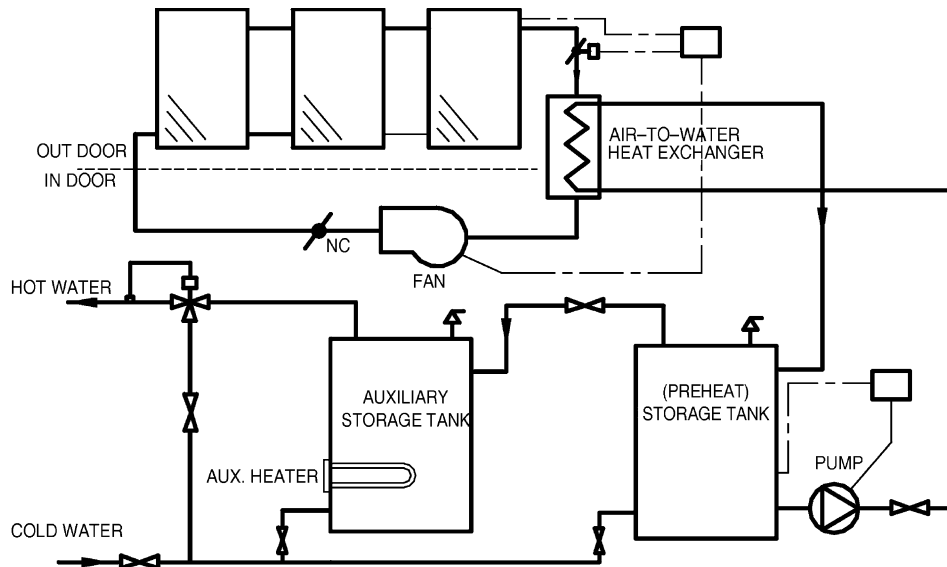


Fig. 33. Air system.

The term passive system is applied to buildings that include as integral part of the building elements, that admit, absorb, store and release solar energy and thus reduce the needs for auxiliary energy for comfort heating. As no solar collectors are employed in the passive systems in this paper, only active systems are considered.

Systems for space heating are very similar to those for water heating, described in Section 5.1, and as the same considerations for combination with an auxiliary source, boiling and freezing, controls, etc., apply to both these may not be repeated again. The most common heat transfer fluids are water, water and antifreeze mixtures and air. The load is the building to be heated. Although it is technically possible to construct a solar heating or cooling system which can satisfy 100% the design load, such a system would be non-viable since it would be oversized for most of the time. The size of the solar system may be determined by a life-cycle cost analysis described in Section 4.7.

Active solar space systems use collectors to heat a fluid, storage units to store solar energy until needed, and distribution equipment to provide the solar energy to the heated spaces in a controlled manner. A complete system includes additionally pumps or fans for transferring the energy to storage or to the load which require a continuous availability of non-renewable energy, generally in the form of electricity.

The load can be space cooling, heating, or a combination of these two with hot water supply. In combination with conventional heating equipment solar heating provides the same levels of comfort, temperature stability, and reliability as conventional systems.

Active solar energy systems can also be combined with heat pumps for water heating and/or space heating. In residential heating the solar system can be used in parallel

with a heat pump, which supplies auxiliary energy when the sun is not available. Additionally, for domestic water systems requiring high water temperatures, a heat pump can be placed in series with the solar storage tank.

During daytime the solar system absorbs solar radiation with collectors and conveys it to storage using a suitable fluid. As the building requires heat it is obtained from storage. Control of the solar system is exercised by differential temperature controllers, i.e. the controller compares the temperature of the collectors and storage and whenever the temperature difference is more than a certain value ($7\text{--}10\text{ }^{\circ}\text{C}$), the solar pump is switched ON. In locations where freezing conditions are possible to occur, a low-temperature sensor is installed on the collector which controls the solar pump when a pre-set temperature is reached. This process wastes some stored heat, but it prevents costly damages to the solar collectors.

Solar cooling of buildings is an attractive idea as the cooling loads and availability of solar radiation are in phase. Additionally, the combination of solar cooling and heating greatly improves the use factors of collectors compared to heating alone. Solar air conditioning can be accomplished by three types of systems: absorption cycles, adsorption (desiccant) cycles and solar mechanical processes. Some of these cycles are also used in solar refrigeration systems and are described in Section 5.3. The rest of this section deals with solar heating and service hot water production. It should be noted that the same solar collectors are used for both space heating and cooling systems when both are present.

A review of the various solar heating and cooling systems is presented in Ref. [139]. A review of solar and low energy cooling technologies is presented in Ref. [140].

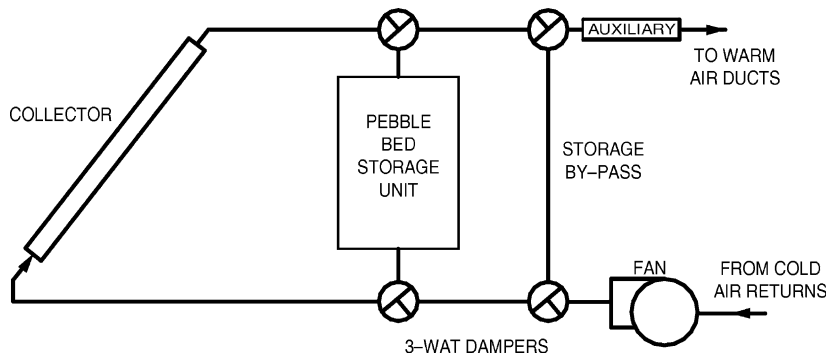


Fig. 34. Schematic of basic hot air system.

5.2.1. Space heating and service hot water

It is useful to consider solar systems as having five basic modes of operation, depending on the conditions that exist in the system at a particular time [97]:

1. If solar energy is available and heat is not needed in the building, energy gain from the collector is added to storage.
2. If solar energy is available and heat is needed in the building, energy gain from the collector is used to supply the building need.
3. If solar energy is not available, heat is needed in the building, and the storage unit has stored energy in it, the stored energy is used to supply the building need.
4. If solar energy is not available, heat is needed in the building, and the storage unit has been depleted, auxiliary energy is used to supply the building need.
5. The storage unit is fully heated, there are no loads to met, and the collector is absorbing heat.

When the last mode occurs, there is no way to use or store the collected energy, and this energy must be discarded. This can be achieved through the operation of pressure relief valves or if the stagnant temperature will not be detrimental to the collector materials, the flow of fluids is turned off, thus the collector temperature will rise until the absorbed energy is dissipated by thermal losses. This is more suitable to solar air collectors.

Additional operational modes can also be employed such as to provide service hot water. It is also possible to combine modes, i.e. to operate in more than one mode at a time. Moreover, many systems do not allow direct heating from solar collector to building, but always transfer heat from collector to storage whenever this is available and from storage to load whenever needed. In Europe solar heating systems for combined space and water heating are known as combisystems. The following sections describe the design of residential-scale installations.

5.2.2. Air systems

A schematic of a basic solar heating system using air as the heat transfer fluid, with pebble bed storage unit and

auxiliary heating source is shown in Fig. 34. The various modes of operations are achieved by appropriate positioning of the dampers. In most air systems it is not practical to combine the modes of adding energy to and removing energy from storage at the same time. Auxiliary energy can be combined with energy supplied from collector or storage to top-up the air temperature in order to cover the building load. As shown in Fig. 34, it is possible to bypass the collector and storage unit when auxiliary alone is being used to provide heat. Fig. 35 shows a more detailed schematic of an air system. Blowers, controls, means of obtaining service hot water, and more details of ducting are shown.

The advantages of using air as a heat transfer fluid are outlined in water heating air systems (Section 5.1.5). Additionally, other advantages include the high degree of stratification possible in the pebble bed which leads to lower collector inlet temperatures. The working fluid is air, and warm air heating systems are in common use. Control equipment that can be applied to those systems is also readily available. Additional to the disadvantages of water heating air systems (Section 5.1.5) is the difficulty of adding solar air conditioning to the systems. Finally, air collectors are operated at lower fluid capacitance rates and thus with lower values of F_R than the liquid heating collectors.

Usually, air heating collectors in space heating systems are operated at fixed air flow rates, thus the outlet temperature varies through the day. It is also possible to operate them at a fixed outlet temperature by varying the flow rate. This however results in reduced F_R and thus reduced collector performance when flow rates are low.

5.2.3. Water systems

There are many variations of systems used for both solar space heating and service hot water production. The basic configuration is similar to the solar water heating systems outlined in Sections 5.1.3 and 5.1.4. When used for both space and hot water production this system allows independent control of the solar collector-storage and storage-auxiliary-load loops as solar-heated water can be added to storage at the same time that hot water is removed from storage to meet building loads. Usually, a bypass is

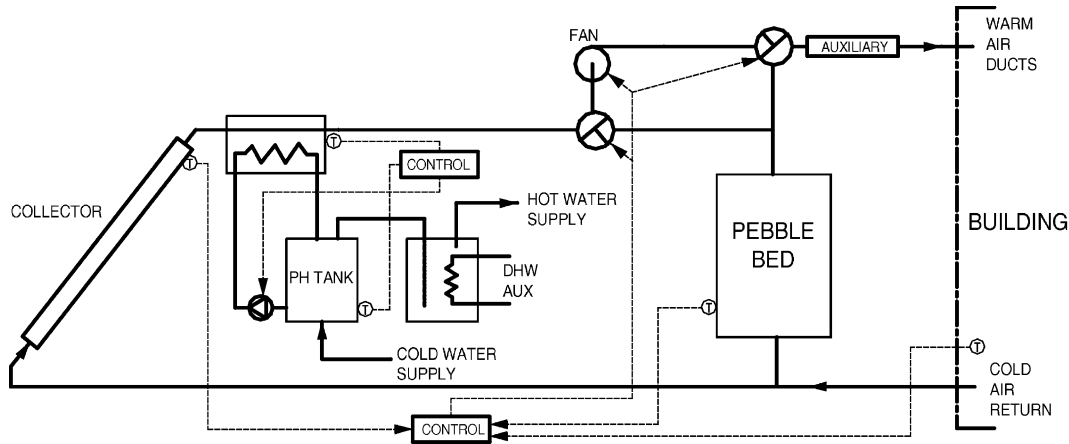


Fig. 35. Detail schematic of a solar air heating system.

provided around the storage tank to avoid heating the storage tank, which can be of considerable size, with auxiliary energy.

A detailed schematic of a liquid-based system is shown in Fig. 36 [97]. In this case a collector heat exchanger is shown between the collector and the storage tank, which allows the use of antifreeze solutions to the collector circuit. Relief valves are also required for dumping excess energy if the collector temperature reaches saturation. Means of extracting energy for service hot water are indicated. Auxiliary energy for heating is added so as to ‘top off’ that available from solar energy system.

A load heat exchanger is shown in Fig. 36 to transfer energy from the tank to the air in the heated spaces. The load heat exchanger must be adequately designed to avoid excessive temperature drop and corresponding increase in the tank and collector temperatures.

Advantages of liquid heating systems include high collector F_R , smaller storage volume, and relatively easy adaptation to supply energy to absorption air conditioners (Section 5.3.2).

5.2.4. Heat pump systems

Heat pumps use mechanical energy to transfer thermal energy from a source at a lower temperature to a sink at a higher temperature. Electrically driven heat pump heating systems have two advantages compared to electric resistance heating or expensive fuels. The heat pump’s COP is high enough to yield 11 to 15 MJ of heat for each kW h of energy supplied to the compressor [21], which saves on purchase of energy, and usefulness for air conditioning in the summer. Water-to-air heat pumps, which use solar heated water from the storage tank as the evaporator energy source, are an alternative auxiliary heat source. Use of water

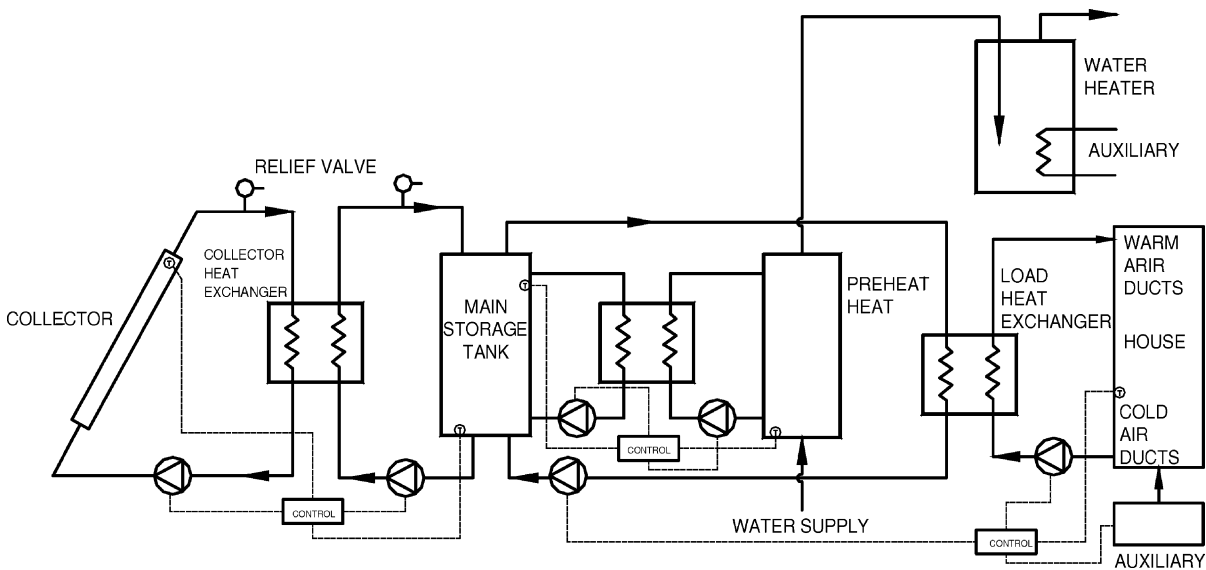


Fig. 36. Detail schematic of a solar water heating system.

involves freezing problems which need to be taken into consideration. Solar heating systems using liquids will operate at lower temperatures than conventional hydronic systems and will require more baseboard heater area to transfer heat into the building.

5.3. Solar refrigeration

Solar cooling can be considered for two related processes: to provide refrigeration for food and medicine preservation and to provide comfort cooling. Solar refrigeration systems usually operate at intermitted cycles and produce much lower temperatures (ice) than in air conditioning. When the same cycles are used in space cooling they operate on continuous cycles. The cycles employed for solar refrigeration are the absorption and adsorption. During the cooling portion of the cycles, the refrigerant is evaporated and reabsorbed. In these systems the absorber and generator are separate vessels. The generator can be integral part of the collector, with refrigerant absorbent solution in the tubes of the collector circulated by a combination of a thermosyphon and a vapour lift pump.

There are many options available which enable the integration of solar energy into the process of ‘cold’ production. Solar refrigeration can be accomplished by using either a thermal energy source supplied from a solar collector or electricity supplied from photovoltaics. This can be achieved by using either thermal adsorption or absorption units or conventional refrigeration equipment powered from photovoltaics. Solar refrigeration is employed mainly to cool vaccine stores in areas with no mains electricity and for solar space cooling.

Photovoltaic refrigeration, although uses standard refrigeration equipment which is an advantage, has not achieved widespread use because of the low efficiency and high cost of the photovoltaic cells. As photovoltaics are not covered in this paper details are given only on the solar adsorption and absorption units with more emphasis on the latter.

5.3.1. Adsorption units

Porous solids, called adsorbents, can physically and reversibly adsorb large volumes of a vapour, called the adsorbate. Though this phenomenon, called solar adsorption, was recognised in the 19th century its practical application in the field of refrigeration is relatively recent. The concentration of adsorbate vapours in a solid adsorbent is a function of the temperature of the pair, i.e. the mixture of adsorbent and adsorbate, and the vapour pressure of the latter. The dependence of adsorbate concentration on temperature, under constant pressure conditions, makes it possible to adsorb or desorb the adsorbate by varying the temperature of the mixture. This forms the basis of the application of this phenomenon in the solar-powered intermittent vapour sorption refrigeration cycle.

An adsorbent–refrigerant working pair for a solar refrigerator requires the following characteristics:

1. A refrigerant with a large latent heat of evaporation.
2. A working pair with high thermodynamic efficiency.
3. A small heat of desorption under the envisaged operating pressure and temperature conditions.
4. A low thermal capacity.

Water–ammonia has been the most widely used sorption–refrigeration pair and research has been undertaken to utilise the pair for solar-operated refrigerators. The efficiency of such systems is limited by the condensing temperature, which cannot be lowered without introduction of advanced and expensive technology. For example, cooling towers or desiccant beds have to be used to produce cold water to condensate ammonia at lower pressure. Amongst the other disadvantages inherent in using water and ammonia as the working pair are the heavy gauge pipe and vessel walls required to withstand the high pressure, the corrosiveness of ammonia, and the problem of rectification, i.e. removing water vapour from ammonia during generation. A number of different solid adsorption working pairs such as zeolite–water, zeolite–methanol, and activated carbon–methanol, have been studied in order to find the one that performed better. The activated carbon–methanol working pair was found to perform the best [19].

Because complete physical property data are available for only a few potential working pairs, the optimum performance remains unknown at the moment. In addition, the operating conditions of a solar-powered refrigerator, i.e. generator and condenser temperature, vary with its geographical location [19].

The development of three solar/biomass adsorption air conditioning refrigeration systems is presented by Critoph [141]. All systems use active carbon–ammonia adsorption cycles and the principle of operation and performance prediction of the systems are given.

Thorpe [142] presented an adsorption heat pump system which uses ammonia with granular active adsorbate. A high COP is achieved and the cycle is suitable for the use of heat from high temperature (150–200 °C) solar collectors for air conditioning.

5.3.2. Absorption units

Absorption is the process of attracting and holding moisture by substances called desiccants. Desiccants are sorbents, i.e. materials that have an ability to attract and hold other gases or liquids, which have a particular affinity for water. During absorption the desiccant undergoes a chemical change as it takes on moisture; for example, the table salt, which changes from a solid to a liquid as it absorbs moisture. The characteristic of the binding of desiccants to moisture, makes the desiccants very useful in chemical separation processes [143].

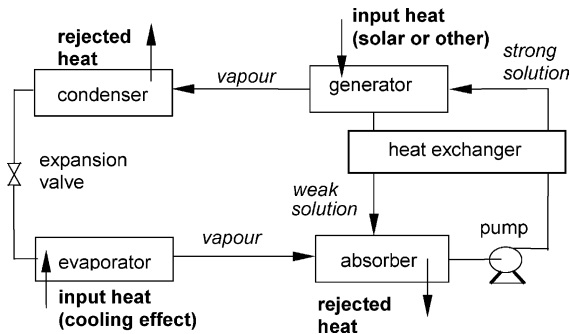


Fig. 37. Basic principle of the absorption air conditioning system.

Absorption systems are similar to vapour-compression air conditioning systems but differ in the pressurisation stage. In general an absorbent, on the low-pressure side, absorbs an evaporating refrigerant. The most usual combinations of fluids include lithium bromide–water ($\text{LiBr-H}_2\text{O}$) where water vapour is the refrigerant and ammonia–water ($\text{NH}_3\text{-H}_2\text{O}$) systems where ammonia is the refrigerant.

The pressurisation is achieved by dissolving the refrigerant in the absorbent, in the absorber section (Fig. 37). Subsequently, the solution is pumped to a high pressure with an ordinary liquid pump. The addition of heat in the generator is used to separate the low-boiling refrigerant from the solution. In this way the refrigerant vapour is compressed without the need of large amounts of mechanical energy that the vapour-compression air conditioning systems demand.

The remainder of the system consists of a condenser, expansion valve and evaporator, which function in a similar way as in a vapour-compression air conditioning system.

The $\text{NH}_3\text{-H}_2\text{O}$ system is more complicated than the $\text{LiBr-H}_2\text{O}$ system, since it needs a rectifying column that assures that no water vapour enters the evaporator where it could freeze. The $\text{NH}_3\text{-H}_2\text{O}$ system requires generator temperatures in the range of 125–170 °C with air-cooled absorber and condenser and 95–120 °C when water-cooling is used. These temperatures cannot be obtained with FPCs. The coefficient of performance (COP), which is defined as the ratio of the cooling effect to the heat input, is between 0.6 and 0.7.

The $\text{LiBr-H}_2\text{O}$ system operates at a generator temperature in the range of 70–95 °C with water used as a coolant in the absorber and condenser and has COP higher than the $\text{NH}_3\text{-H}_2\text{O}$ systems. The COP of this system is between 0.6 and 0.8 [97]. A disadvantage of the $\text{LiBr-H}_2\text{O}$ systems is that their evaporator cannot operate at temperatures much below 5 °C since the refrigerant is water vapour. Commercially available absorption chillers for air conditioning applications usually operate with a solution of lithium bromide in water and use steam or hot water as the heat source. In the market two types of chillers are available, the single and the double effect.

The single effect absorption chiller is mainly used for building cooling loads, where chilled water is required at 6–7 °C. The COP will vary to a small extent with the heat source and the cooling water temperatures. Single effect chillers can operate with hot water temperature ranging from about 80 to 150 °C when water is pressurised [118].

The double effect absorption chiller has two stages of generation to separate the refrigerant from the absorbent. Thus the temperature of the heat source needed to drive the high-stage generator is essentially higher than that needed for the single-effect machine and is in the range of 155–205 °C. Double effect chillers have a higher COP of about 0.9–1.2 [144]. Although double effect chillers are more efficient than the single-effect machines they are obviously more expensive to purchase. However, every individual application must be considered on its merits since the resulting savings in capital cost of the single-effect units can largely offset the extra capital cost of the double effect chiller.

The Carrier Corporation pioneered lithium–bromide absorption chiller technology in the United States, with early single-effect machines introduced around 1945. Due to the success of the product soon other companies joined the production. The absorption business thrived until 1975. Then the generally held belief that natural gas supplies were lessening, let to US government regulations prohibiting the use of gas in new constructions and together with the low cost of electricity led to the declination of the absorption refrigeration market [145]. Today the major factor on the decision on the type of system to install for a particular application is the economic trade-off between the different cooling technologies. Absorption chillers typically cost less to operate, but they cost more to purchase than vapour compression units. The payback period depends strongly on the relative cost of fuel and electricity assuming that the operating cost for the needed heat is less than the operating cost for electricity.

The technology was exported to Japan from the US early in the 1960s, and the Japanese manufacturers set a research and development program to improve further the absorption systems. The program led to the introduction of the direct-fired double-effect machines with improved thermal performance.

Today gas-fired absorption chillers deliver 50% of commercial space cooling load worldwide, but less than 5% in the US, where electricity-driven vapour compression machines carry the majority of the load [145].

Many researchers have developed solar assisted absorption refrigeration systems. Most of them have been produced as experimental units and computer codes were written to simulate the systems. Some of these designs are presented here.

Hammad and Audi [146] described the performance of a non-storage, continuous, solar operated absorption refrigeration cycle. The maximum ideal COP of the system was

determined to be equal to 1.6, while the peak actual COP was determined to be equal to 0.55.

Haim et al. [147] performed a simulation and analysis of two open-cycle absorption systems. Both systems comprise a closed absorber and evaporator as in conventional single stage chillers. The open part of the cycle is the regenerator, used to reconcentrate the absorber solution by means of solar energy. The analysis was performed with a computer code developed for modular simulation of absorption systems under varying cycle configurations (open- and closed-cycle systems) and with different working fluids. Based on the specified design features, the code calculates the operating parameters in each system. Results indicate a definite performance advantage of the direct-regeneration system over the indirect one.

Hawladar et al. [148] developed a lithium bromide absorption cooling system employing an $11 \times 11 \text{ m}^2$ collector/regenerator unit. They also have developed a computer model, which they validated against real experimental values with good agreement. The experimental results showed a regeneration efficiency varying between 38 and 67% and the corresponding cooling capacities ranged from 31 to 72 kW.

Ameel et al. [149] give performance predictions of alternative low-cost absorbents for open cycle absorption using a number of absorbents. The most promising of the absorbents considered, was a mixture of two elements, lithium chloride and zinc chloride. The estimated capacities per unit absorber area were 50–70% less than those of lithium bromide systems.

Ghaddar et al. [150] presented modelling and simulation of a solar absorption system for Beirut. The results showed that, for each ton of refrigeration, it is required to have a minimum collector area of 23.3 m^2 with an optimum water storage capacity ranging from 1000 to 1500 l, for the system to operate solely on solar energy for about 7 h per day. The monthly solar fraction of total energy use in cooling is determined as a function of solar collector area and storage tank capacity. The economic analysis performed showed that the solar cooling system is marginally competitive only when it is combined with domestic water heating.

Erhard and Hahne [151] simulated and tested a solar-powered absorption cooling machine. The main part of the device is an absorber/desorber unit, which is mounted inside a concentrating solar collector. Results obtained from field tests are discussed and compared with the results obtained from a simulation program developed for this purpose.

Hammad and Zurigat [152] described the performance of a 1.5 ton solar cooling unit. The unit comprises a 14 m^2 flat-plate solar collector system and five shell and tube heat exchangers. The unit was tested in April and May in Jordan. The maximum value obtained for actual COP was 0.85.

Zinian and Ning [153] describe a solar absorption air conditioning system which uses an array of 2160 evacuated tubular collectors of total aperture area of 540 m^2 and a LiBr absorption chiller. Thermal efficiencies of the collector

array are 40% for space cooling, 35% for space heating and 50% for domestic water heating. It was found that the cooling efficiency of the entire system is around 20%.

A new family of ICPC designs was developed by Winston et al. [154] which allows a simple manufacturing approach to be used and solves many of the operational problems of previous ICPC designs. A low concentration ratio is used that requires no tracking together with an off-the-shelf 20 ton double effect LiBr direct fired absorption chiller, modified to work with hot water. The new ICPC design and double effect chiller was able to produce cooling energy for the building using a collector field that was about half the size of that required for a more conventional collector and chiller.

A method to design, construct and evaluate the performance of a single stage lithium bromide–water absorption machine is presented in Ref. [155]. In this the necessary heat and mass transfer relations and appropriate equations describing the properties of the working fluids are specified. Information on designing the heat exchangers of the LiBr–water absorption unit is also presented. Single-pass vertical-tube heat exchangers have been used for the absorber and for the evaporator. The solution heat exchanger was designed as a single-pass annulus heat exchanger. The condenser and the generator were designed using horizontal tube heat exchangers.

5.4. Industrial process heat

Beyond the low temperature applications there are several potential fields of application for solar thermal energy at a medium and medium–high temperature level (80–240 °C). The most important of them is heat production for industrial processes. The industrial heat demand constitutes about 15% of the overall demand of final energy requirements in the southern European countries. The present energy demand in the EU for medium and medium-high temperatures is estimated to be about 300 T W h/yr [117].

From a number of studies on industrial heat demand, several industrial sectors have been identified with favourable conditions for the application of solar energy. The most important industrial processes using heat at a mean temperature level are: sterilising, pasteurising, drying, hydrolysing, distillation and evaporation, washing and cleaning, and polymerisation. Some of the most important processes and the range of the temperatures required for each are outlined in Ref. [20].

Large-scale solar applications for process heat benefit from the effect of scale. Therefore, the investment costs should be comparatively low, even if the costs for the collector are higher. One way to cause economically easy terms is to design systems without heat storage, i.e. the solar heat is fed directly into a suitable process (fuel saver). In this case the maximum rate at which the solar energy system delivers energy must not be appreciably larger than the rate

at which the process uses energy. This system however cannot be cost-effective in cases, where heat is needed at the early or late hours of the day or at nighttimes when the industry operates on a double shift basis.

The types of industries that spent most of the energy are the food industry and the manufacture of non-metallic mineral products. Particular types of food industries, which can employ solar process heat, are the milk and cooked pork meats (sausage, salami, etc.) industries and breweries. Most of the process heat is used in food and textile industry for such diverse applications as drying, cooking, cleaning, extraction and many others. Favourable conditions exist in food industry, because food treatment and storage are processes with high energy consumption and high running time. Temperature for these applications may vary from near ambient to those corresponding to low-pressure steam, and energy can be provided either from flat-plate or low concentration ratio concentrating collectors.

The principle of operation of components and systems outlined in the previous sections apply directly to industrial process heat applications. The unique features of the latter lie in the scale on which they are used, and the integration of the solar energy supply system with the auxiliary energy source and the industrial process.

The two primary problems that need to be considered when designing an industrial process heat application concern the type of energy to be employed and the temperature at which the heat is to be delivered. For example, if a process requires hot air for direct drying, an air heating system is probably the best solar energy system option. If hot water is needed for cleaning in food processing, the solar energy will be a liquid heater. If steam is needed to operate an autoclave or sterilizer, the solar energy system must be designed to produce steam probably with concentrating collectors. Another important factor in determination of the most suitable system for a particular application is the temperature of the fluid to the collector. Other requirements concern the fact that the energy may be needed at particular temperature or over a range of temperatures and possible sanitation requirements

of the plant that must also be met as for example in food processing applications.

The investments in industrial processes are generally large, and the transient and intermittent characteristics of solar energy supply are so unique that the study of options in solar industrial applications can be done by modelling methods (Section 4.6) at costs that are very small compared to the investments.

Many industrial processes use large amounts of energy in small spaces. If solar is to be considered for these applications, the location of collectors can be a problem. It may be necessary to locate the collector arrays on adjacent buildings or grounds, resulting in long runs of pipes or ducts. Where feasible, collectors can be mounted on the roof of a factory especially when no land area is available. In this case shading between adjacent collector rows should be avoided and considered. However, collector area may be limited by roof area and orientation. Existing buildings are generally not designed or orientated to accommodate arrays of collectors, and in many cases structures to support collector arrays must be added to the existing structures. New buildings can be readily designed, often at little or no incremental cost, to allow for collector mounting and access.

In a solar process heat system, interfacing of the collectors with conventional energy supplies must be done in a way compatible with the process. The easiest way to accomplish this is by using heat storage, which can also allow the system to work in periods of low irradiation and/or nighttime.

The central system for heat supply in most factories uses hot water or steam at a pressure corresponding to the highest temperature needed in the different processes. Hot water or low pressure steam at medium temperatures ($< 150\text{ }^{\circ}\text{C}$) can be used either for preheating of water (or other fluids) used for processes (washing, dyeing, etc.) or for steam generation or by direct coupling of the solar system to an individual process working at temperatures lower than that of the central steam supply (Fig. 38). In the case of water preheating, higher efficiencies are obtained due to the low input temperature to the solar system, thus low-technology

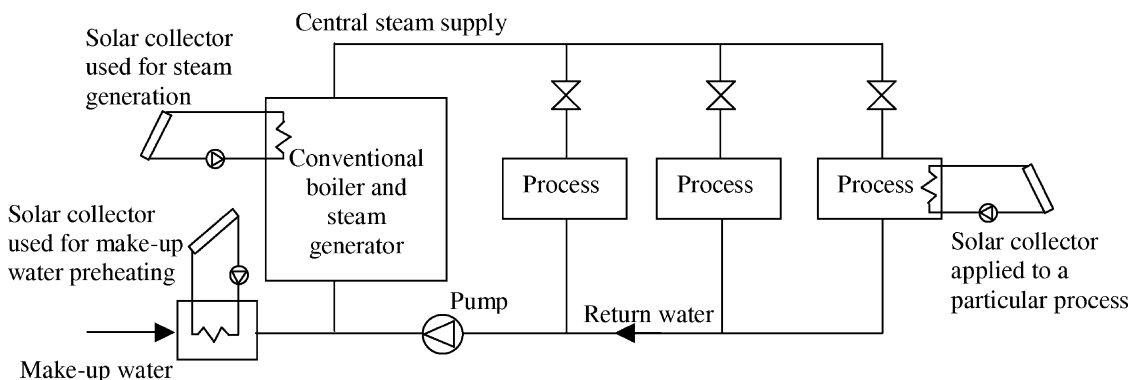


Fig. 38. Possibilities of combining the solar system with the existing heat supply.

collectors can work effectively and the required load supply temperature has no or little effect on the performance of the solar system.

A number of research papers on the subject have been presented recently by a number of researchers. Norton [156] presented the most common applications of industrial process heat. In particular the history of solar industrial and agricultural process applications were presented and practical examples were described.

A system for solar process heat for decentralised applications in developing countries was presented by Spate et al. [157]. The system is suitable for community kitchen, bakeries and post-harvest treatment. The system employs a fix-focus parabolic collector, a high temperature FPC and a pebble bed oil storage.

Benz et al. [158] presented the planning of two solar thermal systems producing process heat for a brewery and a dairy in Germany. In both industrial processes the solar yields were found to be comparable to the yields of solar systems for domestic solar water heating or space heating. In another paper, Benz et al. [159] presented a study for the application of non-concentrating collectors for food industry in Germany. In particular the planning of four solar thermal systems producing process heat for a large and a small brewery, a malt factory and a dairy are presented. In the breweries, the washing machines for the returnable bottles were chosen as a suitable process to be fed by solar energy, in the dairy the spray-dryers for milk and whey powder production and in the malt factory the wither and kiln processes. Up to 400 kW h/m² per annum were delivered from the solar collectors, depending on the type of collector.

5.4.1. Solar industrial air and water systems

There are two types of applications employing solar air collectors the open circuit, and the recirculating applications. In open circuit, heated ambient air is used in industrial applications where because of contaminants recirculation of air is not possible. Examples are drying, paint spraying, and supplying fresh air to hospitals. It should be noted that heating of outside air is an ideal operation for the collector, as it operates very close to ambient temperature, thus more efficiently.

In recirculating air systems a mixture of recycled air from the dryer and ambient air is supplied to the solar collectors. Solar-heated air supplied to a drying chamber, can be applied to a variety of materials, including food crops, and lumber. In these applications, adequate control of the rate of drying, which can be obtained by controlling the temperature and humidity of the supply air, can lead to improved product quality.

Similarly, there are also two types of applications employing solar water collectors the once-through systems and the recirculating water heating applications. The latter are exactly similar to domestic water heating systems presented in Section 5.1. Once-through systems are employed in cases where large quantities of water are

used for cleaning in food industries, and recycling of used water is not practical because of the contaminants picked up by the water in the cleaning process.

5.4.2. Solar steam generation systems

PTC are frequently employed for solar steam generation, because relatively high temperatures can be obtained without any serious degradation in the collector efficiency. Low temperature steam can be used in industrial applications, sterilisation, and for powering desalination evaporators.

Three methods have been employed to generate steam using PTC [160]:

1. The steam-flash concept, in which pressurised water is heated in the collector and then flashed to steam in a separate vessel.
2. The direct or in situ concept, in which two phase flow is allowed in the collector receiver so that steam is generated directly.
3. The unfired-boiler concept, in which a heat-transfer fluid is circulated through the collector and steam is generated via heat-exchange in an unfired boiler.

All these systems have certain advantages and disadvantages. In a steam-flash system, shown schematically in Fig. 39, water, pressurised to prevent boiling, is circulated through the collector and then flashed across a throttling valve into a flash vessel. Treated feedwater input maintains the level in the flash vessel and the subcooled liquid is recirculated through the collector. The in situ boiling concept, shown in Fig. 40, uses a similar system configuration without a flash valve. Subcooled water is heated to boiling and steam forms directly in the receiver tube. Capital costs associated with a direct-steam and a flash-steam system would be approximately the same [161].

Although both systems use water, a superior heat transport fluid, the in situ boiling system is more advantageous. The flash system uses a sensible heat change in the working fluid, which makes the temperature differential across the collector relatively high. The rapid increase in water vapour pressure with temperature requires

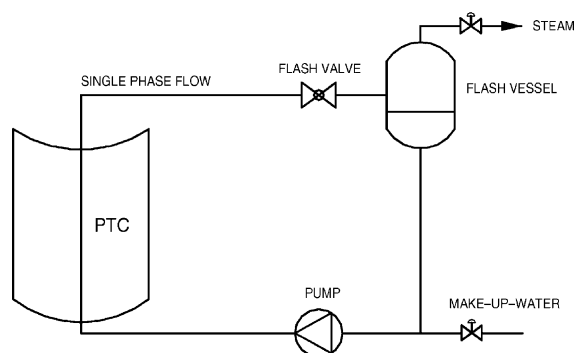


Fig. 39. The steam-flash steam generation concept.

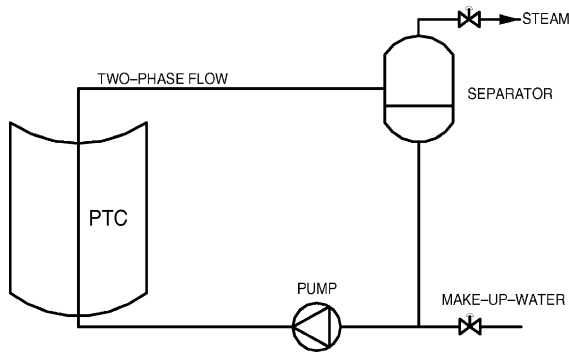


Fig. 40. The direct steam generation concept.

corresponding increase in system operating pressure to prevent boiling. Increased operating temperatures reduce the thermal efficiency of the solar collector. Increased pressures within the system require a more robust design of collector components, such as receivers and piping. The differential pressure over the delivered steam pressure required to prevent boiling is supplied by the circulation pump and is irreversibly dissipated across the flash valve. When boiling occurs in the collectors, as in an in situ boiler, the system pressure drop and consequently, electrical power consumption is greatly reduced. In addition, the latent heat-transfer process minimises the temperature rise across the solar collector. Disadvantages of in situ boiling are the possibility of a number of stability problems [162] and the fact that even with a very good feedwater treatment system, scaling in the receiver is unavoidable. In multiple row collector arrays, the occurrence of flow instabilities could result in loss of flow in the affected row. This in turn could result in tube dryout with consequent damage of the receiver selective coating. No significant instabilities were reported by Hurtado and Kast [161] when experimentally testing a single row 36 m system. Recently, once through systems are developed on a pilot scale for direct steam generation in which PTC are used inclined at 2–4° [163].

A diagram of an unfired boiler system is shown in Fig. 41. In this system, the heat-transfer fluid should be non-freezing and non-corrosive, system pressures are low and control is

straightforward. These factors largely overcome the disadvantages of water systems, and are the main reasons for the predominant use of heat-transfer oil systems in current industrial steam-generating solar systems.

The major disadvantage of the system result from the characteristics of the heat-transfer fluid. These fluids are hard to contain, and most heat-transfer fluids are flammable. Decomposition, when the fluids are exposed to air, can greatly reduce ignition-point temperatures, and leaks into certain types of insulation can cause combustion at temperatures that are considerably lower than measured self-ignition temperatures. Heat-transfer fluids are also relatively expensive and present a potential pollution problem that makes them unsuitable for food industry applications [164]. Heat-transfer fluids have much poorer heat-transfer characteristics than water. They are more viscous at ambient temperatures, are less dense, and have lower specific heats and thermal conductivities than water. These characteristics mean that higher flow rates, higher collector differential temperatures, and greater pumping power are required to obtain the equivalent quantity of energy transport when compared to a system using water. In addition, heat-transfer coefficients are lower, so there is a larger temperature differential between the receiver tube and the collector fluid. Higher temperatures are also necessary to achieve cost effective heat exchange. These effects result in reduced collector efficiency.

For every application the suitable system has to be selected by taking into consideration all the above factors and constrains.

5.5. Solar desalination systems

Water is one of the most abundant resources on earth, covering three-fourths of the planet's surface. About 97% of the earth's water is salt water in the oceans; 3% of all fresh water is in ground water, lakes and rivers, which supply most of human and animal needs. Water is essential to life. The importance of supplying potable water can hardly be overstressed. Man has been dependent on rivers, lakes and underground water reservoirs for fresh water requirements in domestic life, agriculture and industry. However, rapid

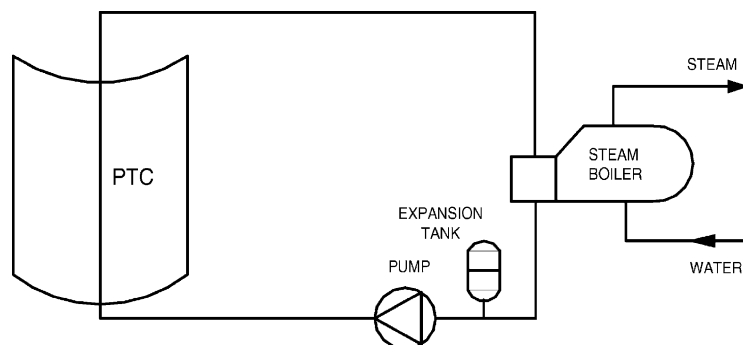


Fig. 41. The unfired-boiler steam generation concept.

industrial growth and the population explosion all over the world have resulted in a large escalation of demand for fresh water. Added to this is the problem of pollution of rivers and lakes by industrial wastes and the large amounts of sewage discharged. On a global scale, manmade pollution of natural sources of water is becoming the single largest cause for fresh water shortage [17]. The only nearly inexhaustible sources of water are the oceans. Their main drawback, however, is their high salinity. It would be attractive to tackle the water-shortage problem with desalination of this water.

Desalination can be achieved by using a number of techniques. These may be classified into the following categories:

- (i) phase-change or thermal processes; and
- (ii) membrane or single-phase processes.

In Table 11, the most important technologies in use are listed. In the phase-change or thermal processes, the distillation of sea water is achieved by utilising a thermal energy source. The thermal energy may be obtained from a conventional fossil-fuel source, nuclear energy or from a non-conventional solar energy source. In the membrane processes, electricity is used either for driving high pressure pumps or for ionisation of salts contained in the sea water.

Desalination processes require significant quantities of energy to achieve separation. This is highly significant as it is a recurrent cost which few of the water-short areas of the world can afford. Many countries in the Middle East, because of oil income, have enough money to invest and run desalination equipment. People in many other areas of the world have neither the cash nor the oil resources to allow them to develop in a similar manner. It is estimated that the installed capacity of desalinated water systems in year 2000 is about 25 million m³/day, which is expected to increase drastically in the next decades. The dramatic increase in desalinated water supply will create a series of problems, the most significant of which are those related to energy

consumption. It has been estimated that the production of 25 million m³/day requires 230 million tons of oil per year. Even if oil were much more widely available, could we afford to burn it on the scale needed to provide everyone with fresh water? Given current understanding of the greenhouse effect and the importance of CO₂ levels, this use of oil is debatable. Thus, apart from satisfying the additional energy demand, environmental pollution would be a major concern. Fortunately, there are many parts of the world that are short of water but have exploitable renewable sources of energy that could be used to drive desalination processes.

Solar energy can be used for sea-water desalination either by producing the thermal energy required to drive the phase-change processes or by producing electricity required to drive the membrane processes. Solar desalination systems are thus classified into two categories, i.e. direct and indirect collection systems. As their name implies, direct collection systems use solar energy to produce distillate directly in the solar collector, whereas in indirect collection systems, two sub-systems are employed (one for solar energy collection and one for desalination). Conventional desalination systems are similar to solar systems since the same type of equipment is applied. The prime difference is that in the former, either a conventional boiler is used to provide the required heat or mains electricity is used to provide the required electric power, whereas in the latter, solar energy is applied.

A representative example of direct collection systems is the conventional solar still, which uses the greenhouse effect to evaporate salty water. It consists of a basin, in which a constant amount of seawater is enclosed in a veeshaped glass envelope. The sun's rays pass through the glass roof and are absorbed by the blackened bottom of the basin. As the water is heated, its vapour pressure is increased. The resultant water vapour is condensed on the underside of the roof and runs down into the troughs, which conduct the distilled water to the reservoir. The still acts as a heat trap because the roof is transparent to the incoming sunlight, but it is opaque to the infrared radiation emitted by the hot water (greenhouse effect). The roof encloses all of the vapour, prevents losses and, at the same time, keeps the wind from reaching the salty water and cooling it. The stills require frequent flushing, which is usually done during the night. Flushing is performed to prevent salt precipitation [165]. Design problems encountered with solar stills are brine depth, vapour tightness of the enclosure, distillate leakage, methods of thermal insulation, and cover slope, shape and material [165,166]. A typical still efficiency, defined as the ratio of the energy utilised in vaporising the water in the still to the solar energy incident on the glass cover, is 35% (maximum) and daily still production is about 34 l/m² [167]. The interested readers can find more details and a survey of indirect systems in Ref. [18]. For these systems a number of collectors ranging from stationary to low concentration ratio PTC can be used according to the temperature required by the desalination process. The usual temperature that

Table 11
Desalination processes

Phase-change processes	Membrane processes
(1) Multistage flash (MSF)	(1) Reverse osmosis (RO)
(2) Multiple effect boiling (MEB)	RO without energy
(3) Vapour compression (VC)	recovery
(4) Freezing	RO with energy
(5) Humidification/dehumidification	recovery (ER-RO)
(6) Solar stills	(2) Electrodialysis (ED)
Conventional stills	
special stills	
wick-type stills	
multiple-wick-type stills	

the thermal desalination evaporators work is around 100 °C. The use of PTC for seawater desalination is described in Ref. [168].

5.6. Solar thermal power systems

Conversion of solar to mechanical and electrical energy has been the objective of experiments for more than a century, starting from 1872 when Mouchot exhibited a steam-powered printing press at the Paris Exposition. The idea is to use concentrating collectors to produce and supply steam to heat engines. A historical review of this and other experiments is given in Section 1. Much of the early attention to solar thermal–mechanical systems was for small scale applications (up to 100 kW) and most of them were designed for water pumping. Since 1975 there have been several large-scale power systems constructed and operated. Commercial plants of 30 and 80 MW electric (peak) generating capacity are nowadays in operation for more than a decade.

The process of conversion of solar to mechanical and electrical energy by thermal means is fundamentally similar to the traditional thermal processes. These systems differ from the ones considered so far as these operate at much higher temperatures.

This section is concerned with generation of mechanical and electrical energy from solar energy by processes based mainly on concentrating collectors and heat engines. There are also another three kinds of power systems, which are not covered in this paper. These are the photovoltaic cells for the direct conversion of solar to electrical energy by solid state devices, solar-biological processes that produce fuels for operation of conventional engines or power plants and solar ponds.

The basic process for conversion of solar to mechanical energy is shown schematically in Fig. 42. Energy is collected by concentrating collectors, stored (if appropriate), and used to operate a heat engine. The main problem of these systems is that the efficiency of the collector is reduced as its operating temperature increases, whereas the efficiency of the heat engine increases as its operating

temperature increases. The maximum operating temperature of stationary collectors is low relative to desirable input temperatures of heat engines, therefore concentrating collectors are used exclusively for such applications.

Identifying the best available sites for the erection of solar thermal power plants is a basic issue of project development. Recently the planning tool STEPS was developed by the German Aerospace Centre (DLR) [169], which uses satellite and Geographic Information System (GIS) data in order to select a suitable site. The factors taken into account are the slope of the terrain, land use (forest, desert, etc.), geomorphological features, hydrographical features, the proximity to infrastructure (power lines, roads, etc.) and of course solar irradiation of the area.

Three system architectures have been used for such applications, the PTC system, the power tower system, and the dish system. These are described in this section.

5.6.1. Parabolic trough collector systems

Several parabolic trough solar thermal systems have been build and operated throughout the world. Most of these systems provide process steam to industry. They displace fossil fuels such as oil or natural gas as the energy source for producing steam. These systems incorporate fields of PTC having aperture areas from 500 to 5000 m². Most of these systems however supply industrial process steam from 150 to 200 °C.

The most current example of power production using parabolic trough is the nine commercial solar energy generating systems (SEGS). The total installed capacity of SEGS is 354 MW and are designed, installed and operated in the Mojave Desert of Southern California. These plants are based on large parabolic trough concentrators providing steam to Rankine power plants. The first of these plants is a 14 MW electric (MW_e) plant, the next six are 30 MW_e plants, and the two latest are 80 MW_e [65].

The plants can supply peaking power, using solely solar energy, solely natural gas, or a combination of the two, regardless of time or weather, within the constraint of the annual limit on gas use. The most critical time for power generation and delivery, and the time in which the selling price of the power per kW h is highest. This is between noon

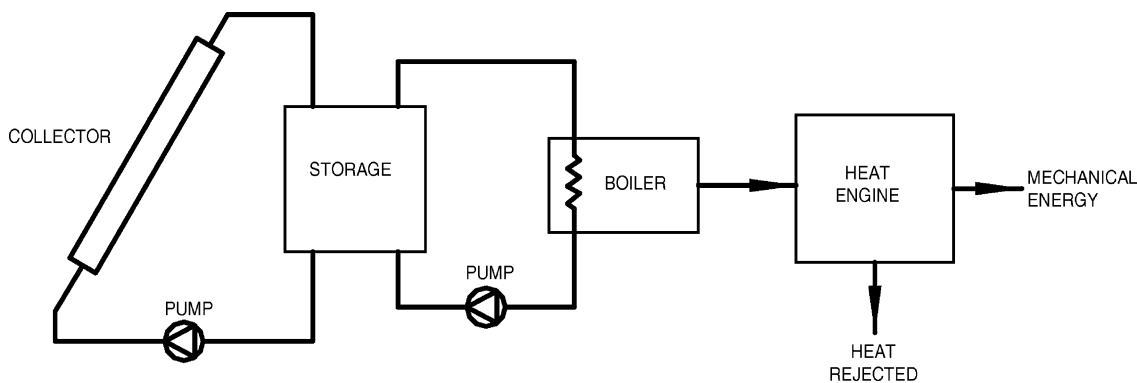


Fig. 42. Schematic of a solar-thermal conversion system.

and 6 p.m. in the months from June to September. Operating strategy is designed to maximise solar energy use. Natural gas is used to provide power during cloudy periods. The turbine-generator efficiency is best at full load, therefore the use of natural gas supplement to allow full-load operation maximises plant output.

A schematic of a typical plant is shown in Fig. 43. As it can be seen the solar and natural gas loops are in parallel to allow operation with either or both of the energy resources. The plants do not have energy storage facilities. The major components in the systems are the collectors, the fluid transfer pumps, the power generation system, the natural gas auxiliary subsystem, and the controls.

A synthetic heat transfer fluid is heated in the collectors and is piped to the solar steam generator and superheater where it generates the steam which drives the turbine. Reliable high-temperature circulating pumps are critical to the success of the plants, and significant engineering effort has gone into assuring that pumps will stand the high fluid temperatures and temperature cycling. The normal temperature of the fluid returned to the collector field is 304 °C and that leaving the field is 390 °C. Experience indicates that availability of the collector fields is about 99% [97].

The power generation system consists of a conventional Rankine cycle reheat steam turbine with feedwater heaters deaerators, etc. The condenser cooling water is cooled in forced draft cooling towers.

The reflectors are made of black-silvered, low-iron float-glass panels which are shaped over parabolic forms. Metallic and lacquer protective coatings are applied to the back of the silvered surface, and no measurable degradation of the reflective material has been observed [97]. The glass is mounted on truss structures, with the position of large arrays of modules adjusted by hydraulic drive motors. The reflectance of the mirrors is 0.94 when clean. Maintenance of high reflectance is critical to plant operation. With a total of $2.32 \times 10^6 \text{ m}^2$ of mirror area, mechanised equipment has been developed for cleaning the reflectors, which is done regularly at intervals of about 2 weeks.

The receivers are 70 mm diameter steel tubes with cement selective surfaces surrounded by a vacuum glass jacket in order to minimise heat losses. The selective surfaces have an absorptance of 0.96 and an emittance of 0.19 at 350 °C.

The collectors rotate about horizontal north–south axes, an arrangement which results in slightly less energy incident on them over the year but favours summertime operation when peak power is needed and its sale brings the greatest revenue. Tracking of the collectors is controlled by a system that utilise an optical system to focus radiation on two light-sensitive sensors. Any imbalance of radiation falling on the sensors causes corrections in the positioning of the collectors. There is a sensor and controller on each collector assembly, the resolution of the sensor is 0.5°.

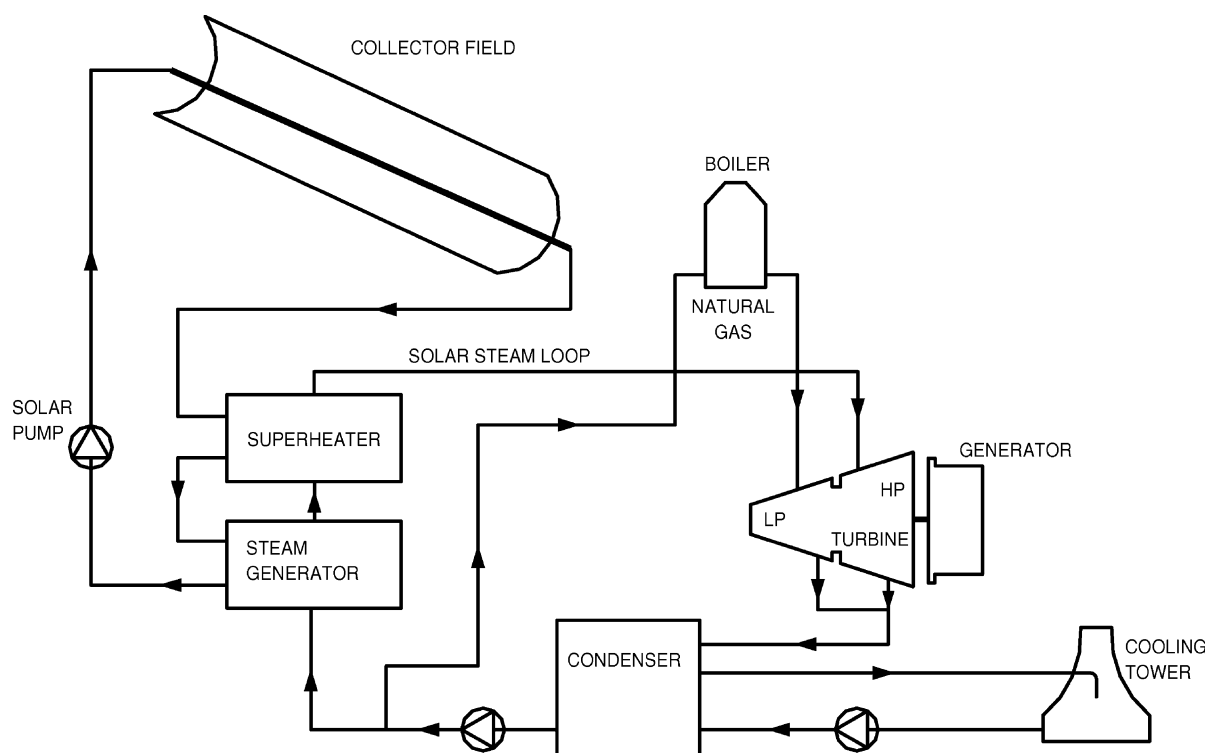


Fig. 43. Typical schematic of SEGs plants.

A promising new configuration that combined SEGS parabolic-trough technology with a gas-turbine combined-cycle power plant is conceived to meet utility needs for continuous operation and peaking power with minimal environmental damage. Such a hybrid combined-cycle plant uses the solar field as the evaporation stage of an integrated system, with the gas-turbine exhaust being recycled for superheating and preheating, thus, the solar field serves as the boiler in an otherwise conventional combined-cycle plant. This approach has several advantages:

1. The direct steam generation system can take advantage of the steam turbine, generator, and other facilities of the combined-cycle plant at a modest increase in capital cost.
2. Adding the direct steam generation facility requires no additional operators or electrical interconnection equipment.
3. Thermodynamic efficiencies are maximized because steam is evaporated outside the waste-heat recovery system; only the remaining thermal-heat exchange processes take place in the recovery heat exchanger. Thus, higher working-steam conditions can be achieved for the same degree of heat use which increases overall cycle efficiency.

This new configuration is preferable from the perspective of the second law of thermodynamics because the solar field reduces the production of entropy in the system.

5.6.2. Power tower systems

In power tower systems, heliostats reflect and concentrate sunlight onto a central tower-mounted receiver where the energy is transferred to a heat transfer fluid. This energy is then passed either to storage or to power-conversion systems which convert the thermal energy into electricity and supply it to the grid.

The major components of the system are the heliostat field, the heliostat controls, the receiver, the storage system, and the heat engine which drives the generator. The heliostat design must ensure that radiation is delivered to the receiver at the desired flux density at minimum cost. Various receiver shapes have been considered, including cavity receivers and cylindrical receivers. The optimum shape is a function of the radiation intercepted and absorbed, thermal losses, receiver cost and design of the heliostat field. For a large heliostat field a cylindrical receiver has advantages when used with Rankine cycle engines, particularly for radiation from heliostats at the far edges of the field. Cavity receivers with larger tower height to heliostat field area ratios are used for higher temperatures required for the operation of Brayton cycle turbines.

As the collector represents the largest cost in the system an efficient engine is justified to obtain maximum useful conversion of the collected energy. Several possible thermodynamic cycles can be considered. Brayton or

Stirling gas cycle engines operated at inlet temperatures of 800–1000 °C provide high engine efficiencies, but are limited by low gas heat transfer coefficients and by practical constraints on collector design (i.e. the need for cavity receivers) imposed by the requirements of very high temperatures. Rankine cycle engines employing turbines driven from steam generated in the receiver at 500–550 °C and have several advantages over the Brayton cycle. Heat transfer coefficients in the steam generator are high, allowing the use of high energy densities and smaller receivers. Cavity receivers are not needed and cylindrical receivers that are usually employed permit larger heliostat fields to be used. The use of reheat cycles improves steam turbine performance, but entail mechanical design problems. Additionally, it is also possible to use steam turbines with steam generated from an intermediate heat transfer fluid circulated through the collector or boiler. With such systems the fluids could be molten salts or liquid metals, and cylindrical receivers could be operated at around 600 °C. In fact, these indirect systems are the only ones that can be combined with thermal storage.

Power tower plants are defined by the options chosen for a heat transfer fluid, for the thermal storage medium and for the power-conversion cycle. The heat transfer fluid may be water/steam, molten nitrate salt, liquid metals or air. Thermal storage may be provided by phase change materials or ceramic bricks. Power tower systems usually achieve concentration ratios of 300–1500, can operate at temperatures up to 1500 °C, and are quite large, generally 10 MW_e or more.

Power tower systems currently under development use either nitrate salt or air as the heat transfer medium. In the USA, the Solar One plant in Barstow, CA was originally a water/steam plant and is now converted to Solar Two, a nitrate salt system. The use of nitrate salt for storage allow the plant to avoid tripping off line during cloudy periods and also allow the delivery of power after sunset. The heliostat system consists of 1818 individually oriented reflectors, each consisting of 12 concave panels with a total area of 39.13 m², for a total array of 71 100 m². The reflective material is back-silvered glass. The receiver is a single pass superheated boiler, generally cylindrical in shape, 13.7 m high, 7 m in diameter, with the top 90 m above the ground. It is an assembly of 24 panels, each 0.9 m wide and 13.7 m long. Six of the panels on the south side, which receives the least radiation, are used as feedwater preheaters and the balance are used as boilers. The panels are coated with a non-selective flat black paint which was heat cured in place with solar radiation. The receiver was designed to produce 50 900 kg/h of steam at 516 °C with absorbing surface operating at a maximum temperature of 620 °C [66].

Meanwhile the PHOEBUS consortium, a European industry group, is leading the way with air-based systems. Gaseous heat transfer media allow for significantly higher receiver outlet temperatures, but require higher operating pressures. Pressure-tolerant gas-cooled ceramic-tube

receivers have, however, relatively high heat losses compared to water/steam or advance receivers. The PHOEBUS consortium is developing a novel Technology Solar Air (TSA) receiver, a volumetric air receiver which distributes the heat-exchanging surface over a three-dimensional volume and operates at ambient pressures. Because of its relative simplicity and safety, these plants can be used for applications in developing countries [170].

Future work will concentrate on the scaling up of the nitrate salt and TSA/PHOEBUS systems. The target size for nitrate salt plants in south-west USA is 100–200 MW_e, while a 30 MW_e plant is the aim for the PHOEBUS consortium. In addition to these two systems, a 20 MW Solgas plant, using a combined cycle plant with a solar power tower back-up, is planned for southern Spain [66].

Recent research and development efforts have focused on polymer reflectors and stretched-membrane heliostats. A stretched-membrane heliostat consists of a metal ring, across which two thin metal membranes are stretched. A focus control system adjusts the curvature of the front membrane, which is laminated with a silvered-polymer reflector, usually by adjusting the pressure (a very slight vacuum) in the plenum between the two membranes. Stretched-membrane heliostats are potentially much cheaper than glass/metal heliostats because they weigh less and have fewer parts.

5.6.3. Parabolic dish systems

A parabolic dish concentrates solar energy onto a receiver at its focal point. The receiver absorbs the energy and converts it into thermal energy. This can be used directly as heat or supply for power generation. The thermal energy can either be transported to a central generator for conversion, or it can be converted directly into electricity at a local generator coupled to the receiver.

Dishes track the sun on two axes, and thus they are the most efficient collector systems because they are always focussed. Concentration ratios usually range from 600 to 2000, and they can achieve temperatures in excess of 1500 °C. Rankine-cycle engines, Brayton-cycle engines, and sodium-heat engines have been considered for systems using dish-mounted engines the greatest attention though was given to Stirling-engine systems.

Current developments in the USA and Europe are focussed on 7.5 kW_e systems for remote applications. In Europe, three dish/Stirling systems are demonstrated at PSA in Spain, whereas in the USA a program has been set to demonstrate water pumping and village power applications [171]. Stretched-membrane concentrators are currently the focus of considerable attention because they are most likely to achieve the goals of low production cost and adequate performance. Both multifaceted and single-facet designs are being pursued. Recently, a 7-meter single-facet dish was developed, which demonstrated excellent performance in tests.

The greatest challenge facing distributed-dish systems is developing a power-conversion unit, which would have low capital and maintenance costs, long life, high conversion efficiency, and the ability to operate automatically. Several different engines, such as gas turbines, reciprocating steam engines, and organic Rankine engines, have been explored, but in recent years, most attention has been focused on Stirling-cycle engines. These are externally heated piston engines in which heat is continuously added to a gas (normally hydrogen or helium at high pressure) that is contained in a closed system. The gas cycles between hot and cold spaces in the engine stores and releases the heat that is added during expansion and rejected during compression.

5.7. Solar furnaces

Solar furnaces are made of high concentration and thus high temperature collectors of the parabolic dish and heliostat type. They are primarily used for material processing. Solar material processing involves affecting the chemical conversion of materials by their direct exposure to concentrated solar energy. A diverse range of approaches are being researched for applications related to high added-value products such as fullerenes, large carbon molecules with major potential commercial applications in semiconductors and superconductors, to commodity products such as cement [172]. None of these processes however, have achieved large-scale commercial adoption. Some pilot systems are shortly described here.

A solar thermochemical process has been developed by Steinfeld et al. [173] which combines the reduction of zinc oxide with reforming of natural gas leading to the co-production of zinc, hydrogen and carbon monoxide. At the equilibrium chemical composition in a black-body solar reactor operated at a temperature of 1250 K at atmospheric pressure with solar concentration of 2000, efficiencies between 0.4 and 0.65 have been found, depending on product heat recovery. A 5 kW solar chemical reactor has been employed to demonstrate this technology in a high-flux solar furnace. Particles of zinc oxide were introduced continuously in a vortex flow natural gas contained within a solar cavity receiver exposed to concentrated insolation from a heliostat field. The zinc oxide particles are exposed directly to the high radiative flux avoiding the inefficiencies and cost of heat exchangers.

A 2 kW concentrating solar furnace has been used to study the thermal decomposition of titanium dioxide at temperatures of 2300–2800 K in an argon atmosphere [174]. The decomposition rate was limited by the rate at which oxygen diffuses from the liquid–gas interface. It was shown that this rate is accurately predicted by a numerical model which couples the equations of chemical equilibrium and steady-state mass transfer [174].

5.8. Solar chemistry applications

Solar energy is essentially unlimited and its utilization is ecologically benign. However, solar radiation reaching the earth is intermittent and not distributed evenly. There is thus a need to store solar energy and transport it from the sunny uninhabited regions to the industrialized populated regions where energy is needed. The way to achieve this is by the thermochemical conversion of solar energy into chemical fuels. This method provides a thermochemically efficient path for storage and transportation. For this purpose high concentration ratio collectors similar to the ones used for power generation are employed. Thus by concentrating solar radiation in receivers and reactors, energy can be supplied to high-temperature processes to drive endothermic reactions. Solar energy can also assist in the processing of energy-intensive and high-temperature materials.

Applications include the solar reforming of low hydrocarbon fuels such as LPG and natural gas and upgrade it into a synthesis gas that can be used in gas turbines. Thus weak gas resources diluted with carbon dioxide can be used directly as feed components for the conversion process. Therefore, natural gas fields currently not exploited due to high CO₂ content might be opened to the market. Furthermore, gasification products of non-conventional fuels like biomass, oil shale and waste asphaltene can also be fed into the solar upgrade process [175].

Other applications include the solar gasification of biomass and the production of solar aluminium the manufacture of which is one of the most energy intensive processes. Another interesting application is the solar zinc and syngas production which are both very valuable commodities. Zinc finds application in Zn/air fuel cells and batteries. Zinc can also react with water to form hydrogen which can be further processed for heat and electricity generation. Syngas can be used to fuel highly efficient combined cycles or can be used as the building block of a wide variety of synthetic fuels, including methanol, which is a very promising substitute of gasoline for fuelling cars [175].

A model for solar volumetric reactors for hydrocarbons reforming operation at high temperature and pressure is presented by Yehesket et al. [176]. The system is based on two achievements: the development of a volumetric receiver tested at 5000–10 000 suns, gas outlet temperature of 1200 °C and pressure at 20 atm and a laboratory scale chemical kinetics study of hydrocarbons reforming. Other related applications are a solar driven ammonia based thermochemical energy storage system [177] and an ammonia synthesis reactor for a solar thermochemical energy storage system [178].

Another field of solar chemistry applications is the solar photochemistry. Solar photochemical processes make use of the spectral characteristics of the incoming solar radiation to effect selective catalytic transformations which find

application in the detoxification of air and water and in the processing of fine chemical commodities.

In solar detoxification photocatalytic treatment of non-biodegradable persistent chlorinated water contaminants typically found in chemical production processes is achieved. For this purpose PTC with glass absorbers are employed and the high intensity of solar radiation is used for the photocatalytic decomposition of organic contaminants. The process uses ultraviolet (UV) energy, available in sunlight, in conjunction with the photocatalyst, titanium dioxide, to decompose organic chemicals into non-toxic compounds [179]. Another application concerns the development of a prototype employing lower concentration CPC [175]. Recent developments in photocatalytic detoxification and disinfection of water and air are presented by Goswami [180].

The development of a compound parabolic concentrator technology for commercial solar detoxification applications is given in Ref. [181]. The objective is to develop a simple, efficient and commercially competitive water treatment technology. A demonstration facility is planned to be erected by the project partners at PSA in Southern Spain.

6. Conclusions

Several of the most common types of solar collectors are presented in this paper. The various types of collectors described include flat-plate, compound parabolic, evacuated tube, parabolic trough, Fresnel lens, parabolic dish and Heliostat field collector (HFC). The optical, thermal and thermodynamic analysis of collectors is also presented as well as methods to evaluate their performance. Additionally, typical applications are described in order to show to the reader the extent of their applicability. These include water heating, space heating and cooling, refrigeration, industrial process heat, desalination, thermal power systems, solar furnaces and chemistry applications. It should be noted that the applications of solar energy collectors are not limited to the above areas. There are many other applications which are not described here either because they are not fully developed or are not matured yet. The application areas described in this paper show that solar energy collectors can be used in a wide variety of systems, could provide significant environmental and financial benefits, and should be used whenever possible.

References

- [1] Kreith F, Kreider JF. Principles of solar engineering. New York: McGraw-Hill; 1978.
- [2] Anderson B. Solar energy: fundamentals in building design. New York: McGraw-Hill; 1977.
- [3] Dincer I. Energy and environmental impacts: present and future perspectives. Energy Sources 1998;20(4/5):427–53.

- [4] Dincer I. Renewable energy, environment and sustainable development. Proceedings of the World Renewable Energy Congress V, Florence, Italy; 1998. p. 2559–62.
- [5] Rosen MA. The role of energy efficiency in sustainable development. Technol Soc 1996;15(4):21–6.
- [6] Dincer I, Rosen MA. A worldwide perspective on energy, environment and sustainable development. Int J Energy Res 1998;22(15):1305–21.
- [7] www.worldwatch.org.
- [8] Dincer I. Environmental impacts of energy. Energy Policy 1999;27(14):845–54.
- [9] Colombo U. Development and the global environment. In: Hollander JM, editor. The energy–environment connection. Washington: Island Press; 1992. p. 3–14.
- [10] Sayigh AAW. Renewable energy: global progress and examples. Renewable Energy 2001; WREN 2001;15–17.
- [11] Johanson TB, Kelly H, Reddy AKN, Williams RH. Renewable fuels and electricity for a growing world economy. In: Johanson TB, Kelly H, Reddy AKN, Williams RH, editors. Renewable energy-sources for fuels and electricity. Washington, DC: Island Press; 1993. p. 1–71.
- [12] Meinel AB, Meinel MP. Applied solar energy: an introduction. Reading, MA: Addison-Wesley; 1976.
- [13] Kreider JF, Kreith F. Solar heating and cooling. New York: McGraw-Hill; 1977.
- [14] SERI. Power from the Sun: principles of high temperature solar thermal technology; 1987.
- [15] Kalogirou S. Solar water heating in Cyprus. Current status of technology and problems. Renewable Energy 1997;10:107–12.
- [16] Lysen E. Photovoltaics: an outlook for the 21st century. Renewable Energy World 2003;6(1):43–53.
- [17] Malik MAS, Tiwari GN, Kumar A, Sodha MS. Solar distillation. New York: Pergamon Press; 1985.
- [18] Kalogirou S. Survey of solar desalination systems and system selection. Energy: Int J 1997;22:69–81.
- [19] Norton B. Solar energy thermal technology. London: Springer; 1992.
- [20] Kalogirou S. The potential of solar industrial process heat applications. Appl Energy 2003;76:337–61.
- [21] ASHRAE. Handbook of HVAC Applications, Atlanta; 1995 [chapter 30].
- [22] Spate F, Hafner B, Schwarzer K. A system for solar process heat for decentralised applications in developing countries. Proceedings of ISES Solar World Congress, Jerusalem, Israel on CD-ROM; 1999.
- [23] Schweiger H. Optimisation of solar thermal absorber elements with transparent insulation. Thesis, Universitat Politecnica de Catalunya, Terrassa, Barcelona, Spain; 1997.
- [24] Benz N, Hasler W, Hetfleish J, Tratzky S, Klein B. Flat-plate solar collector with glass TL. Proceedings of Eurosun'98 Conference on CD-ROM, Portoroz, Slovenia; 1998.
- [25] Tripanagnostopoulos Y, Souliotis M, Nousia Th. Solar collectors with colored absorbers. Solar Energy 2000;68:343–56.
- [26] Wazwaz J, Salmi H, Hallak R. Solar thermal performance of a nickel-pigmented aluminium oxide selective absorber. Renewable Energy 2002;27:277–92.
- [27] Orel ZC, Gunde MK, Hutchins MG. Spectrally selective solar absorbers in different non-black colours. Proceedings of WREC VII, Cologne on CD-ROM; 2002.
- [28] Kontinen P, Lund PD, Kilpi RJ. Mechanically manufactured selective solar absorber surfaces. Solar Energy Mater Solar Cells 2003;79(3):273–83.
- [29] Wackelgard E, Niklasson GA, Granqvist CG. Selective solar-absorbing coatings. In: Gordon J, editor. Solar energy: the state of the art. Germany: ISES; 2001. p. 109–44.
- [30] Kreider JF. The solar heating design process. New York: McGraw-Hill; 1982.
- [31] Close DJ. Solar air heaters. For low and moderate temperature applications. Solar Energy 1963;7(3):117–24.
- [32] Gupta CL, Garg HP. Performance studies on solar air heaters. Solar Energy 1967;11(1):25–31.
- [33] Wijeyundera NE, Lee LAh, Tjioe LEK. Thermal performance study of two-pass solar air heaters. Solar Energy 1982;28(5):363–70.
- [34] Samuel TD. Heat withdrawal from multi-layer thermal trap collectors. Solar Energy 1983;30(3):261–70.
- [35] Biondi P, Cicala L, Farina G. Performance analysis of solar air heaters of conventional design. Solar Energy 1988;41(1):101–7.
- [36] Parker BF, Lindley MR, Colliver DG, Murphy WE. Thermal performance of three solar air heaters. Solar Energy 1993;51(6):467–79.
- [37] Kolb A, Winter ERF, Viskanta R. Experimental studies on a solar air collector with metal matrix absorber. Solar Energy 1999;65(2):91–8.
- [38] Klein SA, Beckman WA, Duffie JA. A design procedure for solar air heating systems. Solar Energy 1977;19:509–12.
- [39] Hollands KGT, Shewen EC. Optimization of flow passage geometry for air-heating, plate-type solar collectors. J Solar Energy Engng 1981;103:323–30.
- [40] Francia G. A new collector of solar radiant energy. UN Conf New Sources Energy, Rome 1961;4:572.
- [41] Soltau H. Testing the thermal performance of uncovered solar collectors. Solar Energy 1992;49(4):263–72.
- [42] Molineaux B, Lachal B, Gusian O. Thermal analysis of five outdoor swimming pools heated by unglazed solar collectors. Solar Energy 1994;53(1):21–6.
- [43] Winter F. Twenty-year progress report on the copper development association do-it-yourself solar swimming pool heating manual and on the associated prototype heater. Solar Energy 1994;53(1):33–6.
- [44] Winston R. Solar concentrators of novel design. Solar Energy 1974;16:89–95.
- [45] Pereira M. Design and performance of a novel non-evacuated 1.2x CPC type concentrator. Proceedings of Intersol Biennial Congress of ISES, Montreal, Canada, vol. 2.; 1985. p. 1199–204.
- [46] Rabl A. Optical and thermal properties of compound parabolic collectors. Solar Energy 1976;18:497–511.
- [47] Mills DR, Giutronich JE. Asymmetrical non-imaging cylindrical solar concentrators. Solar Energy 1978;20:45–55.
- [48] McIntire WR. Optimization of stationary nonimaging reflectors for tubular evacuated receivers aligned north-south. Solar Energy 1980;24:169–75.
- [49] O'Gallagher JJ, Snail K, Winston R, Peek C, Garrison JD. A new evacuated CPC collector tube. Solar Energy 1982;29(6):575–7.
- [50] Ronnelid M, Perers B, Karlsson B. Construction and testing of a large-area CPC-collector and comparison with a flat plate collector. Solar Energy 1996;57(3):177–84.

- [51] Rabl A, Goodman NB, Winston R. Practical design considerations for CPC solar collectors. *Solar Energy* 1979;22:373–81.
- [52] Tripanagnostopoulos Y, Yianoulis P. CPC solar collectors with multichannel absorber. *Solar Energy* 1996;58(1–3): 49–61.
- [53] Tripanagnostopoulos Y, Yianoulis P, Papaefthimiou S, Zafeiratos S. CPC collectors with flat bifacial absorbers. *Solar Energy* 2000;69(3):191–203.
- [54] Tripanagnostopoulos Y, Yianoulis P, Papaefthimiou S, Souliotis M, Nousia Th. Cost effective asymmetric CPC solar collectors. *Renewable Energy* 1999;16:628–31.
- [55] Lin Q, Furbo S. Solar heating systems with evacuated tubular solar collector. Proceedings of the Eurosun'98 Conference on CD-ROM, Portoroz, Slovenia; 1998.
- [56] Morrison GL. Solar collectors. In: Gordon J, editor. *Solar energy: the state of the art*. Germany: ISES; 2001. p. 145–221.
- [57] Winston R, O'Gallagher J, Muschaweck J, Mahoney A, Dudley V. Comparison of predicted and measured performance of an integrated compound parabolic concentrator (ICPC). Proceedings of ISES Solar World Congress on CD-ROM, Jerusalem, Israel; 1999.
- [58] Grass C, Benz N, Hacker Z, Timinger A. Tube collector with integrated tracking parabolic concentrator. Proceedings of the Eurosun'2000 Conference on CD-ROM, Copenhagen, Denmark; 2000.
- [59] Kalogirou S, Eleftheriou P, Lloyd S, Ward J. Design and performance characteristics of a parabolic-trough solar-collector system. *Appl Energy* 1994;47:341–54.
- [60] Garg HP, Hrishikesan DS. Enhancement of solar energy on flat-plate collector by plane booster mirrors. *Solar Energy* 1998;40(4):295–307.
- [61] Tabor H. Mirror boosters for solar collectors. *Solar Energy* 1966;10:111–8.
- [62] Seitel SC. Collector performance enhancement with flat reflectors. *Solar Energy* 1975;17:291–5.
- [63] Perers B, Karlsson B, Bergkvist M. Intensity distribution in the collector plane from structured booster reflectors with rolling grooves and corrugations. *Solar Energy* 1994;53(2): 215–26.
- [64] Kalogirou S. Solar energy utilisation using parabolic trough collectors in Cyprus. MPhil Thesis. The Polytechnic of Wales; 1991.
- [65] Kearney DW, Price HW. Solar thermal plants-LUZ concept (current status of the SEGS plants). Proceedings of the Second Renewable Energy Congress, Reading UK, vol. 2.; 1992. p. 582–8.
- [66] Grasse W. Solar PACES Annual Report, DLR Germany; 1995.
- [67] Kalogirou S, Eleftheriou P, Lloyd S, Ward J. Low cost high accuracy parabolic troughs: construction and evaluation. Proceedings of the world renewable energy congress III, Reading, UK, vol. 1.; 1994. p. 384–6.
- [68] Lupfert E, Geyer M, Schiel W, Zarza E, Gonzalez-Angular RO, Nava P. Eurotrough: a new parabolic trough collector with advanced light weight structure. Proceedings of Solar Thermal 2000 International Conference, on CD-ROM, Sydney, Australia; 2000.
- [69] Geyer M, Lupfert E, Osuna R, Esteban A, Schiel W, Schweitzer A, Zarza E, Nava P, Langenkamp J, Mandelberg E. Eurotrough: parabolic trough collector developed for cost efficient solar power generation. Proceedings of 11th Solar PACES International Symposium on Concentrated Solar Power and Chemical Energy Technologies on CD-ROM, Zurich, Switzerland; 2002.
- [70] Bakos GC, Adamopoulos D, Tsagas NF., Sourso M. Design and construction of a line-focus parabolic trough solar concentrator for electricity generation. Proceedings of ISES Solar World Congress on CD-ROM, Jerusalem, Israel; 1999.
- [71] Kalogirou S. Parabolic trough collector system for low temperature steam generation: design and performance characteristics. *Appl Energy* 1996;55(1):1–19.
- [72] Kupta KC, Mirakur PK, Sathe AP. A simple solar tracking system. SUN, Proceedings of the International Solar Energy Society, New Delhi, India: Pergamon Press; 1978.
- [73] Cope NA, Ingley HA, Farber EA, Morrison CA. Dynamic response analysis of a solar powered heliostropic fluid mechanical drive system. University of Florida; 1981.
- [74] Singh TAK, Dinesh PS. Liquid vapour balance based sun tracking system. Proceedings of the 25th National Renewable Energy Convention 2001 of the Solar Society of India, Warangal, India; 2001. p. 401–6.
- [75] Hession PJ, Bonwick WJ. Experience with a Sun tracker system. *Solar Energy* 1984;32:311.
- [76] Zogbi R, Laplaze D. Design and construction of a Sun tracker. *Solar Energy* 1984;33:369–72.
- [77] Mori Y, Hijikata K, Himero N. Fundamental research on heat transfer performances of solar focusing and tracking collector. *Solar Energy* 1977;19:595–600.
- [78] Boultinghouse KD. Development of a solar flux tracker for parabolic trough collectors. Albuquerque, USA: Sandia National Labs; 1982.
- [79] Briggs F. Tracking-refinement modelling for solar-collector control. Albuquerque, USA: Sandia National Labs; 1980.
- [80] Nuwayhid RY, Mrad I, Abu-Said R. The realisation of a simple solar tracking concentrator for university research applications. *Renewable Energy* 2001;24:207–22.
- [81] Kalogirou SA. Design and construction of a one-axis Sun-tracking mechanism. *Solar Energy* 1996;57(6):465–9.
- [82] Kruger D, Heller A, Hennecke K, Duer K. Parabolic trough collectors for district heating systems at high latitudes: a case study. Proceedings of Eurosun'2000 on CD ROM, Copenhagen, Denmark; 2000.
- [83] Dudley V. SANDIA Report test results for industrial solar technology parabolic trough solar collector. SAND94-1117, Albuquerque, USA: Sandia National Laboratory; 1995.
- [84] Riffelmann KJ, Fend Th, Pitz-Paal R. Parabolic trough collector efficiency improvement activities. In: Kreetz H, Lovegrove K, Meike W, editors. 10th International Symposium—Solar PACES—Solar Thermal Concentrating Technologies, Sydney, Australia. 2000. p. 121–9.
- [85] Francia G. Pilot plants of solar steam generation systems. *Solar Energy* 1968;12:51–64.
- [86] Mills DR. Solar thermal electricity. In: Gordon J, editor. *Solar energy: the state of the art*. Germany: ISES; 2001. p. 577–651.
- [87] Nelson DT, Evans DL, Bansal RK. Linear Fresnel lens concentrators. *Solar Energy* 1975;17:285–9.
- [88] Collares-Pereira M. High temperature solar collector with optimal concentration: non-focusing Fresnel lens with secondary concentrator. *Solar Energy* 1979;23:409–20.

- [89] Kritchman EM, Friesem AA, Yekutieli G. Efficient Fresnel lens for solar concentration. *Solar Energy* 1989;22:119–23.
- [90] Lorenzo E, Minano JC. Design of one-axis tracked linear Fresnel lenses. *Solar Energy* 1986;36(6):531–4.
- [91] Feuermann D, Gordon JM. Analysis of a two-stage linear Fresnel reflector solar concentrator. *ASME J Solar Energy Engng* 1991;113:272–9.
- [92] Pitz-Paal R. Concentrating solar technologies: the key to renewable electricity and process heat for a wide range of applications. Proceedings of the World Renewable Energy Congress VII on CD-ROM, Cologne, Germany; 2002.
- [93] Romero M, Buck R, Pacheco JE. An update on solar central receiver systems projects and technologies. *J Solar Energy Engng* 2002;124(2):98–108.
- [94] Schwarzbözl P, Pitz-Paal R, Meinecke W, Buck R. Cost-optimized solar gas turbine cycles using volumetric air receiver technology. Proceedings of the Renewable Energy for the New Millennium, Sydney, Australia; 2000. p. 171–7.
- [95] Chavez JM, Kolb GJ, Meinecke W. In: Becker M, Klimas PC, editors. Second generation central receiver technologies: a status report. Karlsruhe, Germany: Verlag; 1993.
- [96] Prapas DE, Norton B, Probert SD. Optics of parabolic trough solar energy collectors possessing small concentration ratios. *Solar Energy* 1987;39:541–50.
- [97] Duffie JA, Beckman WA. *Solar engineering of thermal processes*. New York: Wiley; 1991.
- [98] Klein SA. Calculation of flat plate collector loss coefficients. *Solar Energy* 1975;17:79–80.
- [99] Sodha MS, Mathur SS, Malik MAS, Reviews of renewable energy resources, vol. 2. New York: Wiley; 1984.
- [100] Jeter MS. Geometrical effects on the performance of trough collectors. *Solar Energy* 1983;30:109–13.
- [101] Guven HM, Bannerot RB. Derivation of universal error parameters for comprehensive optical analysis of parabolic troughs. Proceedings of the ASME-ISES Solar Energy Conference, Knoxville, USA; 1985. p. 168–74.
- [102] Guven HM, Bannerot RB. Determination of error tolerances for the optical design of parabolic troughs for developing countries. *Solar Energy* 1986;36:535–50.
- [103] Jeter MJ. Calculation of the concentrated flux density distribution in parabolic trough collectors by a semi-finite formulation. *Solar Energy* 1986;37(5):335–45.
- [104] Karimi A, Guven HM, Thomas A. Thermal analysis of direct steam generation in parabolic trough collectors. Proceedings of the ASME Solar Energy Conference; 1986. p. 458–64.
- [105] Bejan A, Kearney DW, Kreith F. Second law analysis and synthesis of solar collector systems. *J Solar Energy Engng* 1981;103:23–8.
- [106] Bejan A. *Entropy generation minimization*. 2nd ed. Boca Raton: CRC Press; 1995. [chapter 9].
- [107] Petela R. Exergy of heat radiation. *ASME J Heat Transfer* 1964;68:187.
- [108] ASHRAE Standard 93. Methods of testing to determine the thermal performance of solar collectors, ANSI/ASHRAE 93-1986; 1986.
- [109] ISO 9806-2, Solar energy-test methods for solar energy collectors. Part 2. Qualification test procedures. Geneva: International Standards Organisation; 1995.
- [110] Kalogirou S, Papamarcou C. Modelling of a thermosyphon solar water heating system and simple model validation. *Renewable Energy* 2000;21(3/4):471–93.
- [111] TRNSYS Program Manual. Solar Energy Laboratory, University of Wisconsin, Madison, USA; 1996.
- [112] Kreider JF, Kreith F. *Solar energy handbook*. New York: McGrawHill; 1981.
- [113] Beckman WA. Modern computing methods in solar energy analysis. Proceedings of Eurosun'98 on CD-ROM, Portoroz, Slovenia; 1998.
- [114] Oishi M, Noguchi T. The evaluation procedure on performance of SDHW system by TRNSYS simulation for a yearly performance prediction. Proceedings of Eurosun'2000 on CD-ROM, Copenhagen, Denmark; 2000.
- [115] Jordan U, Vajen K. Influence of the DHW load profile on the fractional energy savings: a case study of a solar combi-system with TRNSYS simulations. Proceedings of Eurosun'2000 on CD-ROM, Copenhagen, Denmark; 2000.
- [116] Benz N, Gut M, Belkircher Th, Russ W. Solar process heat with non-concentrating collectors for food industry. Proceedings of ISES Solar world Congress on CD-ROM, Jerusalem, Israel; 1999.
- [117] Schweiger H, Mendes JF, Benz N, Hennecke K, Prieto G, Gusi M, Goncalves H. The potential of solar heat in industrial processes. a state of the art review for Spain and Portugal. Proceedings of Eurosun'2000 Copenhagen, Denmark on CD-ROM; 2000.
- [118] Florides G, Kalogirou S, Tassou S, Wrobel L. Modelling and simulation of an absorption solar cooling system for Cyprus. *Solar Energy* 2002;72(1):43–51.
- [119] *Watsun Users Manual and Program Documentation*. Watsun Simulation Laboratory, University of Waterloo, Canada; 1992.
- [120] *Polysun. User's manual for Polysun 3.3, SPF, Switzerland; 2000.*
- [121] Gantner M. Dynamische simulation thermischer solaranlagen. Diploma Thesis, Hochschule für Technik Rapperswil (HSR), Switzerland; 2000.
- [122] Beckman WA, Klein SA, Duffie JA. *Solar heating design by the f-chart method*. New York: Wiley/Interscience; 1977.
- [123] Klein SA, Beckman WA. *F-Chart User's Manual*, University of Wisconsin; 1981.
- [124] Datta G, Broman L, Garg HP. Optimisation of collector tilts using F-chart method. Proceedings of the Second World Renewable Energy Congress, Reading, UK; 1992. p. 1051–5.
- [125] Kalogirou S, Lloyd S. Use of solar parabolic trough collectors for hot water production in Cyprus. A feasibility study. *Renewable Energy* 1992;2(2):117–24.
- [126] Kalogirou S. Artificial neural networks in renewable energy systems: a review. *Renewable Sustainable Energy Rev* 2001; 5(4):373–401.
- [127] Kalogirou S. Economic analysis of solar energy systems using spreadsheets. Proceedings of the World Renewable Energy Congress IV, Denver, Colorado, USA, vol. 2; 1996. p. 1303–7.
- [128] Morrison G, Wood B. Packaged solar water heating technology: twenty years of progress. Proceedings of ISES Solar World Congress on CD-ROM, Jerusalem, Israel; 1999.
- [129] Gupta GL, Garg HP. System design in solar water heaters with natural circulation. *Solar Energy* 1968;12:163–82.
- [130] Ong KS. A finite difference method to evaluate the thermal performance of a solar water heater. *Solar Energy* 1974;16: 137–47.

- [131] Ong KS. An improved computer program for the thermal performance of a solar water heater. *Solar Energy* 1976;18: 183–91.
- [132] Kudish AI, Santamura P, Beaufort P. Direct measurement and analysis of thermosyphon flow. *Solar Energy* 1985;35: 167–73.
- [133] Morrison GL, Braun JE. System modelling and operation characteristics of thermosyphon solar water heaters. *Solar Energy* 1985;34:389–405.
- [134] Hobson PA, Norton B. A design nomogram for direct thermosyphon solar energy water heaters. *Solar Energy* 1989;43:89–95.
- [135] Shariah AM, Shalabi B. Optimal design for a thermosyphon solar water heater. *Renewable Energy* 1997;11:351–61.
- [136] Tripanagnostopoulos Y, Souliotis M, Nousia Th. CPC type integrated collector storage systems. *Solar Energy* 2002; 72(4):327–50.
- [137] Kalogirou S. Design, construction, performance evaluation, and economic analysis of an integrated collector storage system. *Renewable Energy* 1997;12(2):179–92.
- [138] McIntire WR. Truncation of nonimaging cusp concentrators. *Solar Energy* 1979;23:351–5.
- [139] Hahne E. Solar heating and cooling. Proceedings of Eurosun'96, Freiburg, Germany, vol. 1; 1996. p. 3–19.
- [140] Florides G, Tassou S, Kalogirou S, Wrobel L. Review of solar and low energy cooling technologies for buildings. *Renewable Sustainable Energy Rev* 2002;6(6):557–72.
- [141] Critoph RE. Development of three solar/biomass adsorption air conditioning refrigeration systems. Proceedings of the World Renewable Energy Congress VII on CD-ROM, Cologne, Germany; 2002.
- [142] Thorpe R. Progress towards a highly regenerative adsorption cycle for solar thermal powered air conditioning. Proceedings of the World Renewable Energy Congress VII on CD-ROM, Cologne, Germany; 2002.
- [143] ASHRAE. Handbook of fundamentals, Atlanta; 1989.
- [144] Dorgan CB, Leight SP, Dorgan CE. Application guide for absorption cooling/refrigeration using recovered heat. American Society of Heating, Refrigerating and Air Conditioning Engineers, Inc.; 1995.
- [145] Keith EH. Design challenges in absorption chillers. *Mech Engng: CIME* 1995;117(10):80–4.
- [146] Hammad MA, Audi MS. Performance of a solar LiBr–water absorption refrigeration system. *Renewable Energy* 1992; 2(3):275–82.
- [147] Haim I, Grossman G, Shavit A. Simulation and analysis of open cycle absorption systems for solar cooling. *Solar Energy* 1992;49(6):515–34.
- [148] Hawlader MNA, Noval KS, Wood BD. Unglazed collector/regenerator performance for a solar assisted open cycle absorption cooling system. *Solar Energy* 1993;50(1):59–73.
- [149] Ameel TA, Gee KG, Wood BD. Performance predictions of alternative, Low cost absorbents for open-cycle absorption solar cooling. *Solar Energy* 1995;54(2):65–73.
- [150] Ghaddar NK, Shihab M, Bdeir F. Modelling and simulation of solar absorption system performance in Beirut. *Renewable Energy* 1997;10(4):539–58.
- [151] Erhard A, Hahne E. Test and simulation of a solar-powered absorption cooling machine. *Solar Energy* 1997;59(4–6): 155–62.
- [152] Hammad M, Zurigat Y. Performance of a second generation solar cooling unit. *Solar Energy* 1998;62(2):79–84.
- [153] Zinian HE, Ning Z. A solar absorption air-conditioning plant using heat-pipe evacuated tubular collectors. Proceedings of ISES Solar World Congress on CD-ROM, Jerusalem, Israel; 1999.
- [154] Winston R, O'Gallagher J, Duff W, Henkel T, Muschaweck J, Christiansen R, Bergquam J. Demonstration of a new type of icpc in a double-effect absorption cooling system. Proceedings of ISES Solar World Congress on CD-ROM, Jerusalem, Israel; 1999.
- [155] Florides G, Kalogirou S, Tassou S, Wrobel L. Design and construction of a lithium bromide–water absorption machine. *Energy Conversion Mgmt* 2003;44(15):2483–508.
- [156] Norton B. Solar process heat: distillation, drying, agricultural and industrial uses. Proceedings of ISES Solar World Congress, Jerusalem, Israel on CD-ROM, Jerusalem, Israel; 1999.
- [157] Spate F, Hafner B, Schwarzer K. A system for solar process heat for decentralised applications in developing countries. Proceedings of ISES Solar World Congress on CD-ROM, Jerusalem, Israel; 1999.
- [158] Benz N, Gut M, Rub W. Solar process heat in breweries and dairies. Proceedings of EuroSun 98, Portoroz, Slovenia on CD-ROM; 1998.
- [159] Benz N, Gut M, Beikircher T. Solar process heat with non-concentrating collectors for food industry. Proceedings of ISES Solar World Congress on CD ROM, Jerusalem, Israel; 1999.
- [160] Kalogirou S, Lloyd S, Ward J. Modelling optimisation and performance evaluation of a parabolic trough collector steam generation system. *Solar Energy* 1997;60(1):49–59.
- [161] Hurtado P, Kast M. Experimental study of direct in-situ generation of steam in a line focus solar collector, SERI; 1984.
- [162] Peterson RJ, Keneth E. Flow instability during direct steam generation in line-focus solar collector system, SERI/TR-1354; 1982.
- [163] Zarza E, Hennecke K, Coebel O. Project DISS (Direct Solar Steam) update on project status and future planning. Proceedings of ISES Solar World Congress on CD-ROM, Jerusalem, Israel; 1999.
- [164] Murphy LM, Keneth E. Steam generation in line-focus solar collectors: a comparative assessment of thermal performance, operating stability, and cost issues. SERI/TR-1311; 1982.
- [165] Mustacchi C, Cena V. Solar desalination: design, performances, economics, Sogesta; 1981.
- [166] Eibling JA, Talbert SG, Lof GOG. Solar stills for community use: digest of technology. *Solar Energy* 1971;13:263.
- [167] Daniels F. Direct use of the sun's energy. 6th ed. London: Yale University Press; 1974 [chapter 10].
- [168] Kalogirou S. Use of parabolic trough solar energy collectors for sea-water desalination. *Appl Energy* 1998; 60(2):65–88.
- [169] Kronshage S, Schillings C, Trieb F. Country analysis for solar thermal power stations using remote sensing methods. Proceedings of the World Renewable Energy Congress VII on CD-ROM, Cologne, Germany; 2002.
- [170] Meurer C, Barthels H, Brocke WA, Emonts B, Groehn HG. PHOEBUS: an autonomous supply system with renewable energy-six years of operational experience and advanced

- concepts. Proceedings of ISES Solar World Congress on CD-ROM, Jerusalem, Israel; 1999.
- [171] Solar Thermal Power and Solar Chemical Energy Systems, Solar PACES Program of the International Energy Agency. Birmingham, UK: The Franklin Company Consultants Ltd; 1994.
- [172] Norton B. Solar process heat. In: Gordon J, editor. Solar energy: the state of the art. Germany: ISES; 2001. p. 477–96.
- [173] Steinfeld A, Larson C, Palumbo R, Foley M. Thermodynamic analysis of the co-production of zinc and synthesis gas using solar process heat. *Energy* 1996;21:205–22.
- [174] Palumbo R, Rouanet A, Pichelin G. Solar thermal decomposition of TiO_2 at temperatures above 2200 K and its use in the production of Zn and ZnO. *Energy* 1995;20:857–68.
- [175] Grasse W. Solar PACES Annual Report. DLR Germany; 1998.
- [176] Yehesket J, Rubin R, Berman A, Karni J. Chemical kinetics of high temperature hydrocarbons reforming using a solar reactor. Proceedings of Eurosun'2000 on CD-ROM, Copenhagen, Denmark; 2000.
- [177] Lovegrove K, Luzzi A, Kreetz H. A solar driven ammonia based thermochemical energy storage system. Proceedings of ISES Solar World Congress on CD-ROM, Jerusalem, Israel; 1999.
- [178] Kreetz H, Lovegrove K. Theoretical analysis and experimental results of a $1 \text{ kW}_{\text{chem}}$ ammonia synthesis reactor for a solar thermochemical energy storage system. Proceedings of ISES Solar World Congress on CD-ROM, Jerusalem, Israel; 1999.
- [179] Mehos M, Turchi C, Pacheco J, Boegel AJ, Merrill T, Stanley R. Pilot-scale study of the solar detoxification of VOC-contaminated groundwater, NREL/TP-432-4981; 1992.
- [180] Goswami DY. Recent developments in photocatalytic detoxification and disinfection of water and air. Proceedings of ISES Solar World Congress on CD-ROM, Jerusalem, Israel; 1999.
- [181] Blanco J, Malato S, Fernandez P, Vidal A, Morales A, Trincado P, Oliveira J, Minero C, Musci M, Casalle C, Brunotte M, Tratzky S, Dischinger N, Funken K, Sattler C, Vincent M, Collares-Pereira M, Mendes J, Rangel C. Compound parabolic concentrator technology development to commercial solar detoxification applications. Proceedings of ISES Solar World Congress on CD-ROM, Jerusalem, Israel; 1999.